

# MAN-MADE RADIO NOISE

## PART I: ESTIMATES FOR BUSINESS, RESIDENTIAL, AND RURAL AREAS

A. D. SPAULDING  
R. T. DISNEY



U.S. DEPARTMENT OF COMMERCE  
Frederick B. Dent, Secretary

Betsy Ancker-Johnson, Ph. D.  
Assistant Secretary for Science and Technology

OFFICE OF TELECOMMUNICATIONS  
John M. Richardson, Acting Director



JUNE 1974

**UNITED STATES DEPARTMENT OF COMMERCE  
OFFICE OF TELECOMMUNICATIONS  
STATEMENT OF MISSION**

The mission of the Office of Telecommunications in the Department of Commerce is to assist the Department in fostering, serving, and promoting the nation's economic development and technological advancement by improving man's comprehension of telecommunication science and by assuring effective use and growth of the nation's telecommunication resources.

In carrying out this mission, the Office

- Performs analysis, engineering, and related administrative functions responsive to the needs of the Director of the Office of Telecommunications Policy, Executive Office of the President, in the performance of his responsibilities for the management of the radio spectrum
- Conducts research needed in the evaluation and development of telecommunication policy as required by the Office of Telecommunications Policy, pursuant to Executive Order 11556
- Conducts research needed in the evaluation and development of other policy as required by the Department of Commerce
- Assists other government agencies in the use of telecommunications
- Conducts research, engineering, and analysis in the general field of telecommunication science to meet government needs
- Acquires, analyzes, synthesizes, and disseminates information for the efficient use of the nation's telecommunication resources.

## TABLE OF CONTENTS

	Page
LIST OF FIGURES	v
LIST OF TABLES	xi
ABSTRACT	1
1. INTRODUCTION	2
2. NOISE PARAMETERS	3
3. ESTIMATION METHODS AND THE DATA BASE	8
4. MAN-MADE RADIO NOISE ESTIMATES	12
4.1 Available Noise Power, $F_a$	12
4.1.1 Estimates of $F_a$ for Typical Areas	13
4.1.2 Power Lines	36
4.2 The Average and Logarithmic Moments, $V_d$ and $L_d$	44
4.3 Amplitude and Time Statistics	63
5. USE OF THE MAN-MADE NOISE ESTIMATES IN DETERMINING SYSTEM PERFORMANCE	86
6. MATHEMATICAL MODELING OF THE NOISE PROCESS	90
7. CONCLUSIONS AND DISCUSSION	93
8. ACKNOWLEDGMENTS	97
9. REFERENCES	99
APPENDIX A. MEASUREMENT METHODS USED TO OBTAIN THE DATA BASE	A1
REFERENCES, APPENDIX A	A12
APPENDIX B. THE USE OF TRAFFIC DENSITY INFORMATION AS A NOISE PREDICTOR	B1
REFERENCES, APPENDIX B	B11



## LIST OF FIGURES

	Page
Figure 1. Estimates of median values of man-made noise expected at typical locations.	23
Figure 2. Distribution of location median values of man-made noise, 20 MHz residential area data.	24
Figure 3. Distribution of $F_a$ values for a given location.	25
Figure 4. Expected variation of man-made radio noise levels at a location within an hour.	26
Figure 5. Estimates of man-made noise levels and their variation within an hour for business areas.	27
Figure 6. Estimates of man-made noise levels and their variation within an hour for residential areas.	28
Figure 7. Estimates of man-made noise levels and their variation within an hour for rural areas.	29
Figure 8. Estimates of man-made noise levels and their variation within an hour for interstate highways.	30
Figure 9. Estimates of man-made noise levels and their variation within an hour for parks and university campuses.	31
Figure 10. Radio-noise measurements, Dept. of Commerce Boulder Labs, end of Wing 1.	32
Figure 11. Radio-noise measurements, Dept. of Commerce Boulder Labs, end of Wing 1.	33
Figure 12. Hourly median values of radio noise, measured near highway in front of Dept. of Commerce Boulder Labs, October 25-28, 1967.	34
Figure 13. Horizontal versus vertical component of man-made radio noise at 250 MHz.	35

Figure 14. Decrease in power line noise with distance at 0.5 MHz.	39
Figure 15. Decrease in power line noise with distance at 102 MHz.	40
Figure 16. Power line noise measurements taken moving parallel to a 115 kV line in rural Wymoing, both under the line and 1/4 mile from the line.	41
Figure 17. Expected decrease of radio noise radiated from 115 kV H-frame power line with distance from line.	42
Figure 18. Expected radio noise power, $F_a$ , and its standard deviation, $\sigma_{F_a}$ , from 115 kV, H-frame power transmission line. Receiving antenna under and 0.01 mi. (16.09 meters) from power line.	43
Figure 19. Mean of location median values of $V_d$ , values measured in a 4-kHz bandwidth.	49
Figure 20. Mean of location median values of $L_d$ , values measured in a 4-kHz bandwidth.	50
Figure 21. Mean of location median values of $V_d$ , values measured in a 10-kHz bandwidth.	51
Figure 22. Mean of location median values of $L_d$ , values measured in a 10-kHz bandwidth.	52
Figure 23. Expected median values of $V_d$ and $L_d$ for business areas.	53
Figure 24. Expected median values of $V_d$ and $L_d$ for residential areas.	54
Figure 25. Expected median values of $V_d$ and $L_d$ for rural areas.	55
Figure 26. Distribution of $V_d$ within an hour for a residential area.	56
Figure 27. Distribution of $L_d$ within an hour for a residential area.	57

Figure 28.	Median values of $V_d$ measured along interstate highways, in parks, and on university campuses.	58
Figure 29.	Median values of $L_d$ measured along interstate highways, in parks, and on university campuses.	59
Figure 30.	$V_d$ for horizontal component of man-made noise versus $V_d$ for vertical component.	60
Figure 31.	Correlation of $V_d$ and $L_d$ for man-made noise.	61
Figure 32.	Lack of correlation of $F_a$ and $V_d$ for man-made noise.	62
Figure 33.	Amplitude probability distribution of envelope of man-made radio noise at 48 MHz.	67
Figure 34.	Amplitude probability distribution of man-made noise at 102 MHz.	68
Figure 35.	Amplitude probability distribution of man-made noise at 102 MHz.	69
Figure 36.	Amplitude probability distribution of man-made noise at 102 MHz.	70
Figure 37.	Amplitude probability distribution of man-made noise at 48 MHz, 10 kHz bandwidth.	71
Figure 38.	Randomly selected 200 ms sample of noise envelope from a 6-minute, 250 MHz central Colorado Springs recording.	
Figure 39.	Normalized autocovariance for the noise sample of figure 38.	73
Figure 40.	Amplitude probability distribution for a 6-minute sample of noise recorded in central Colorado Springs.	74
Figure 41.	Average positive crossing rate characteristic for the sample of noise of figure 40.	75
Figure 42.	Pulse duration distributions for the sample of noise of figure 40.	76

Figure 43.	Pulse spacing distributions for the sample of noise of figure 40.	77
Figure 44.	Randomly selected 200 ms sample of noise envelope from a 6-minute 48 MHz, Denver, Colorado, residential area.	78
Figure 45.	Normalized autocovariance for the noise sample of figure 44.	79
Figure 46.	Randomly selected 200 ms sample of noise envelope from a 6-minute, 48 MHz, Denver, Colorado, residential area.	80
Figure 47.	Normalized autocovariance for the noise sample of figure 46.	81
Figure 48.	Amplitude probability distribution for a 6-minute sample of noise recorded in a residential area of Denver, Colorado.	82
Figure 49.	Average positive crossing rate characteristic for the sample of noise of figure 48.	83
Figure 50.	Pulse duration distributions for the sample of noise of figure 48.	84
Figure 51.	Pulse spacing distributions for the sample of noise of figure 48.	85
Figure 52.	Comparison of present estimates with JTAC (1968) estimates.	98
Figure A1.	Block diagram of the measuring and recording facilities in the OT/ITS mobile radio noise lab.	A13
Figure A2.	Block diagram of the analog -recording -playback system.	A14
Figure A3.	Block diagram of the correlation measurement system.	A15
Figure A4.	OT/ITS mobile radio-noise lab system noise factors.	A16



- Figure B1. Regression of 5.0 MHz  $F_{a\mu}$  with log population density of SLA's. B12
- Figure B2. Linear regression of  $F_{a\mu}$  vs. log hourly traffic count along 26 thoroughfares at 48 MHz. B12
- Figure B3. Correlation coefficients along with the 95 percent confidence limits for each of measurement frequencies,  $F_{a\mu}$  vs. log hourly traffic count. B13
- Figure B4. Hourly median values of radio noise power and hourly traffic count. Broadway, Boulder, Colorado, October 25-27, 1967, noise values recorded 100 ft west of highway center. B14
- Figure B5. Distribution of radio noise power at 20 MHz radiated from 958 individual vehicles, values measured at 50 ft from vehicle. B15
- Figure B6. Distribution of radio noise power at 48 MHz radiated from 958 individual vehicles, values measured at 50 ft from vehicle. B15



## LIST OF TABLES

	Page
Table 1. Expected Variation of Median Values about Estimates for Business, Residential, and Rural Locations.	15
Table 2. Expected Variation, Man-Made Radio Noise Levels, about the Median Value for a Location, within the Hour.	17
Table 3. Variation of the Median Value of $V_d$ and $L_d$ with Location for a Given Frequency and Bandwidth.	45

## MAN-MADE RADIO NOISE

### PART I: ESTIMATES FOR BUSINESS, RESIDENTIAL, AND RURAL AREAS

A. D. Spaulding and Robert T. Disney\*

The Office of Telecommunications, Institute for Telecommunication Sciences (OT/ITS), over the past several years, has accumulated a data base of man-made radio noise measurements in the frequency range from 250 kHz through 250 MHz taken in a number of geographical areas. This data base has been analyzed to provide estimates of the expected characteristics of man-made radio noise in business, residential, and rural areas. The parameters used are the average available power spectral density, the ratio of the rms to the average voltage of the noise envelope, and the ratio of the rms to the average logarithm of the envelope voltage. The variation of these parameters as a function of frequency, location, and time are shown and discussed. Examples of amplitude and time statistics of the received man-made radio noise process also are shown and discussed. The use of the estimates is shown (principally by references in Part II, Bibliography) in the solution of problems encountered in frequency management and telecommunication system design.

Key words: Man-made radio noise, noise levels, noise characteristics, non-Gaussian noise, impulsive noise, system performance.

---

\* The authors are with the Institute for Telecommunication Sciences, Office of Telecommunications, U.S. Department of Commerce, Boulder, Colorado 80302.

## 1. INTRODUCTION

The interference environment present at a receiving terminal of a telecommunications system is one of the factors determining whether or not that link of the system will perform satisfactorily. In either the solution of a spectrum management problem or the design of a particular system, the determination of system performance is a prime consideration. In spectrum management, not only is information on the effect of the interference environment on the proposed system necessary, but also the change in the environment caused by the proposed system must be considered. In the design of any proposed system, these two effects need to be considered, though the effect of the environment on the system is generally the primary concern.

The interference environment will consist of all discrete signals present other than the desired signal (usually referred to as unwanted or undesired signals), broadband impulsive noise, the receiver's own internally generated noise, and various other unintended radiations. Often this composite interference environment, whether predominantly noise or unwanted signals, is referred to simply as "noise." In this report, the impulsive noise background will be termed "noise." This radio noise, as distinguished from unwanted signal interference, is a broad-band phenomenon often covering several octaves in frequency, and its spectrum can be considered flat across any bandwidth that is a small percentage of the center frequency of the receiving system.

In order to estimate the behavior of a telecommunications system at some future time, two types of interference information are required. One is the determination of the effect of all of the various kinds of interference environments on the system under consideration, and the other is the estimate of the interference environment that will be present at the time and place of actual system operation. The latter

involves a prediction process for estimating the characteristics of the environment within some degree of accuracy. The primary purpose here is to provide the best estimate possible of those characteristics of the noise process basic to systems design and analysis. In addition, some guidance in the use of these estimates in determining system performance is given in the text and in the references. To provide a better understanding of the estimates, short descriptions of the data base used for preparing the estimates and the equipment employed in the measurement program are included.

Part II of the report is a bibliography listing publications which give man-made noise measurements, techniques of measurement, and system design and analysis in impulsive noise environments.

## 2. NOISE PARAMETERS

The characteristics of the interference environment that determine the performance of a system will be dependent on the modulation-demodulation scheme employed; however, some characteristics of the radio noise process will greatly influence the operation of any system regardless of the detection scheme used. The most basic single parameter of the broadband interference is its power spectral density; that is, the noise power per unit bandwidth (OTP, 1970). This parameter must be known as a function of time, location, and frequency and should be given in a form which allows it to be compared with and combined with other types of interference, such as unwanted signals, internal receiver noise, etc. For the proper design or analysis of any modem, the probability density function of the detected noise envelope is generally required. This is generally given as the percentage of time the envelope voltage exceeds various voltage levels and as such is the amplitude probability distribution (APD). While the APD gives the amplitude behavior of the noise process, the time behavior is

also of importance for many types of interference. The time statistics most generally required for system analysis are the autocovariance function, the average crossing rates of the noise envelope (ACR), pulse spacing distributions (PSD), and pulse duration distributions (PDD). The last three, the ACR, PSD, and PDD, are a function of envelope voltage level. The above statistics are for the detected noise envelope; that is, for the noise process as seen by the receiving system under consideration (Montgomery, 1954; Watt et al., 1958; Middleton, 1960; CCIR, 1964, 1966; Wozencraft and Jacobs, 1965; Conda, 1965; Halton and Spaulding, 1966; Hall, 1966; JTAC, 1968; Bello and Esposito, 1969, 1970; Crippen et al., 1970; Akima et al., 1969; Omura, 1969; Shaver et al., 1972; Gilliland, 1972; and others in Part II, Bibliography). The envelope statistics are required since we are, in general, dealing with a narrowband noise process (i.e., describable by an envelope and phase) and the phase is uniformly distributed.

The basic unit used to describe the noise in these predictions is the power spectral density expressed in terms of an effective antenna noise factor,  $F_a$  (CCIR, 1957, 1964; OTP, 1970). The definition of  $F_a$  is

$$F_a = 10 \log_{10} f_a , \quad (1)$$

where

$$f_a = \frac{P_n}{kT_o b} \quad (2)$$

and  $p_n$  is the external noise power available from an equivalent lossless antenna in bandwidth  $b$ , in watts,  $k$  is Boltzmann's constant =  $1.38 \times 10^{-23}$  Joules/°K,  $T_o$  is the reference temperature = 288° K, and  $b$  is the noise power bandwidth in hertz. Note that  $f_a$  is a dimen-

sionless quantity, being the ratio of two powers. The quantity  $f_a$ , however, gives, numerically, the available power spectral density in terms of  $kT_o$  and the available power in terms of  $kT_o b$ . For this reason, one commonly sees  $F_a$  with units attached (i. e.,  $\text{dB} > kT_o$  or  $\text{dB} > kT_o b$ ).

Relation (2) can be given as

$$P_n = F_a + B - 204 \text{ dBW} , \quad (3)$$

where  $P_n = 10 \log p_n$ ,  $B = 10 \log b$ , and  $-204 = 10 \log kT_o$ .

Other methods commonly used to express the noise power are related simply to  $F_a$  (CCIR, 1957). For example, for the case of a short ( $h \ll \lambda$ ) grounded vertical monopole, the corresponding vertical component of the rms field strength is given by

$$E_n = F_a + 20 \log f_{\text{MHz}} + B - 95.5 \left( \text{dB} > \frac{1 \mu\text{V}}{\text{m}} \right) , \quad (4)$$

where  $E_n$  is the rms field strength for the bandwidth  $b$  in  $\text{dB} > 1 \mu\text{V}/\text{m}$ ,  $f_{\text{MHz}}$  is the frequency in megahertz, and  $\lambda$  is the wavelength in meters. Similar expressions for  $E_n$  can be derived for other antennas.

The relationship between  $f_a$  and the noise power in terms of an effective antenna noise temperature is given by

$$f_a = T_a / T_o , \quad (5)$$

where  $T_a$  is the effective antenna noise temperature in  $^\circ\text{K}$ .

Since the noise level may result from a combination of noise generated internal to the receiving system and external noise, it is convenient to express the resulting noise by means of Norton's (1953) generalization of Friis' (1944) definition of the noise figure of a radio receiver. The system noise factor can be defined in terms of the



losses and actual temperatures of the various parts of the system. Loss in the circuit is taken here to be the ratio of available input power to available output power and will differ from the loss in delivered power unless a matched load is used. The noise factor of the antenna circuit,  $f_c$ , is

$$f_c = 1 + \frac{T_c}{T_o} (\ell_c - 1), \quad (6)$$

where  $\ell_c$  is the loss factor in the antenna and associated circuit,  $T_c$  is the actual temperature of the antenna circuit and nearby ground, and  $T_o$  is the reference temperature (288°K).

Similarly, the transmission line loss factor,  $\ell_t$ , and temperature,  $T_t$ , will determine a noise factor,  $f_t$ , for the transmission line given by

$$f_t = 1 + \frac{T_t}{T_o} (\ell_t - 1). \quad (7)$$

Using a receiver noise factor of  $f_r$ , and assuming the receiver is free of spurious responses, we can use Friis' method of combining noise figures in cascade to obtain a system noise factor,  $f$ , including external noise,  $f_a$ , which is

$$f = f_a + (\ell_c - 1) \frac{T_c}{T_o} + \ell_c (\ell_t - 1) \frac{T_t}{T_o} + \ell_c \ell_t (f_r - 1). \quad (8)$$

If all temperatures are equal to  $T_o$ , equation (8) becomes

$$f = f_a - 1 + f_c f_t f_r. \quad (9)$$

The rms of the noise envelope voltage was used for all power measurements taken for this report. Calibration techniques allow this rms measurement to be referred to the terminals of an equivalent loss-

less antenna and given in terms of  $F_a$  in decibels. With the exception of the few measurements made using a half wave dipole in a corner reflector, all values of  $F_a$  were obtained using a short vertical antenna.

For an envelope having a deterministic waveform, a definite relationship between the rms voltage, the mean voltage, and other average values (such as the antilog of the mean logarithm, ALML, of the envelope voltage) can be found. A simple case would be a sine wave modulation, and a trivial case would be a constant CW signal. In the case of a random waveform such as that resulting from broadband impulsive noise, no definitive relationship exists. The ratios of the rms to the mean and ALML of the noise envelope voltage vary as the impulsive character of the noise varies with time, location, and frequency. A knowledge of these ratios provide useful information on the impulsive character of the received noise. For example, the ratio of the rms to the mean for white Gaussian noise is approximately 1 dB, while the ratio of the rms to the ALML is approximately 2.5 dB. As the noise becomes more impulsive in nature, these ratios will increase. Thus, if these ratios are known, or can be predicted, some information can be inferred on the distribution of the instantaneous envelope voltages (APD). Since the APD is required information for determining the expected performance of telecommunications systems, estimates of the expected values of these two ratios are useful. The ratio of the rms to the mean voltage is the voltage deviation ( $V_d$  in decibels). The ratio of the rms to the antilog-mean logarithm of the envelope voltage is the log deviation ( $L_d$  in decibels). For detailed definitions, see Crichlow, et al. (1960).

A direct relationship between the predicted moments ( $F_a$ ,  $V_d$ , and  $L_d$ ) and the most likely or expected APD is not presently available for man-made noise in a form such as that given for atmospheric radio noise by Crichlow et al. (1960) and later adopted in a simplified form

by CCIR (1964). A given APD will define a unique set of moments. The converse is not true, however, as a given set of the three moments could have resulted from any one of a family of APD's. The man-made noise generally is composed of contributions from a number of sources and will change rapidly in character with time and location as the noise contributions from the various sources change in relative amplitude. On the average, an APD similar to that observed for atmospheric radio noise is found for man-made radio noise. Typical APD's and their variations have been given for urban residential man-made radio noise by Spaulding et al. (1971).

### 3. ESTIMATION METHODS AND THE DATA BASE

Estimates of future man-made radio noise levels and other characteristics of the noise process can be of two forms. One is based directly on past measurements, and the other depends on the correlation of the noise with some predictable parameter of the environment for use as a "predictor" of the future noise. The first form, based on past measurements of the behavior of the noise at "typical" locations, assumes that the behavior patterns noted will continue into the future. The direct analysis of the available data base will then provide the estimates of the future man-made radio noise conditions that will exist at other locations. This process has been used to obtain the predictions for three types of locations: business areas, residential areas, and rural areas. The business area is defined here as any area where the predominant usage throughout the area is for any type of business. This includes stores and offices, industrial parks, large shopping centers, main streets or highways lined with various business enterprises, etc. The residential area is defined here as any area used predominantly for single or multiple family dwellings with a density of at least two

single family units per acre and no large or busy highways. An occasional isolated business such as a drugstore or filling station can be included, but a city block or more of concentrated business enterprises should be considered a business area. This definition applies to both urban and suburban residential areas. Rural areas are defined here as locations where land usage is primarily for agricultural or similar pursuits, and dwellings are no more than one every five acres.

In attempting to group the measurements in the data base into these classifications, some areas were found unsuitable for inclusion in any of the three groups. Some notable examples of these areas are interstate highways outside of the main towns or cities and fairly large parks and university campuses within cities. The available data for these three types of areas were not included in the general analysis but were analyzed separately to give an indication of what might be expected at such locations. In using the predictions, personal judgment will have to be used in selecting the "typical" area classification to be employed for any specific estimate.

The data base used in this report consists of some 300 hrs of  $F_a$ ,  $V_d$ , and  $L_d$  data collected for each parameter simultaneously on eight frequencies over the period from 1966 through 1971. The measurements were made in six states--Colorado, Maryland, Texas, Virginia, Washington, Wyoming--and in Washington, D.C. The measurements were made in 103 areas; the area size ranging from a few square blocks in a business area to several square miles in some of the rural locations; the criteria usually being that the type of area remain the same for any one set of measurements or a measurement run. The period of measurement for each mobile run varied from approximately 15 min to over an hour. A few stationary measurements were made for a period of 24 hrs or longer. For many of the mobile runs in the business

and residential areas, average vehicle density information was obtained from past vehicle counts made by the local traffic engineering groups for the highways included in the area of the run. During one period, actual traffic counts were obtained during the measurement period.

The measurements used in the analysis for business areas were recorded at 23 areas in Boulder, Colorado Springs, and Denver, Colorado; San Antonio, Texas; Cheyenne, Wyoming; and Washington, D.C. The residential area data consist of measurements made at 38 areas in the cities and suburbs of Boulder, Colorado Springs, and Denver, Colorado; San Antonio, Texas; and Cheyenne, Wyoming. The data used for rural areas were recorded in 31 rural areas in Colorado, Maryland, Virginia, Washington, and Wyoming. Continuous runs were made for 24 hrs on the grounds of the Department of Commerce Boulder Laboratories. Two locations were used for these runs, one near the main radio building and the other near Broadway (the main highway passing in front of the Laboratory grounds). Additional data are in the ITS man-made radio noise data base, but they were not used for the present purpose because of the incomplete frequency coverage of those measurements or because of the specialized nature of the individual measurements.

To insure the complete compatibility of all data used to provide the estimates in this report, only data recorded using the OT/ITS equipment in the mobile radio noise laboratory were considered. A description of this equipment and the mobile noise laboratory is given in Appendix A. With the exception of the 24-hr runs on the Boulder Laboratory grounds, all measurements were made during the daytime hours, generally in the pre-noon period when atmospheric radio noise was at a low enough level so that man-made radio noise was the predominant factor at all frequencies. At times, the atmospheric radio noise dominated the readings at the lower frequencies in rural areas, but

these periods were edited out of the data as well as possible before the analysis was performed.

In some instances, again principally in rural locations, some limitation at 250 MHz was experienced due to the recording system noise factor (Appendix A, fig. A4).

Most of the data were recorded using short vertical monopole antennas essentially at ground level. No attempt has been made here to provide information on the effect of antenna height or direction of arrival of the man-made radio noise. Measurements during a short run using two dipole antennas in corner reflectors at 250 MHz simultaneously with one antenna in a vertical and the other in a horizontal configuration provide some information on the effect of polarization of the received man-made radio noise.

The second type of estimation involves the correlation of the received noise with various aspects of the environment which can be used as "predictors." There are three requirements for a predictor if it is to be of value in determining expected future interference levels. First, of course, the noise must correlate well with the statistics of the predictor. The second requirement is that statistical information concerning the predictor must be readily available, and third, an estimate of the future pattern of behavior of the predictor must be available. If these three requirements are met, then an estimate of the pattern of behavior of the predictor in the future will provide an estimate or prediction of man-made radio noise interference for the same future period. A number of possible predictors have been investigated, including obvious ones such as population density, electrical power consumption, and traffic density. The most successful predictor found to date in the frequency range above about 20 MHz is traffic density (Spaulding, 1971; Spaulding et al., 1971), and a method of estimating noise levels from automotive ignition systems near main highways is given in Appendix

B. This, combined with traffic engineering estimates of future highway usage, may provide the best estimate of future radio noise levels at many locations.

Relatively good correlation was found between power consumption in an area and the radio noise power below 20 MHz. Unfortunately, in most areas, statistics on power consumption are very difficult, if not impossible, to obtain. Statistics on population density are readily available for small areas (called a standard location area or SLA for the 1960 census) from the Census Bureau. Population density in a SLA, however, shows very poor correlation with the noise level measured in the SLA (Spaulding et al., 1971).

#### 4. MAN-MADE RADIO NOISE ESTIMATES

##### 4.1 Available Noise Power, $F_a$

In determining the expected man-made radio noise power and its variation for any given location from measurements made at other locations, several factors must be taken into consideration. The main factor, of course, is the similarity between the areas where the measurements were made and the area in question. For any particular location the noise level may be due to particular sources, such as factories in which a large number of arc welders are employed, power lines, etc. The estimates given here are in terms of business, residential, and rural areas, and a physical examination of the area in question should determine which of these types of areas will most closely correspond to the selected area. In addition to these three basic types of areas, estimates are also given for interstate highways and parks and university campuses. Estimates for power lines are also given.

#### 4.1.1 Estimates of $F_a$ for Typical Areas

Using all accumulated data in the data base, the areas where measurements were made were divided into the business, residential, and rural classifications. These divisions were chosen because they can be easily defined and recognized. All data used in this report were measured at ground level. The man-made noise may be quite different at some elevations above ground level or in areas that cannot be logically placed in one of the three classes of areas chosen due to peculiar local conditions. Since the data given are intended for estimating the noise conditions at average locations, data containing these strictly local, unusual effects have not been used.

After the division of the data into the various classes, each set of data was analyzed using the recorded values of  $F_a$ . Using the individual median values of the sets of mobile runs (see Appendix A) for each type of area, a linear regression line was found by a least squares fit for  $F_a$ , in decibels versus the logarithm of the frequency, for each area. The three regression lines were quite close in slope, showing less than 2 dB per decade of frequency difference. The data for all cases and all frequencies were then combined to find the slope giving the best fit to all the data. A standard statistical test for significance in the differences of the various slopes (one for each of the three types of areas and one for all data) showed that the slopes could all be considered equal to -27.7 dB per decade at the 95 percent confidence level. Linear regression, with the slope constrained to this value, was then used to obtain figure 1. Figure 1 provides an estimate of the median radio noise power spectral density that will be found at that type of location as a function of frequency.

At 250 MHz, at rural locations especially, the system noise figure (Appendix A) was close to the available external radio noise. Since a value related to system noise is recorded (by taking a meter reading



of  $F_a$  with the input connected to a dummy antenna in place of the recording antenna) at the time of calibration, a means of approximately determining the system noise factor for any run is available. When the system noise factor and the recorded values were close to the same level, the values were discarded or corrected to remove the effect of system noise on the value of  $F_a$ . If the recorded value was within 0.5 dB of system noise, the recorded values were discarded. If the recorded value was more than 0.5 dB but less than 6 dB above system noise, the reading was corrected by converting the reading from a decibel value to a power value, subtracting the system noise power and converting the difference back to a value of  $F_a$ . Because of this loss of the lowest values at 250 MHz, there is still an unresolved question of whether the - 27.7 dB/decade rate of change of  $F_a$  with frequency is valid to 250 MHz, since all 250 MHz measured medians (and in some cases, the lower decile values) are above the estimated median value line.

In addition to the expected values of man-made radio noise at business, residential, and rural areas, a value for quiet rural areas from CCIR (1964) is also shown on figure 1. These values were obtained from measurements at rural locations chosen with great care to insure low levels of man-made radio noise and probably represent a lower limit of levels to be found. Galactic noise levels are also shown on figure 1 for frequencies above 10 MHz. The level of the galactic noise will vary greatly between 10 and approximately 30 MHz, depending upon the behavior of the ionosphere. Above these frequencies, though, the levels will remain quite constant (Crichlow et al., 1955).

Since the figure 1 estimates for business, residential, and rural locations represent the average values of all similar locations, the variation about the average must be determined next. This variation from location to location in similar areas is indicated by the standard

Table 1. Expected Variation of Median Values about Estimates for Business, Residential, and Rural Locations.

Frequency in MHz	Standard Deviation, $\sigma$ , in dB		
	Business	Residential	Rural
0.25	6.12	3.54	3.89
0.5	8.21	4.28	4.40
1.0	2.33	2.52	7.13
2.5	9.14	8.06	8.02
5.0	6.08	5.54	7.74
10.0	4.15	2.91	4.03
20.0	4.93	4.65	4.53
48.0	7.13	3.98	3.23
102.0	8.76	2.73	3.82
250.0	3.77	2.87	2.26
$\sigma_T^*$	7.00	5.00	6.45

\*  $\sigma_T$  = Standard deviation of all measured medians about regression line of figure 1.

deviation,  $\sigma_T$ , given in table 1. The value of  $\sigma_T$  is given for each of the three types of areas and is the value obtained by using the data at all frequencies to obtain the standard deviations about the regression line shown for each type of location.

Table 1 also gives the standard deviation,  $\sigma$ , at each of the measurement frequencies. A better estimate of the variation of the median values for these typical areas at any given frequency might possibly be obtained by interpolation of the  $\sigma$ 's for the measurement frequencies rather than using  $\sigma_T$ .

An example of the location variation for a given frequency and area type is shown on figure 2. Shown on figure 2 is the cumulative distribution of the median values obtained from residential areas at 20 MHz. Also shown is the estimate for a residential area at 20 MHz from figure 1 and this estimate plus and minus  $\sigma$  and  $\sigma_T$  (from Table 1).

Once the best estimate of the median value of  $F_a$  for a given location has been found, the next point to consider is the variation of  $F_a$  at that location with time. A number of time periods are of concern in determining the temporal variation to be expected. The first is the expected variation within a period up to one hour. In the noise measurement method used, 10-sec samplings of the running average of  $F_a$  were recorded where the time constant for the power moment,  $F_a$ , was approximately 50 sec. Thus, 360 sample values were obtained for each hour of recording time. Again, using a 20 MHz residential area run, as an example, figure 3 shows a typical cumulative distribution of the individual  $F_a$  values measured within an hour at a location. These values were measured May 4, 1967, between 0839 and 0939 local standard time in Boulder, Colorado. Also shown on figure 3 are the upper and lower decile values.

Table 2 and figure 4 show the estimates of the ratios, in decibels, of the upper decile value to the median,  $D_u$ , and of the median to the lower decile,  $D_l$ . These values can be used to estimate the variation of  $F_a$  about the estimated median (from fig. 1) for periods from several minutes up to one hour.

The data were analyzed to obtain the median value of  $F_a$  for each measurement location and also the ratio in decibels of the upper and lower decile values to the median. Figure 5 shows the results of this analysis for all measurement locations considered business areas, giving the mean value of the business area location medians and the 27.7 dB per decade regression line (from fig. 1) along with the expected variation within an hour. The root-mean-square of all the business locations  $D_u$ 's and  $D_l$ 's for each frequency is given on figure 5 to show the expected variation within an hour. The same information is given on figure 6 for residential areas, figure 7 for rural areas, figure 8 for interstate highways, and figure 9 for parks and university campuses.

Table 2. Expected Variation, Man-Made Radio Noise Levels, about the Median Value for a Location, within the Hour.

Frequency MHz	Business Area		Residential Area		Rural Area	
	D <sub>u</sub> (dB)	D <sub>l</sub> (dB)	D <sub>u</sub> (dB)	D <sub>l</sub> (dB)	D <sub>u</sub> (dB)	D <sub>l</sub> (dB)
0.25	8.1	6.1	9.3	5.0	10.6	2.8
0.5	12.6	8.0	12.3	4.9	12.5	4.0
1.0	9.8	4.0	10.0	4.4	9.2	6.6
2.5	11.9	9.5	10.1	6.2	10.1	5.1
5	11.0	6.2	10.0	5.7	5.9	7.5
10	10.9	4.2	8.4	5.0	9.0	4.0
20	10.5	7.6	10.6	6.5	7.8	5.5
48	13.1	8.1	12.3	7.1	5.3	1.8
102	11.9	5.7	12.5	4.8	10.5	3.1
250	6.7	3.2	6.9	1.8	3.5	0.8

The next longer time period of interest is the diurnal variation that can be expected. Since the measurements of man-made radio noise consisted of values at MF and HF as well as the higher frequencies, most of the measurements (all the measurements discussed to this point) were taken between about 0830 and 1500 LST. During this period, atmospheric radio noise is at its lowest level and is least likely to affect the readings. The predictions so far presented can, therefore, be considered the values of man-made radio noise for the hours of daylight. Several 24-hour continuous runs have been made on the grounds of the Department of Commerce, Boulder Laboratories. Some of these runs were made at the end of wing 1 near the parking areas. The hourly median values of  $F_a$  recorded on April 27-28, 1971, are shown on figure 10. This particular run was started at 0930, LST on April 27 and ended at 0900 LST on April 28. Several items are noteworthy on

this figure. First are the relatively high levels caused by atmospheric radio noise between 1800 on April 27 to 0700 on April 28 on the three lower frequencies, and to a lesser degree, present in the 20 MHz values. A peak is observed between 1600 and 1700 on the 2.5 and 5 MHz, but not on the 250 kHz. This would indicate two things. The levels throughout the day on 250 kHz probably are determined by the atmospheric radio noise rather than man-made. The peak on 2.5 and 5 MHz probably is a true man-made radio noise level and was associated with power lines since it was not nearly as predominant (though noticeable) on the four higher frequencies. The low, rather steady levels on 102 MHz at 8 to 10 dB probably were caused by a combination of set noise and galactic noise. Set noise was measured at 7.4 dB, and the expected galactic noise would be  $6 \pm 2$  dB. Combining these two values would give an expected level of  $9.8 \pm 1$  dB. The balance of the values shown on figure 10 probably are all predominantly man-made radio noise. The data shown on figure 10 for 0.25, 10, and 48 MHz are also shown on figure 11 and compared with the data recorded on April 19 and 20, 1967, and on May 11 and 12, 1971. Most of the noise recorded on 250 kHz was atmospheric in origin though the lower values recorded on April 29 and 30, 1967, were from man-made noise. Perhaps the most interesting feature of this figure is the high spike on May 12, 1971, at 48 MHz and the corresponding high reading on 20 MHz. This particular run was started at 1055 LST, but daylight saving time was in effect, and the clock time was 1155 MDST. Since only 5 min of recordings were used to obtain this value, the median was greatly influenced by the heavy traffic density of employees' leaving for lunch. The hourly medians on frequencies of 20 MHz and above are generally influenced by beginning of work, lunch hour, and end of work times, though the effect is somewhat hidden when the median value for the whole hour is considered. The May 12 recording suggests that a 5-min median could

be expected to increase by some 15 dB near a parking lot during a peak traffic period. The expected galactic noise level is shown for 20 and 48 MHz. The lowest levels on both of these frequencies were greatly influenced by this type of noise. While it appears that the 1967 data are generally lower than the 1971 data, no significant yearly trends can be established on this basis. It is interesting to note that the day-to-day variation shown here is considerably less than that predicted within the hour as indicated by the decile values for business areas, figure 5, and residential areas, figure 6.

A continuous three-day run was made with the mobile radio noise laboratory parked on the DOC Boulder Laboratories grounds near Broadway (a main highway on the east side of the Laboratories). The diurnal variation of the noise measured at this location is shown on figure 12. The days shown are Wednesday afternoon, October 25, 1967, through Saturday morning, October 28, 1967. The levels recorded are greatly influenced by traffic patterns at this location, as is discussed in greater detail in Appendix B. The repeatability of the diurnal variation from such a location can be seen from figure 12. The 24-hr pattern shows little variation on the three work days--Wednesday, Thursday, and Friday. It is especially interesting to note the same pattern is repeated on Saturday after 0800, but that the "morning rush hour noise," between 0600 and 0800, is not present on Saturday, a nonworkday for most. Comparing figures 11 and 12, quite good agreement is found for the measurements between 0100 and 0400 when traffic on Broadway is at the lowest. For the rest of the day, the noise near the highway is 5 to 10 dB higher than the noise at the end of wing 1, which is several hundred feet from the highway.

For certain areas where activities are seasonal (resort areas, industrial areas where the work is seasonal such as canneries, etc.),

an estimate of the seasonal variation of the man-made radio noise levels may be required. In some areas this variation can be estimated on the basis of a change in the type of area. The area may be considered a business area if the increased activity causes an increase in the business or industrial activity during a given season and essentially a residential or rural area during the balance of the year. Since this seasonal variation is so dependent on actual location usage, no general estimates of seasonal variation can be given.

The longest time period of interest is the change of noise levels from year to year. Here again, growth in a given area may change the general nature so that the area may go from rural to residential or residential to business (or in a few cases, the reverse) in a period of one year or more. Therefore, long-range estimates can to some extent be predicated on growth potentials in the area. Trends in the increase in electric power consumption and the number of registered automobiles (both possible predictors of man-made noise) are given for the United States as a whole in JTAC (1968). This type of information indicates that the total man-made interference is increasing in the United States but does not provide data helpful in estimating the noise environment at a given location. In a well established business area where streets are already crowded with vehicles, the annual change will be very small. For example, measurements were made by ITS in downtown Washington, D.C., in 1960 and repeated in 1966. The comparison of the two sets of recordings showed that the change in man-made radio noise was negligible over the 6-yr period. The level at a given location in the area varied by as much as 8 dB between the two sets of measurements, but the median value for the area increased by less than 2 dB in the 6-yr period. Since variations of these magnitudes are found on a day-to-day basis, even in a single area, they cannot be considered significant over the 6-yr period. During this same period,

the number of automobiles registered in and near Washington, D.C., increased considerably as did the population. The measured radio noise was predominantly from power distribution lines at the lower frequencies and from vehicle ignition systems at the higher frequencies. Over the 6-yr period, no major change was made to the power distribution system and only minor changes in types of business and amount of power supplied in the area. It probably is reasonable, therefore, to expect little change in the man-made radio noise levels at the lower frequencies. Improvement in ignition noise suppression techniques used by the manufacturers over this period would explain some of the lack of increase in the measured levels at the higher frequencies. Since the streets were already crowded in 1960, vehicle density in that particular area was not changed to any large extent by the greater number of cars in the larger areas. This does not imply that the man-made radio noise remained constant in surrounding areas. Areas that were rural in 1960 and were developed into residential or business areas by 1966, areas where traffic density showed large increases, and areas that changed in character and/or where power consumption increased drastically probably would have shown an increase in the man-made noise levels.

All of the measurements used in obtaining the above estimates were made using a vertical omnidirectional antenna and, therefore, strictly speaking can be considered only as estimates of the vertical component of the radio noise. Very few data are available on the relationship between the vertically and horizontally polarized components. The information that is available indicates that on the average there probably is very little difference in the rms level of the two components. The AMA (1971) and Doty (1971) show peak voltage measurements on individual automobiles and an array of automobiles using a log periodic



antenna in a horizontal and vertical configuration with the center line of the antenna at a height of 10 ft and measuring over a frequency range from 20 MHz to 1 GHz. These measurements indicate that the vertical component may be higher than the horizontal component between 30 and 36 MHz and between 210 MHz and 1 GHz, and there may be as much as 10 dB difference at certain frequencies. Doty also shows the horizontal component as much as 5 dB higher in the frequency range from 63 to 210 MHz. The spectrum was swept from 20 MHz to 1 GHz in approximately 6 min with the antenna in a horizontal position for one sweep and then in a vertical position for the next.

The results of a small sample of measurements made recently by ITS at 250 MHz using two halfwave dipoles in corner reflectors 10 ft above ground are given in figure 13. Two short runs were made with one antenna in a horizontal and the other in a vertical configuration. The measurements were made simultaneously on the two configurations. During one run, the antennas were separated by a distance of 10 ft, while antenna separation was 50 ft during the other run. The offset of 0.559 dB in the equation for the linear regression line is no doubt due to a slight difference in gain settings in the two channels. Even though a fair amount of spread about the regression line is noted, the best estimate of the difference between the vertical and horizontal components is less than 1 dB. Admittedly, both of these samples are relatively small and, therefore, may or may not be representative of the effects of polarization.

All of the above can be used either in a quantitative or qualitative way to assess the best estimate of the level of the average power of the man-made radio noise for a given location and its variation within various time frames.

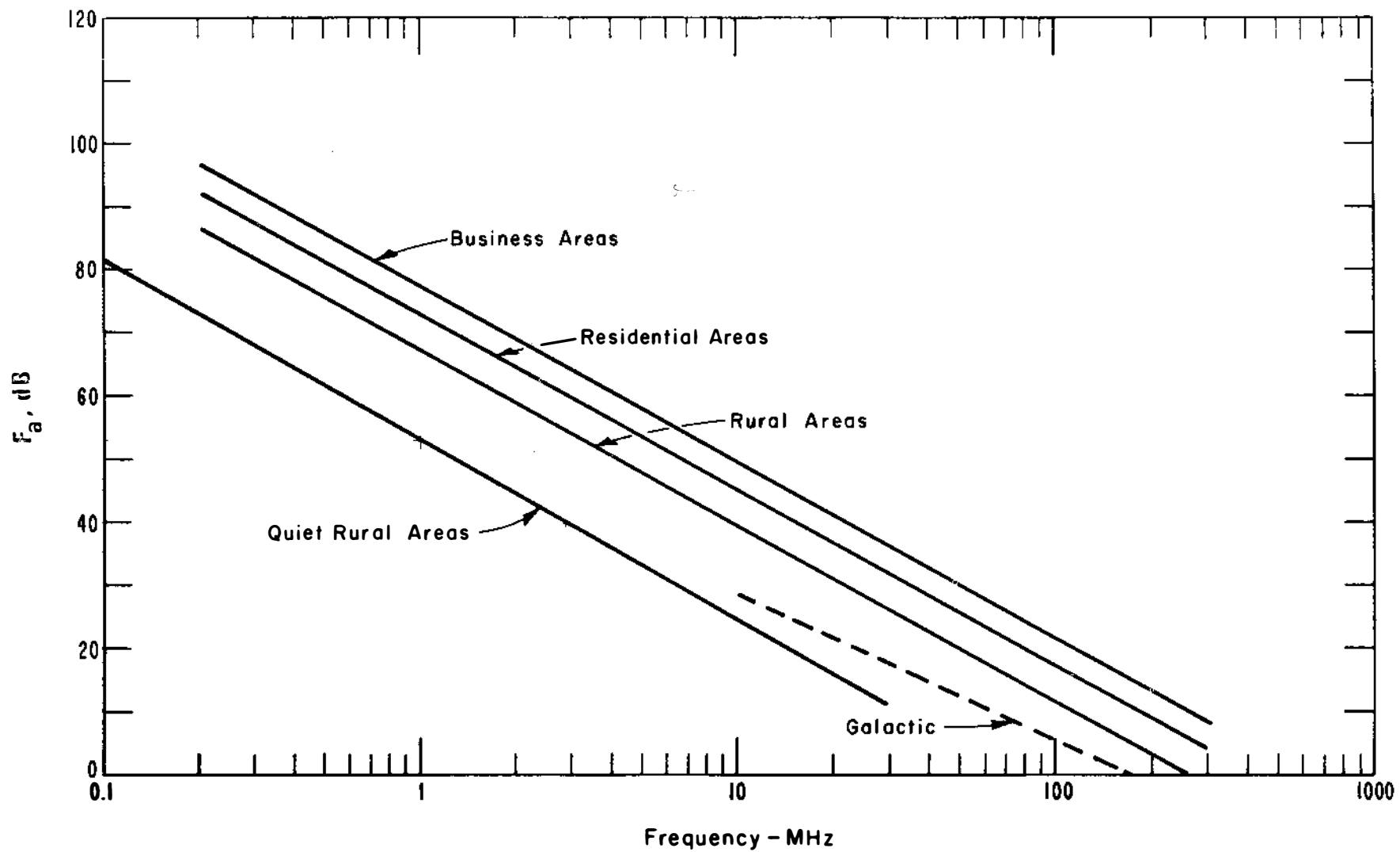


Figure 1. Estimates of median values of man-made noise expected at typical locations.

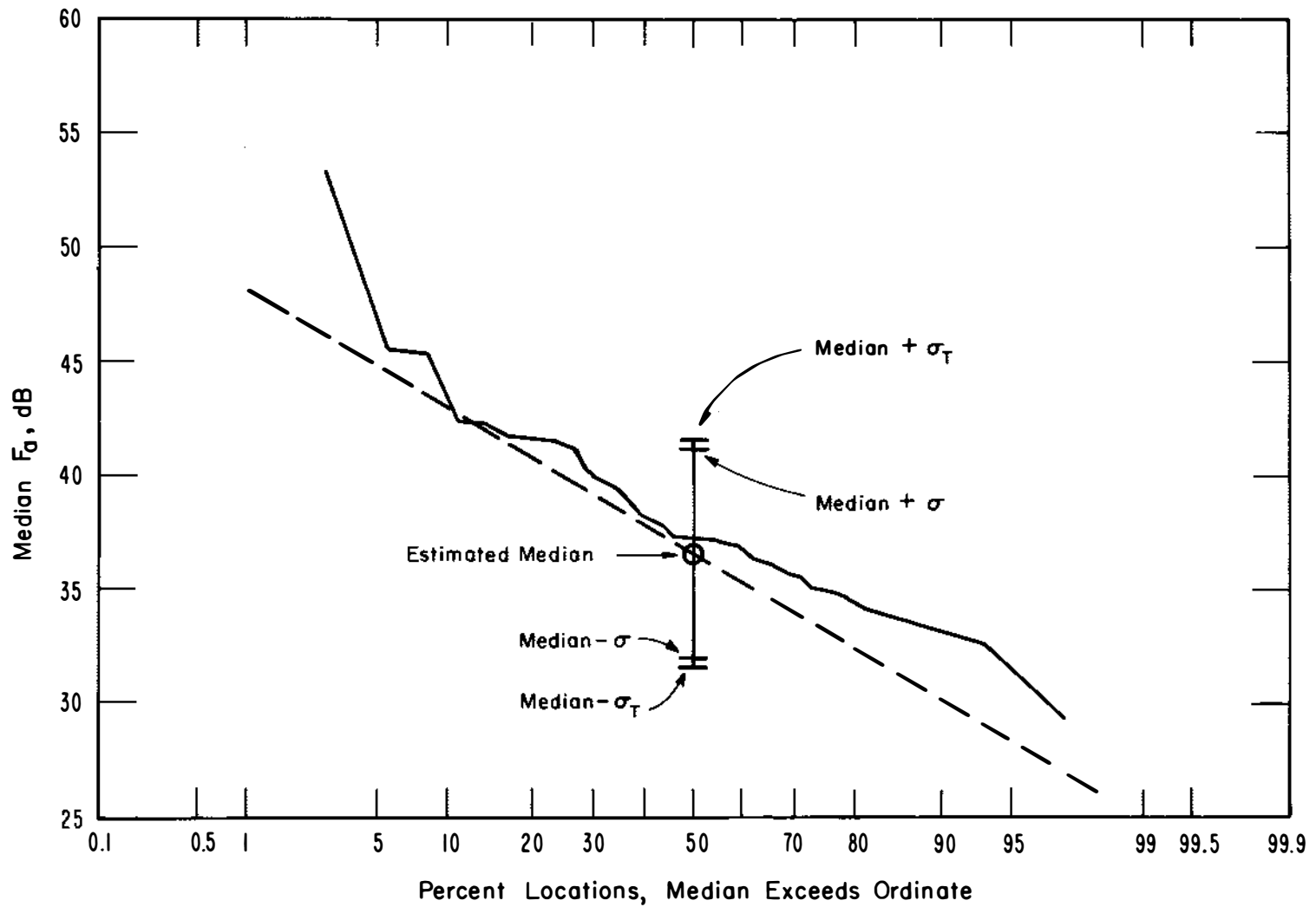


Figure 2. Distribution of location median values of man-made noise, 20 MHz residential area data.

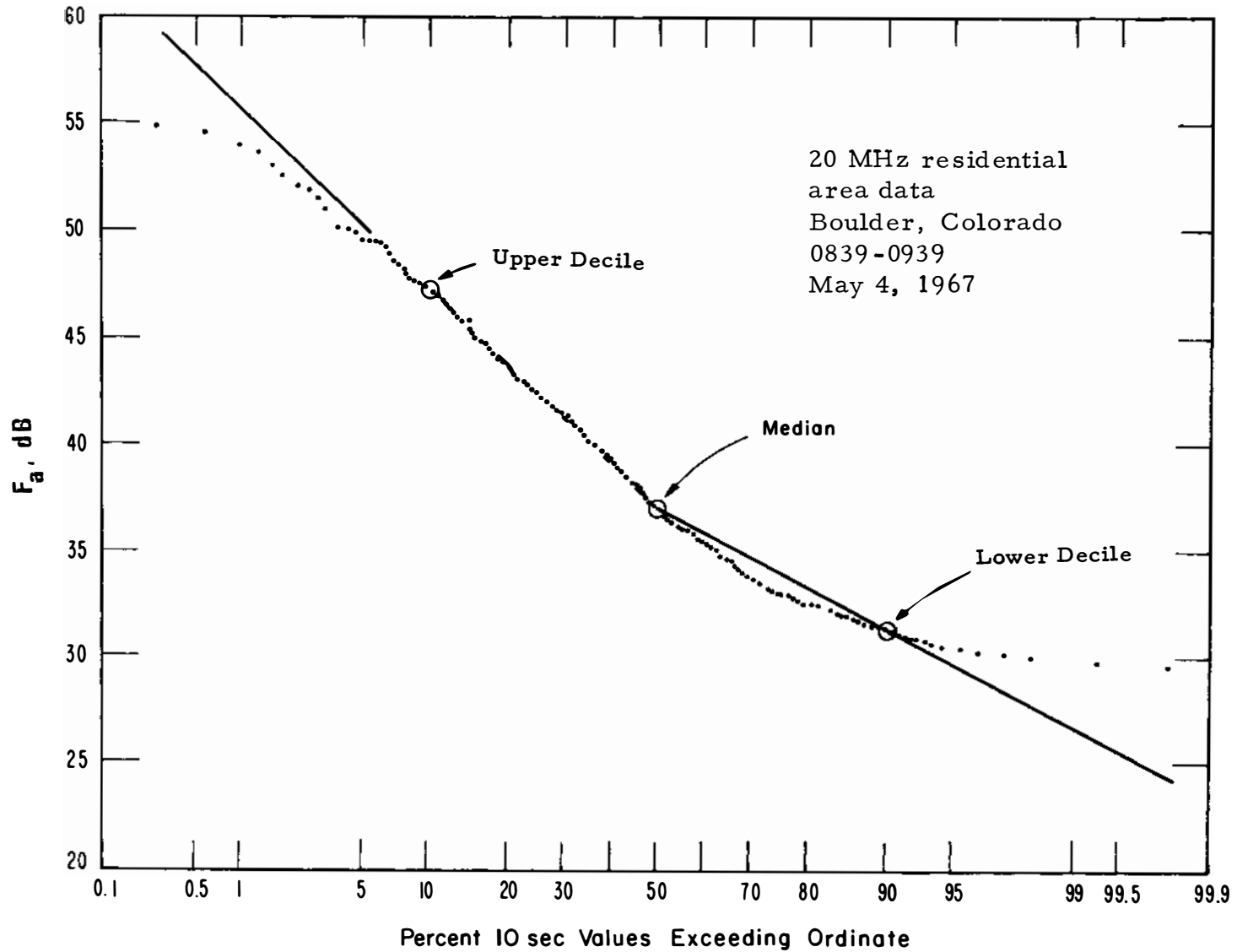


Figure 3. Distribution of  $F_a$  values for a given location.

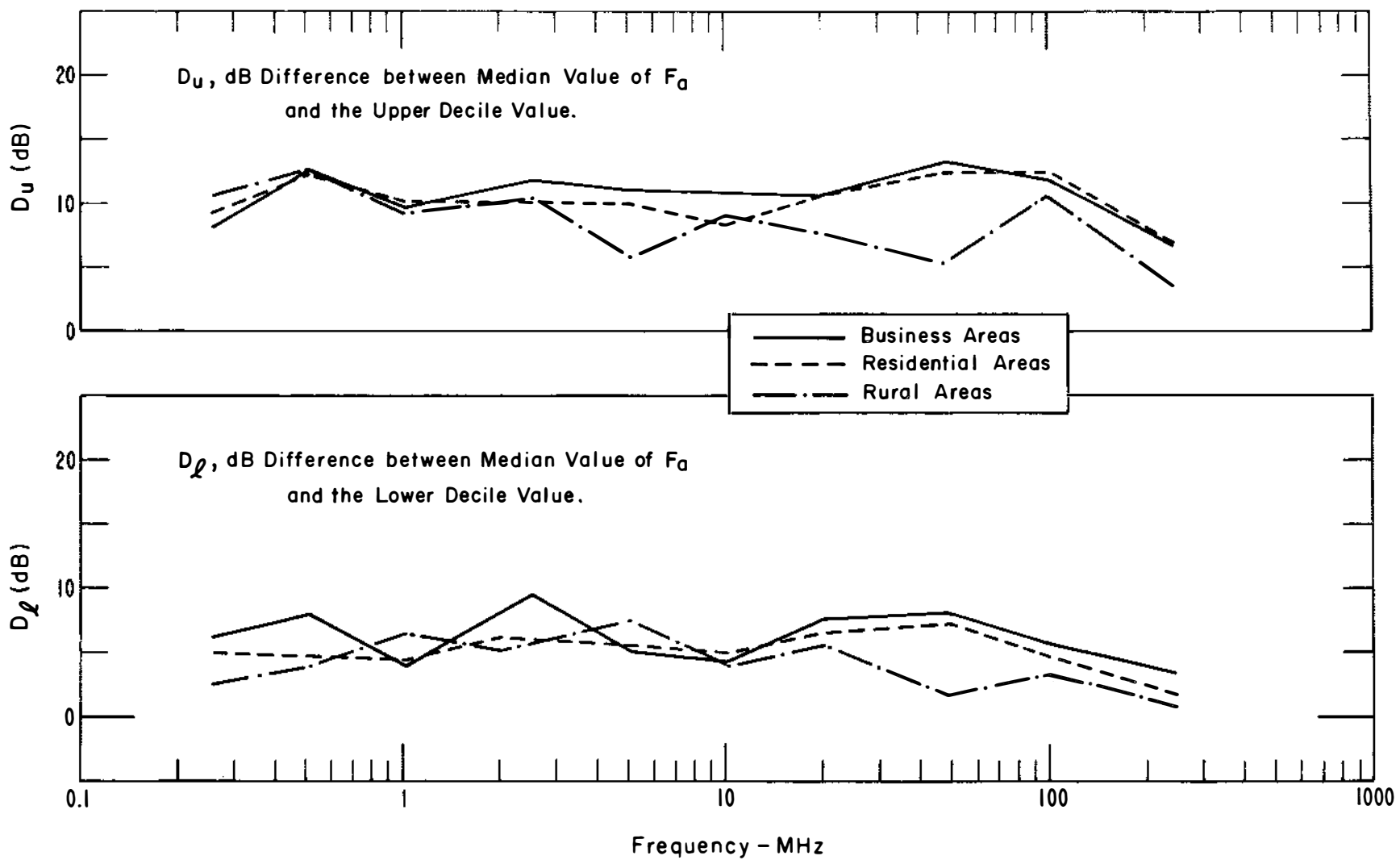


Figure 4. Expected variation of man-made radio noise levels at a location within an hour.

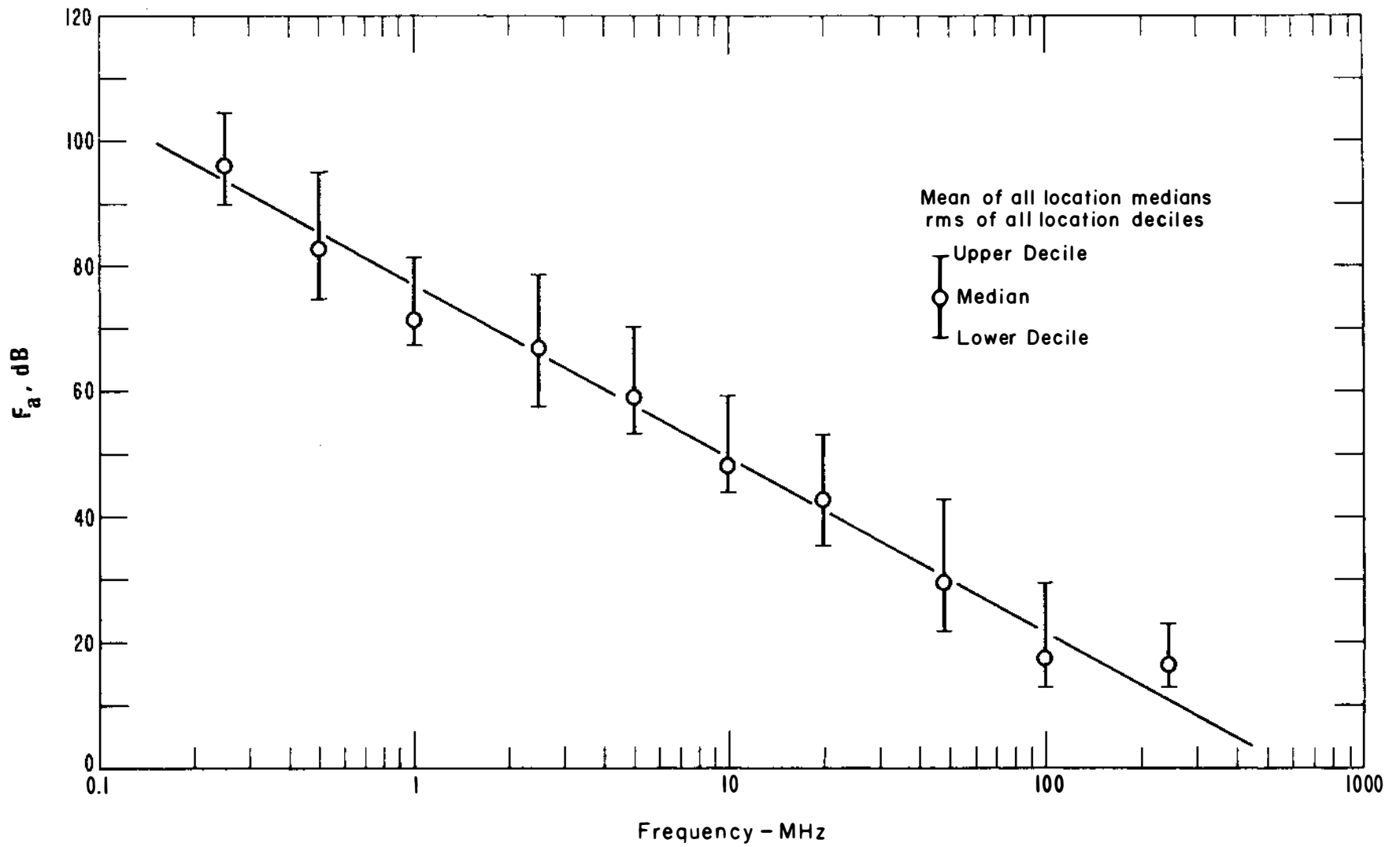


Figure 5. Estimates of man-made noise levels and their variation within an hour for business areas.

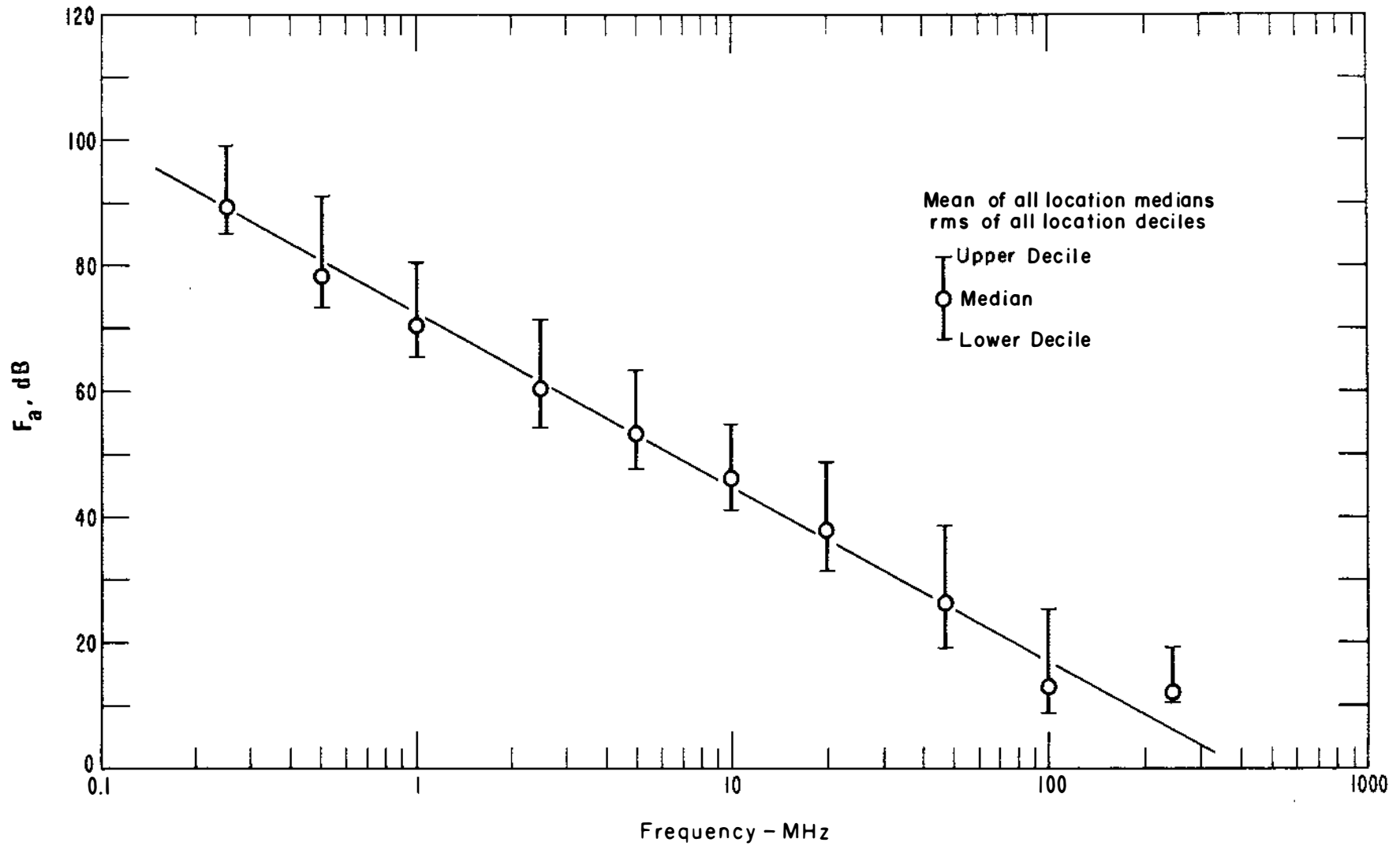


Figure 6. Estimates of man-made noise levels and their variation within an hour for residential areas.

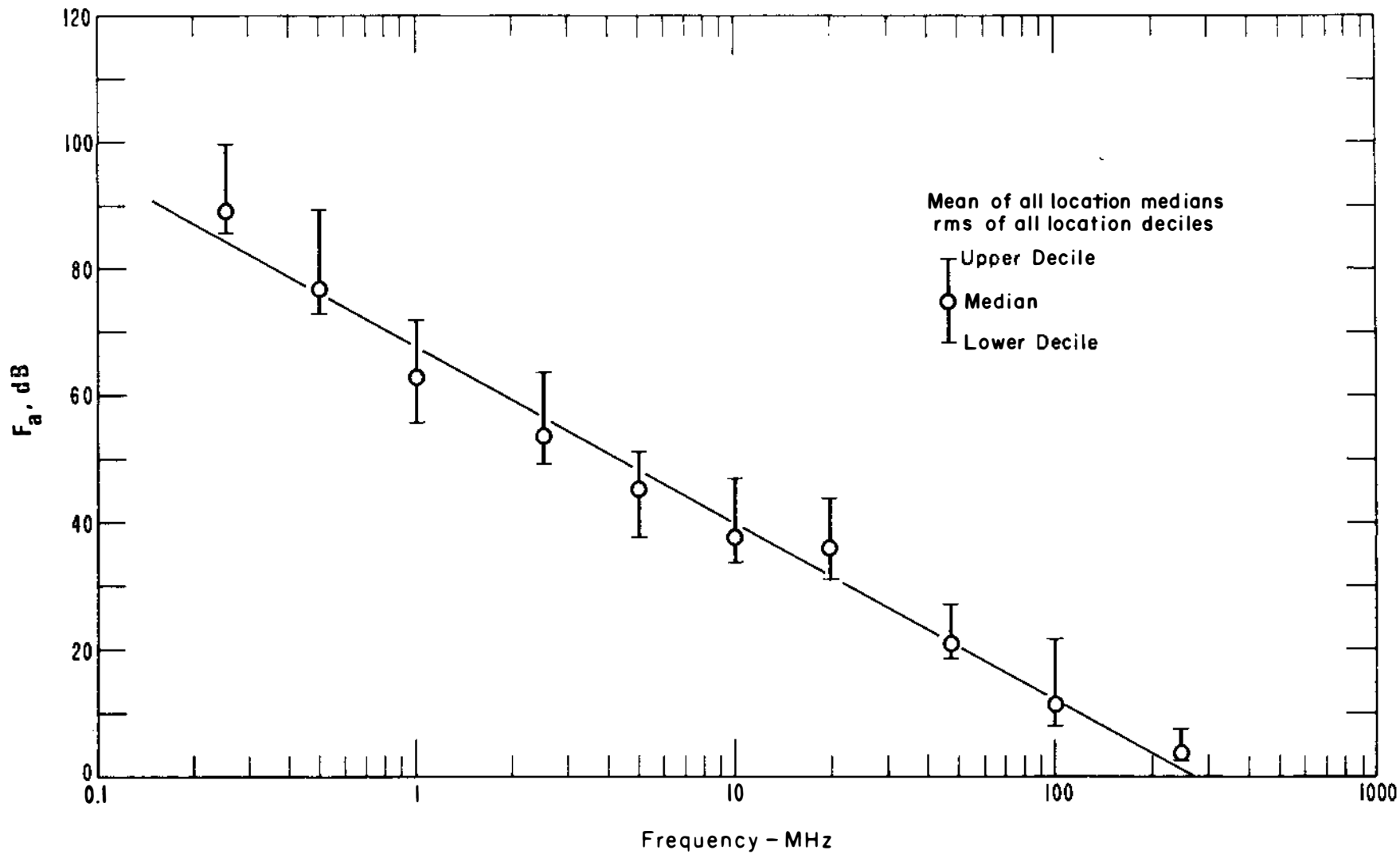


Figure 7. Estimates of man-made noise levels and their variation within an hour for rural areas.



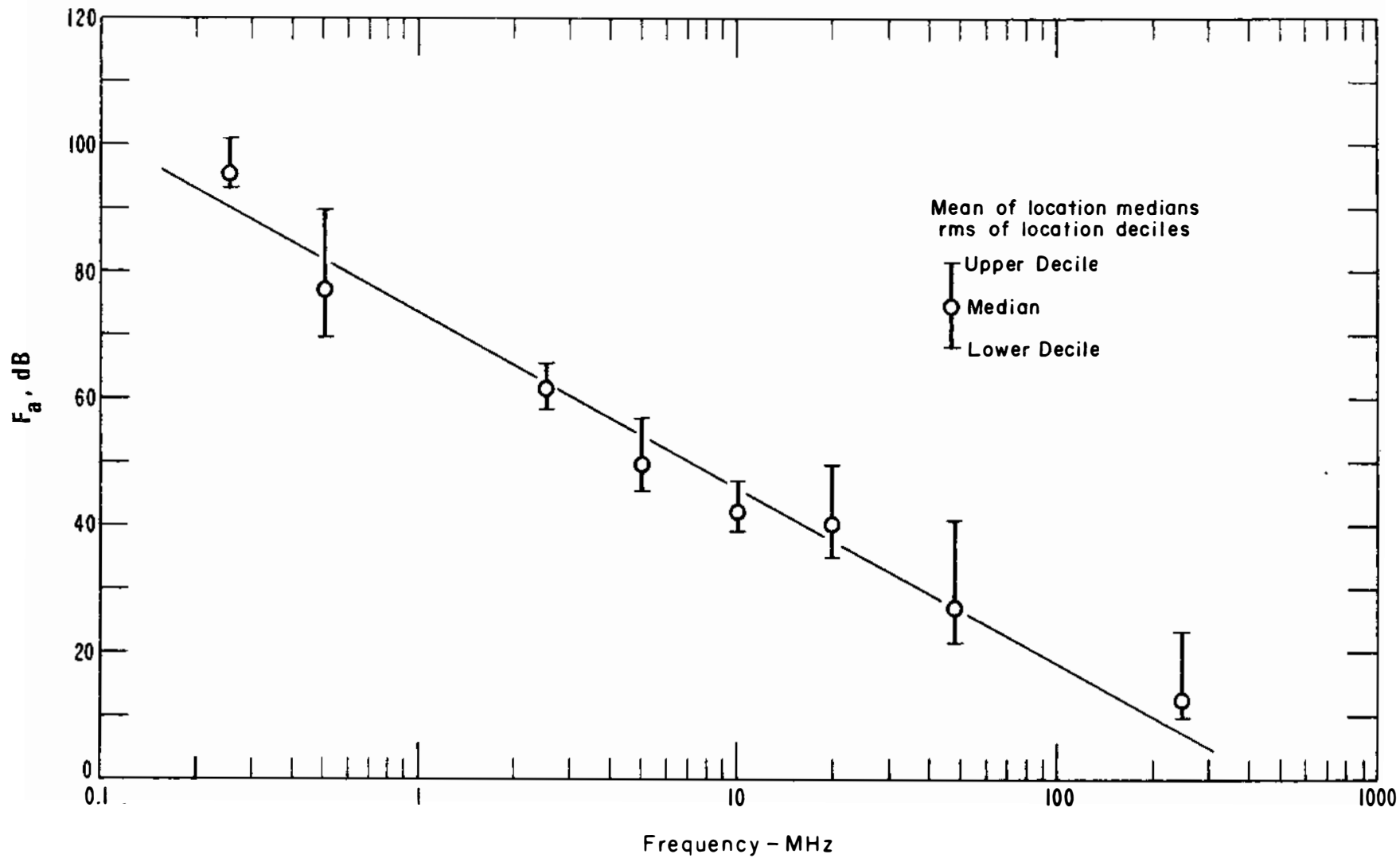


Figure 8. Estimates of man-made noise levels and their variation within an hour for interstate highways.

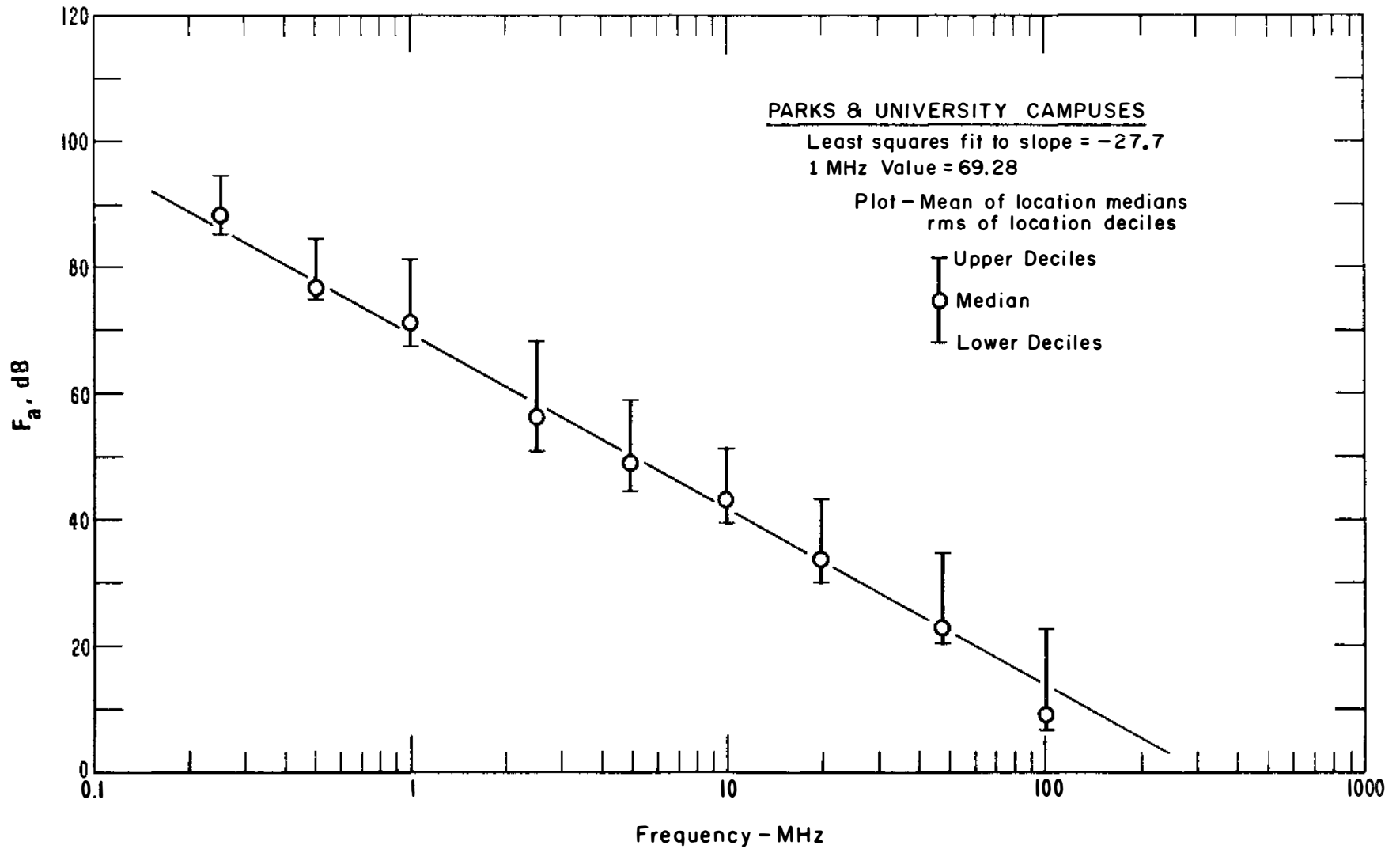


Figure 9. Estimates of man-made noise levels and their variation within an hour for parks and university campuses.

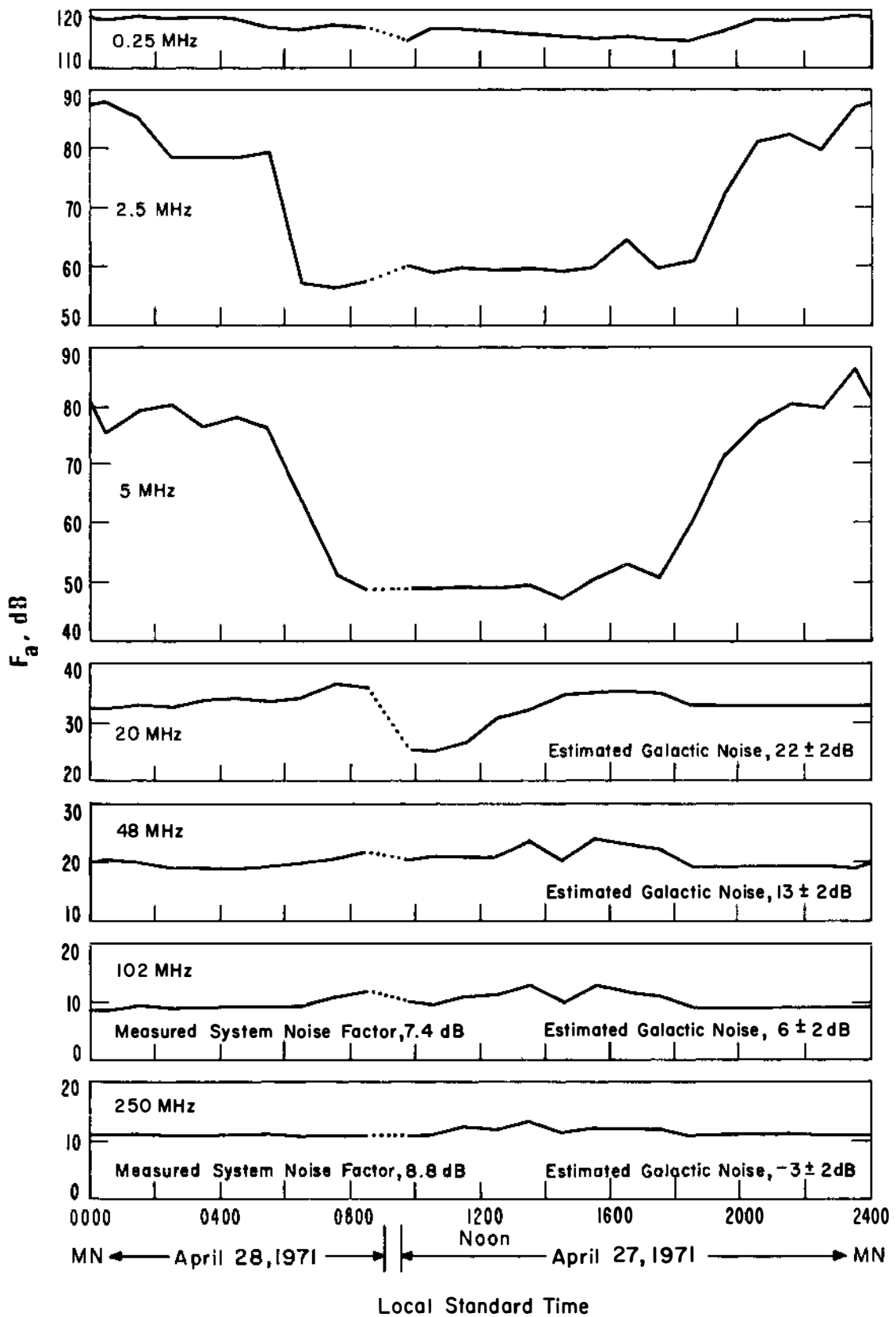


Figure 10. Radio-noise measurements, Dept. of Commerce Boulder Labs, end of Wing 1.

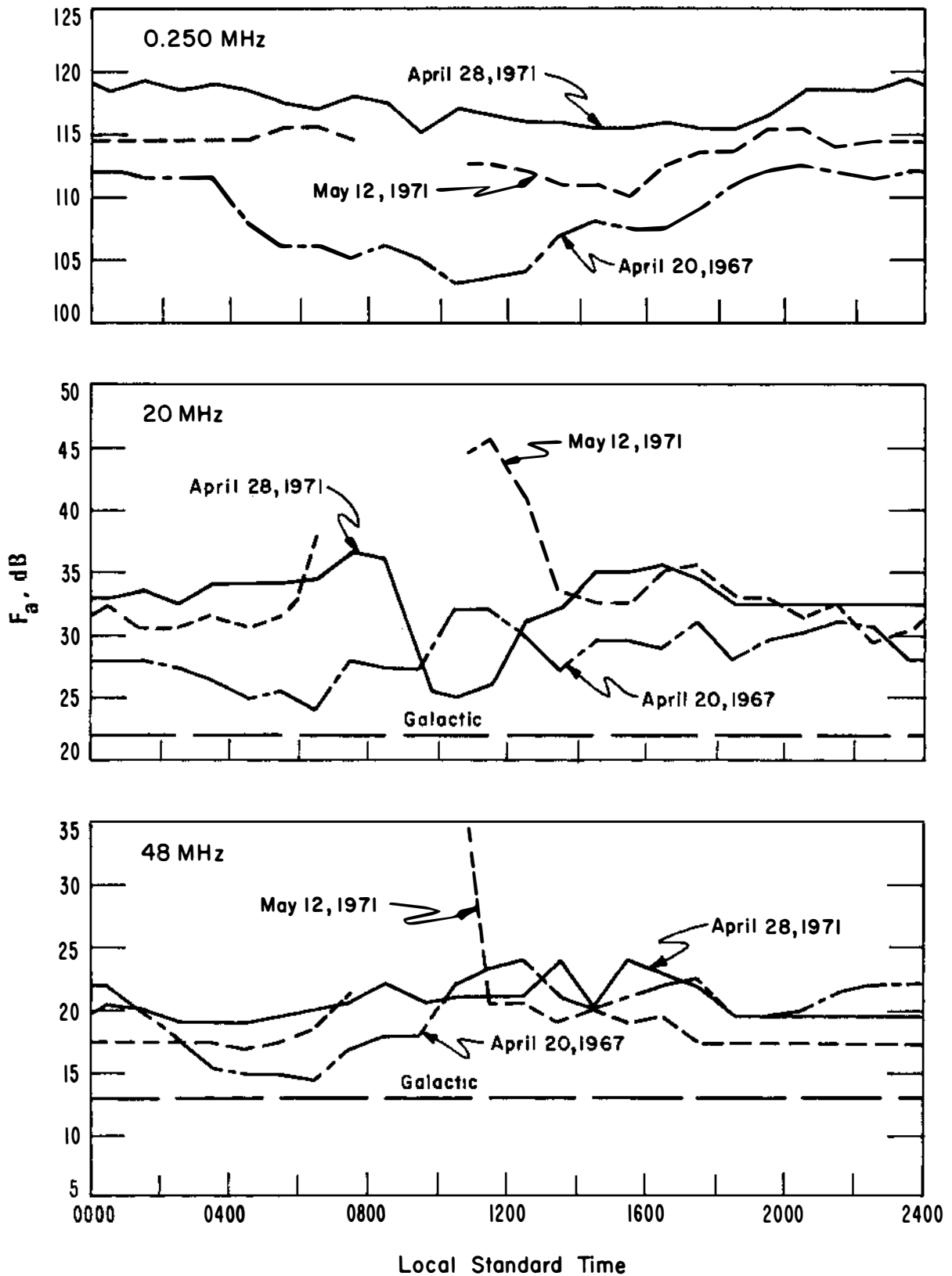


Figure 11. Radio-noise measurements, Dept. of Commerce Boulder Labs, end of Wing 1.

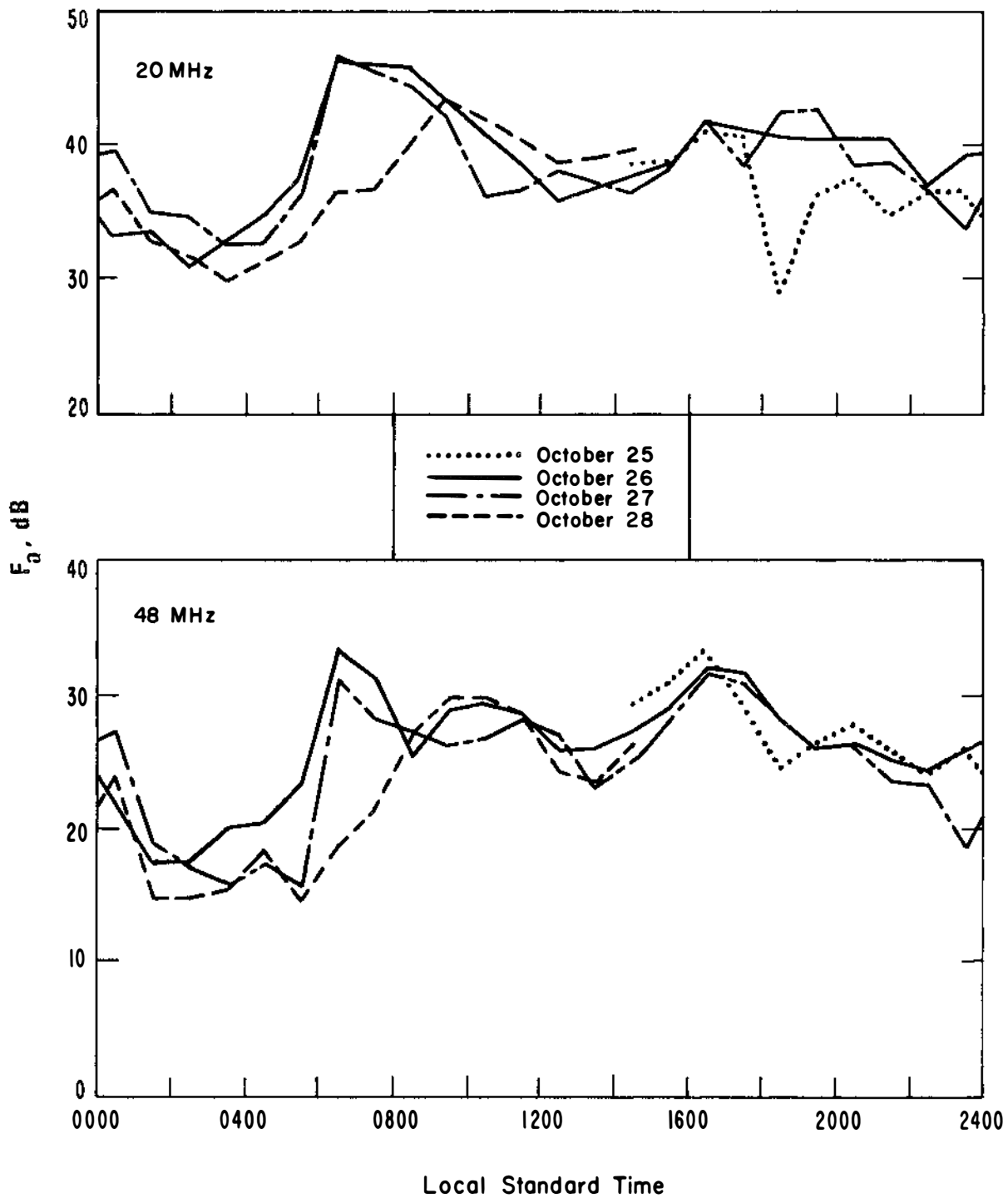


Figure 12. Hourly median values of radio noise, measured near highway in front of Dept. of Commerce Boulder Labs., October 25-28, 1967.

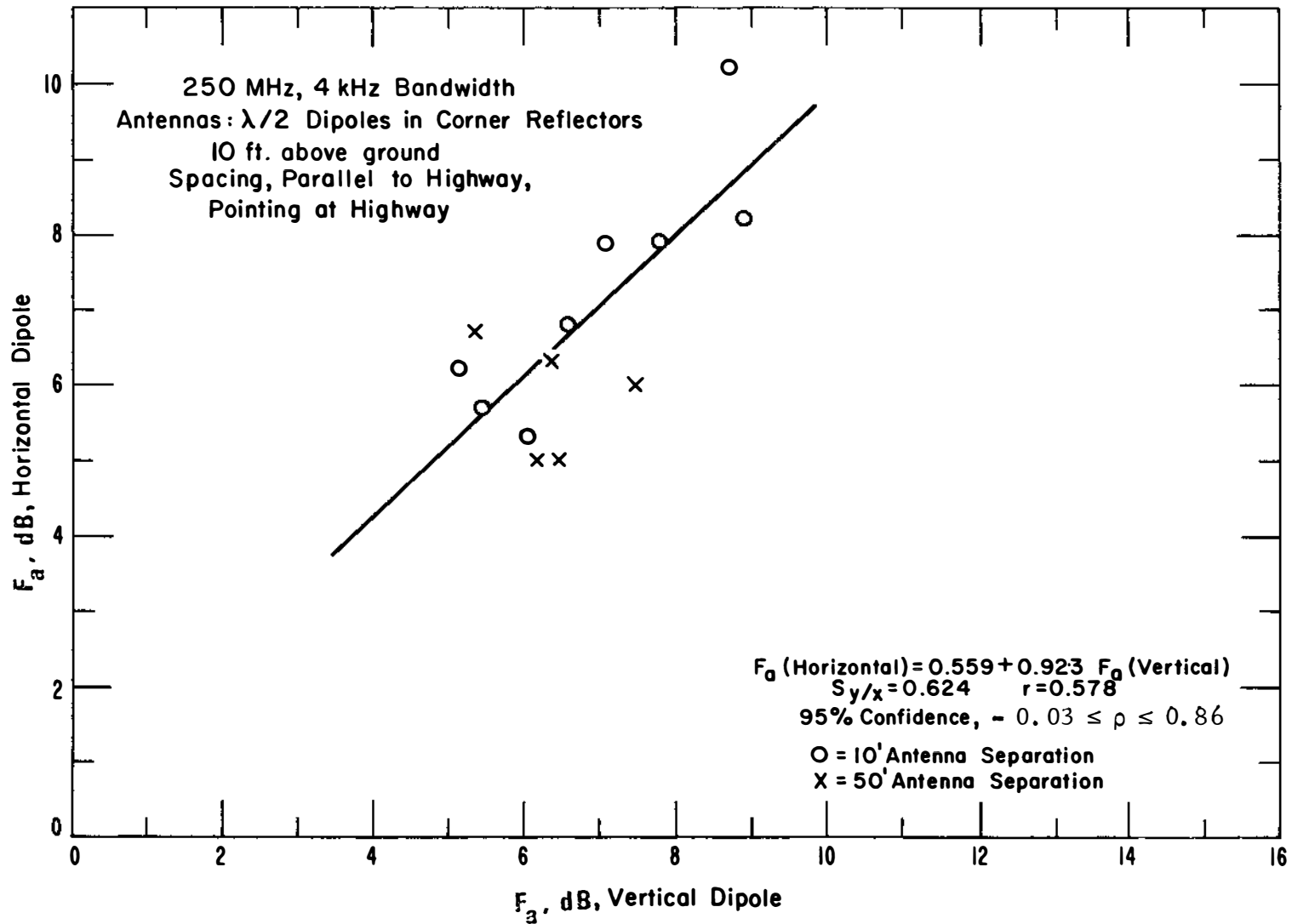


Figure 13. Horizontal versus vertical component of man-made radio noise at 250 MHz.

#### 4.1.2 Power Lines

A number of local features may influence greatly the man-made radio noise level at a given location. One such feature is the proximity of electric power distribution lines. At and below the middle of the HF band, a large part of the received noise is generated by or propagated along power lines. Even in the VHF and UHF bands, however, nearby power lines, especially high voltage lines, can be the source of the predominant man-made radio noise. The mobile radio noise laboratory has been used to measure the decrease in power line noise as a function of distance from the power line. Figures 14 and 15 show examples of such measurements for two power transmission lines. These measurements were made starting directly under the power line and moving perpendicular to the power line until the noise decreased to the ambient level in the area. One set of measurements was made for a 250 kV line located in a rural area of the state of Washington. The 0.5 MHz measurements are shown on figure 14. Another set of measurements was made for a 115 kV line in a rural area in the state of Wyoming. The results of the 102 MHz measurements are shown on figure 15. Both sets of measurements were made using short vertical whip antennas. The physical height of the 0.5 MHz antenna is  $0.003 \lambda$ , and the height of the 102 MHz antenna is  $0.17 \lambda$ . When under the power line, the lowest conductor was approximately 15 ft above the top of the antenna. Because of the antennas used, the fall off of the noise with decreasing distance near the line is almost certain to be due to the antenna pattern rather than a decrease in the actual field. A comparison with figure 1 indicates that, for an average location, the power line noise from a 250 kV line at 0.5 MHz would be equal to the expected ambient noise level at distances of approximately 290 m in business areas, 320 m in residential areas, and 350 m in rural areas. Also, the

expected ambient noise at 102 MHz and the 115 kV power line noise would be equal at approximately 130 m in a business area, 180 m in a residential area, and 240m in a rural area. These probably are good "rule-of-thumb" distances to use in estimating the effect of nearby power lines.

Figure 16 shows the results of measurements taken along a 115 kV line in rural Wyoming, parallel to the line, under the line, and 400 m from it. The figure shows the results for eight measurement frequencies, the values for each frequency being the median value of values taken along approximately 1 mile of the transmission line. Also shown on figure 16 is the general rural noise characteristic from figure 1. The 115 kV line of figures 14 and 15 had steel towers whereas the 115 kV line of figure 16 was similar but used wooden towers.

The above types of measurements were made for five H-frame, 115 kV power transmission lines in the Boulder area, each line being measured at more than one location. Figure 17 summarizes these measurements, giving the decrease in noise power as a function of the perpendicular distance from the lines. Results are shown for seven measurement frequencies, 0.25 MHz to 250 MHz. The results shown give the expected values, based on the mean values of the measurements of the five lines. The results of figure 1 indicate that  $F_a$  decreases with increasing frequency at about 27.7 dB per decade of frequency. The mean value of all the measurements taken under the five H frame, 115 kV lines, and at a distance of 16 meters from the lines are shown on figure 18 along with a least squares fit to the measurements, with the slope restricted to 27.7 dB per decade. Also shown on figure 18 is the standard deviation,  $\sigma_{F_a}$ , for these measurements. The ITS data base does not contain any information on the effect of higher voltage power lines. However, in a recent report (Crippen, 1971), measurements on a 500 kV line indicated that, in



the HF region, the effects of the power line could be noticed in a rural area out to a distance of 400 m.

The noise from power lines will vary over wide limits depending on the condition of the line and insulators, type of supports, etc. Variation also will be noted with weather changes. For example, during periods of precipitation, raindrops or snowflakes hitting the line can cause a corona discharge to take place. The highest noise levels probably will be noted at the beginning of a rainstorm after a dry, windy period when the insulators have become covered with dust. When the rain mixes with the dust and before sufficient rain has fallen to wash the insulators, very strong discharges across the insulators will take place. The line voltage appears to have less effect on the level of the radiated noise than the construction and condition of the line. The lower voltage distribution lines will often be noisier than the high voltage transmission lines. This could be due to a basic design philosophy, age and condition of the line, or a difference in line hardware design.

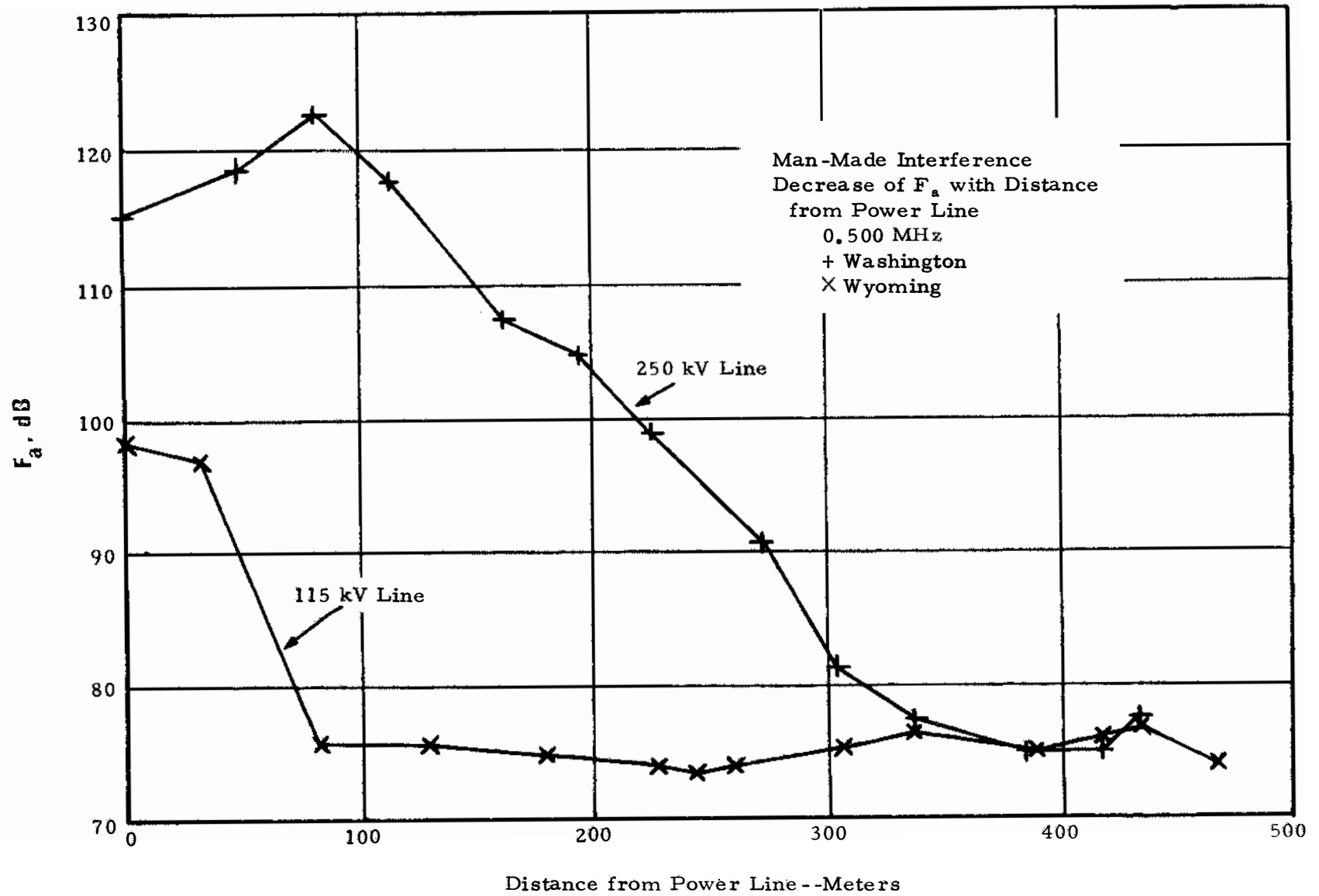


Figure 14. Decrease in power line noise with distance at 0.5 MHz.

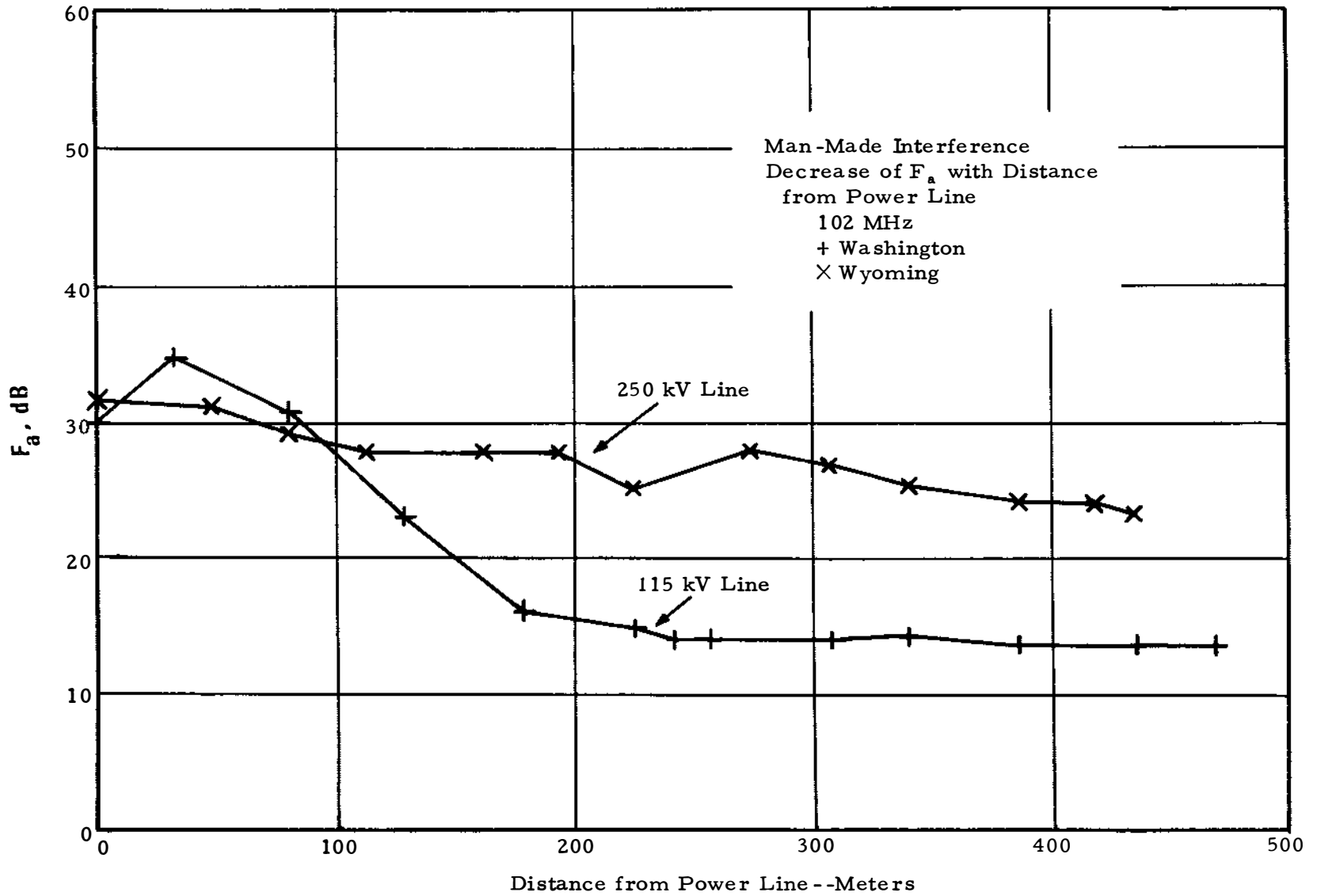


Figure 15. Decrease in power line noise with distance at 102 MHz.

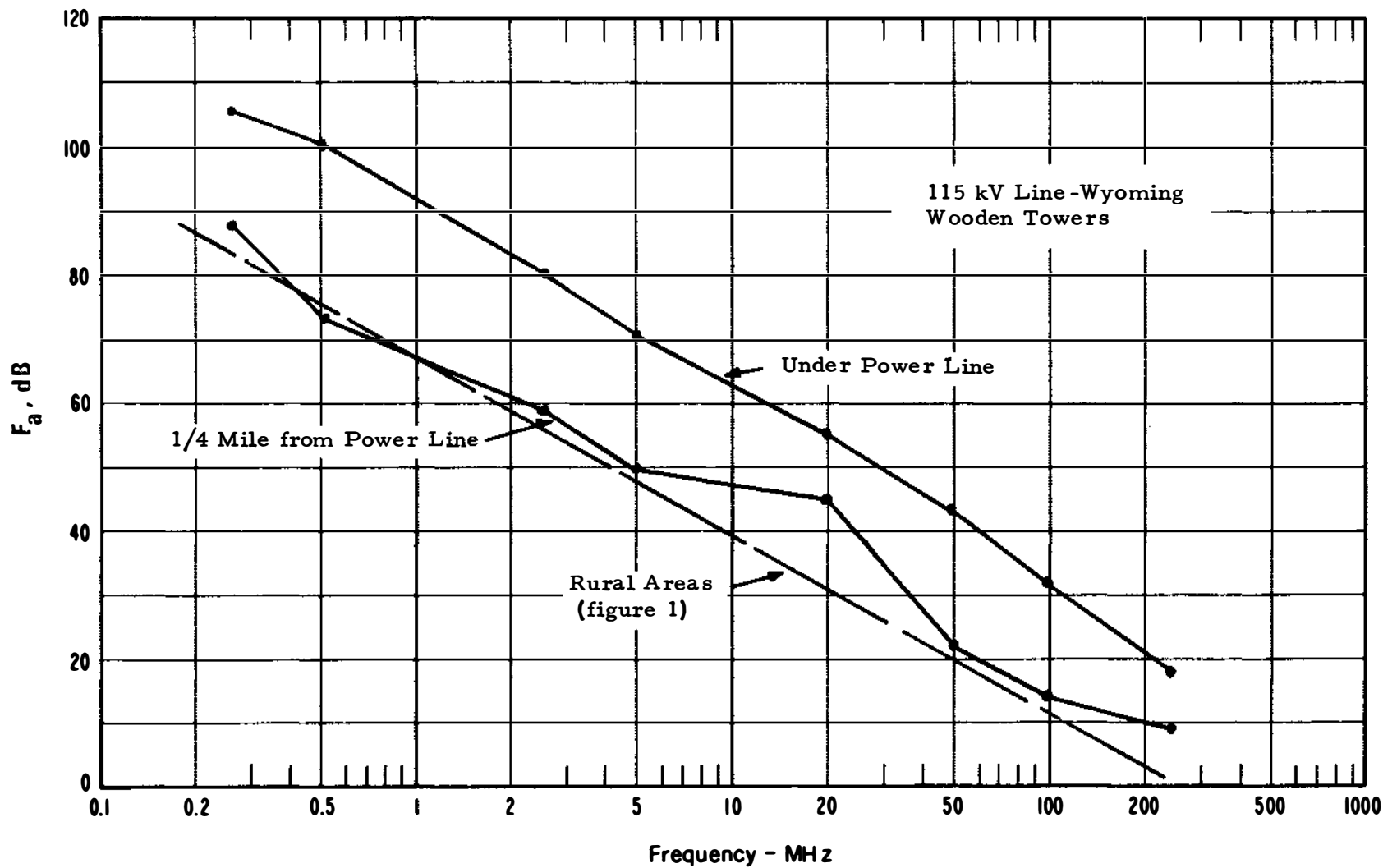


Figure 16. Power line noise measurements taken moving parallel to a 115 kV line in rural Wyoming, both under the line and 1/4 mile from the line.

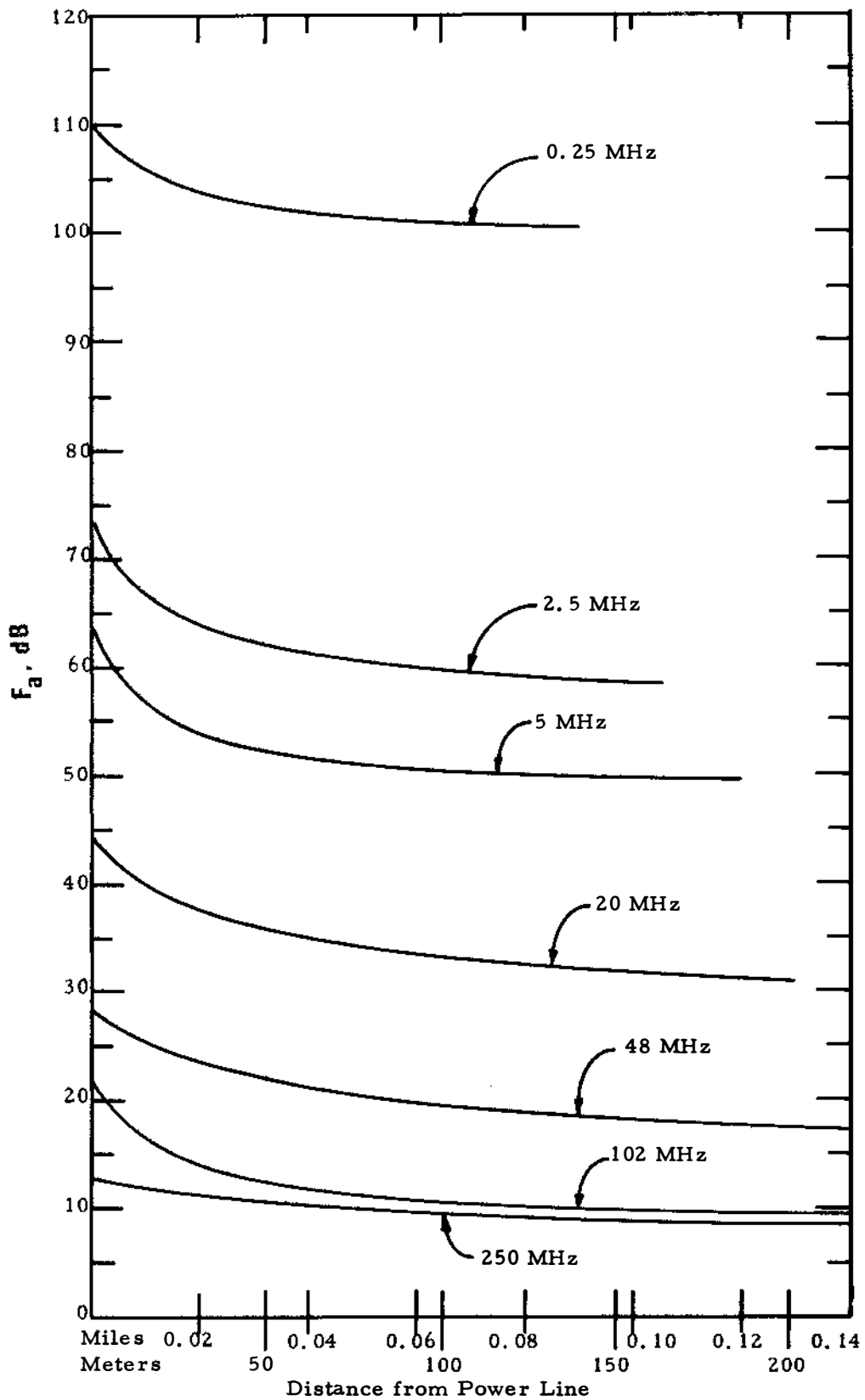


Figure 17. Expected decrease of radio noise radiated from 115 kV H-frame power line with distance from line.

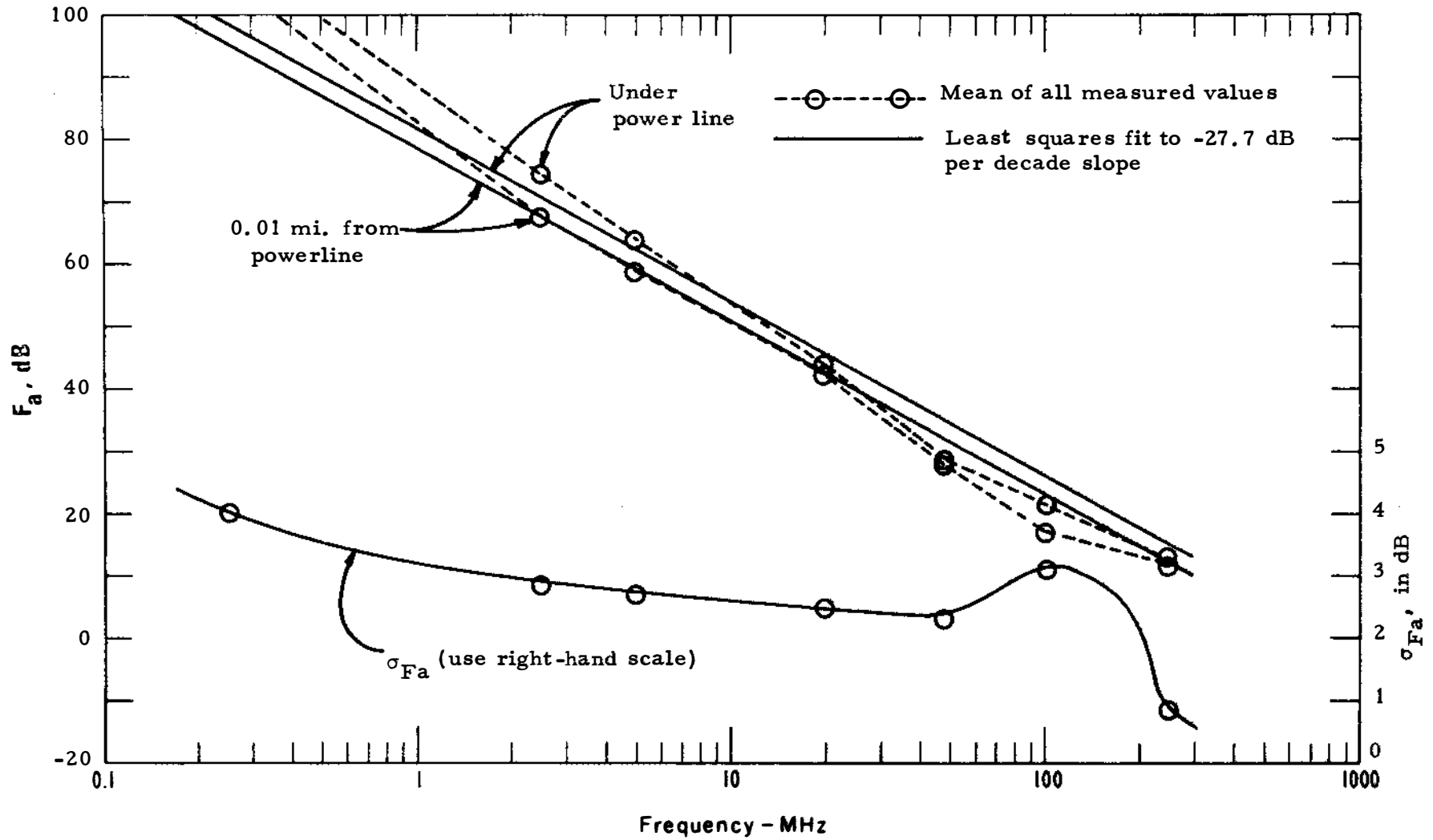


Figure 18. Expected radio noise power,  $F_a$ , and its standard deviation,  $\sigma_{F_a}$ , from 115 kV, H-frame power transmission line. Receiving antenna under and 0.01 mi. (16.09 meters) from power line.

## 4.2 The Average and Logarithmic Moments, $V_d$ and $L_d$

As previously mentioned, the ratio of the rms to the average envelope voltage,  $V_d$ , in decibels, and the ratio of the rms to the antilog of the average logarithm of the envelope voltage,  $L_d$ , in decibels, are indicative of the impulsive nature of the noise (Crichlow et al., 1960).

Values of  $V_d$  and  $L_d$  are available from the same sets of measurements used to obtain the estimates of  $F_a$ . These data were separated into the same groupings as the values of  $F_a$ . Two bandwidths were used in taking the measurements, 4 kHz and 10 kHz. The earlier measurements were all made using the 10 kHz bandwidth. An analog tape recorder (Appendix A) was added to the measurement capability which limited the bandwidth that could be used to 4 kHz. Therefore, all of the latter measurements were made using the 4 kHz bandwidth. Since the values of  $V_d$  and  $L_d$  for radio noise are dependent on bandwidth, the data were further separated into subgroups of 4 kHz and 10 kHz data. The means of the individual location median values for each subgroup are shown plotted on figures 19 through 22. Figures 19 and 20 show values of  $V_d$  and  $L_d$ , respectively, for measurements made in a 4 kHz bandwidth for the three types of areas. Figures 21 and 22 are the corresponding measurements made using a 10 kHz bandwidth. The values of  $V_d$  and  $L_d$  for white Gaussian noise, which are independent of bandwidth and frequency, are also shown on figures 19 through 22. As with the values of  $F_a$ , there is a fairly large variation of the median values from location to location in a particular type of area. This variation is indicated in table 3 where the standard deviations of  $V_d(\sigma_{V_d})$  and  $L_d(\sigma_{L_d})$  are shown for the various types of areas, bandwidths, and frequencies.

As can be seen from figures 19 through 22, there is a definite difference in the character of the noise in the three types of areas. While

Table 3. Variation of the Median Value of  $V_d$  and  $L_d$  with Location for a Given Frequency and Bandwidth

Frequency (MHz)	Standard Deviation of $V_d$ , $\sigma_{V_d}$ (dB)					
	Business Areas		Residential Areas		Rural Areas	
	BW 4 kHz	BW 10 kHz	BW 4 kHz	BW 10 kHz	BW 4 kHz	BW 10 kHz
0.25	1.6	2.2	1.1	1.8	0.6	1.0
0.5	1.2	2.6	0.2	1.2	0.6	0.6
1.0		1.0		0.9		2.3
2.5	2.5	2.6	1.6	2.6	2.0	1.7
5	1.3	1.1	1.4	1.3	0.5	1.0
10		1.5		1.9		0.9
20	2.2	1.8	1.4	1.4	1.4	0.9
48	1.6	1.4	1.8	1.8	1.4	0.4
102	1.4		1.8		1.3	
250	0.7		0.5		0.5	
Average	1.6	1.8	1.2	1.5	1.0	1.1

Frequency (MHz)	Standard Deviation of $L_d$ , $\sigma_{L_d}$ (dB)					
	Business Areas		Residential Areas		Rural Areas	
	BW 4 kHz	BW 10 kHz	BW 4 kHz	BW 10 kHz	BW 4 kHz	BW 10 kHz
0.25	3.1	3.7	1.2	2.7	1.3	1.1
0.5	2.7	4.3	0.6	2.1	1.2	1.1
1.0		1.3		1.2		3.2
2.5	4.2	4.2	1.8	3.5	2.3	2.9
5	1.8	2.0	2.0	1.8	0.9	1.4
10		2.1		2.5		1.3
20	3.3	3.2	2.3	2.4	1.9	1.0
48	2.5	2.7	2.2	2.7	1.4	0.5
102	2.2		2.6		2.8	
250	1.1		1.0		0.6	
Average	2.6	2.9	1.6	2.0	1.6	1.6



there is considerable overlap, considering the values in table 3, the general trends are fairly well defined. Figures 23, for business areas, 24, for residential areas, and 25, for rural areas, give the expected median values of  $V_d$  and  $L_d$ . The solid line is the estimate for a 4 kHz bandwidth and the dashed for 10 kHz. These are estimates for the mean of the individual location median values. The estimates are based on least squares polynomial fits to the measurement data. As with  $F_a$ , the distribution of the location medians, in decibels, can be represented quite well by a normal distribution. The values of  $\sigma_{V_d}$  and  $\sigma_{L_d}$  shown in table 3 can be used in the same manner as  $\sigma_{F_a}$  in table 1 to determine the probability of a median value occurring at any location within a particular type of area.

There will be a variation about the location median with time at any given location, which will generally be larger than the variation from location to location. Again, as with  $F_a$ , this variation within an hour can be represented quite closely by a skewed normal distribution, defined by the median and upper and lower decile values. Using the same 20 MHz residential area recordings used to obtain within the hour variation of  $F_a$  (fig. 3), a distribution of the 10-sec readings of  $V_d$  is shown on figure 26 and of  $L_d$  on figure 27. These distributions are typical of those generally found in business and residential areas. The distributions found in rural areas will have the same form but will usually be much flatter. The ratio, in decibels, of the upper decile to the median value of the distribution shown on figure 26 is 4.8 dB. The average value of this ratio for 20 MHz rural area data is 0.8 dB. Similarly, the ratio of the upper decile to the median for the distribution of the  $L_d$  values in figure 27 is 7.0 dB, while the corresponding rural average value is 1.0 dB.

Interstate highways and parks and university campuses were analyzed separately for values of  $V_d$  and  $L_d$ . The results are shown on figures 28 for  $V_d$  and 29 for  $L_d$ , with the measurement bandwidth indicated. The results for both  $V_d$  and  $L_d$  from the interstate highway measurements are similar to the business area estimate above 10 MHz and similar to the rural area estimate at lower frequencies. This is to be expected, since the man-made noise is caused predominantly by ignition systems at the higher frequencies and power lines at the lower frequencies.

The park and university campus curves appear to fall somewhere between the residential and rural curves. Most parks and campuses have somewhat restricted traffic patterns and few overhead power lines and would be expected, therefore, to approach the general rural conditions.

As with the values of  $F_a$ , the values of  $V_d$  and  $L_d$  were measured using a short vertical antenna. There is even less information on the effect of polarization on  $V_d$  and  $L_d$  than there is on  $F_a$ . At the time the 250 MHz data shown on figure 13 were recorded, the values of  $V_d$  for the two antennas were also recorded. These data are shown plotted on figure 30 along with the best fit regression line. As can be seen, the value of  $V_d$  for the vertical component is generally larger than the value for the horizontal component. The recorded man-made radio noise in this case was almost exclusively from automotive ignition systems. This relationship would indicate that the vertical component was more impulsive for ignition noise than the horizontal component. However, the sample size was extremely small (17 sets of 10 sec measurements).

Two computer plots of the relationships between the three moments,  $F_a$ ,  $V_d$ , and  $L_d$ , are interesting. The high degree of correlation between  $V_d$  and  $L_d$  is shown on figure 31. The values of 673  $V_d$  and the corresponding  $L_d$  location medians obtained by combining the data for

all frequencies and locations are plotted. Since the values of both  $V_d$  and  $L_d$  are dependent upon the instantaneous variations of the noise envelope, a fairly high correlation between the two values would be expected. With as high a correlation coefficient ( $r = 0.94$ ) as was obtained, the value of  $V_d$  may give an adequate definition for the most likely APD as was found to be the case with atmospheric radio noise (Crichlow et al., 1960; CCIR, 1964). Figure 32 shows the lack of correlation between  $V_d$  and  $F_a$ . The very low correlation coefficient ( $r = -0.07$ ) shown by the 673 pairs of  $V_d$  and  $F_a$  indicates that the character of the noise, that is the impulsive nature or instantaneous envelope variations, is not dependent upon the power level. It is a function of the types and number of sources of the composite man-made radio noise and their distribution about the receiving antenna and not of the actual received power level.

Since man-made noise is white (flat spectrum over normal communications bandwidth), the values estimated for  $F_a$  are independent of bandwidth as long as bandwidths limited to a few percent of the center frequency are considered. Since the values of  $V_d$  and  $L_d$  are dependent on bandwidth, the estimates given here are only applicable to these measurement bandwidths.

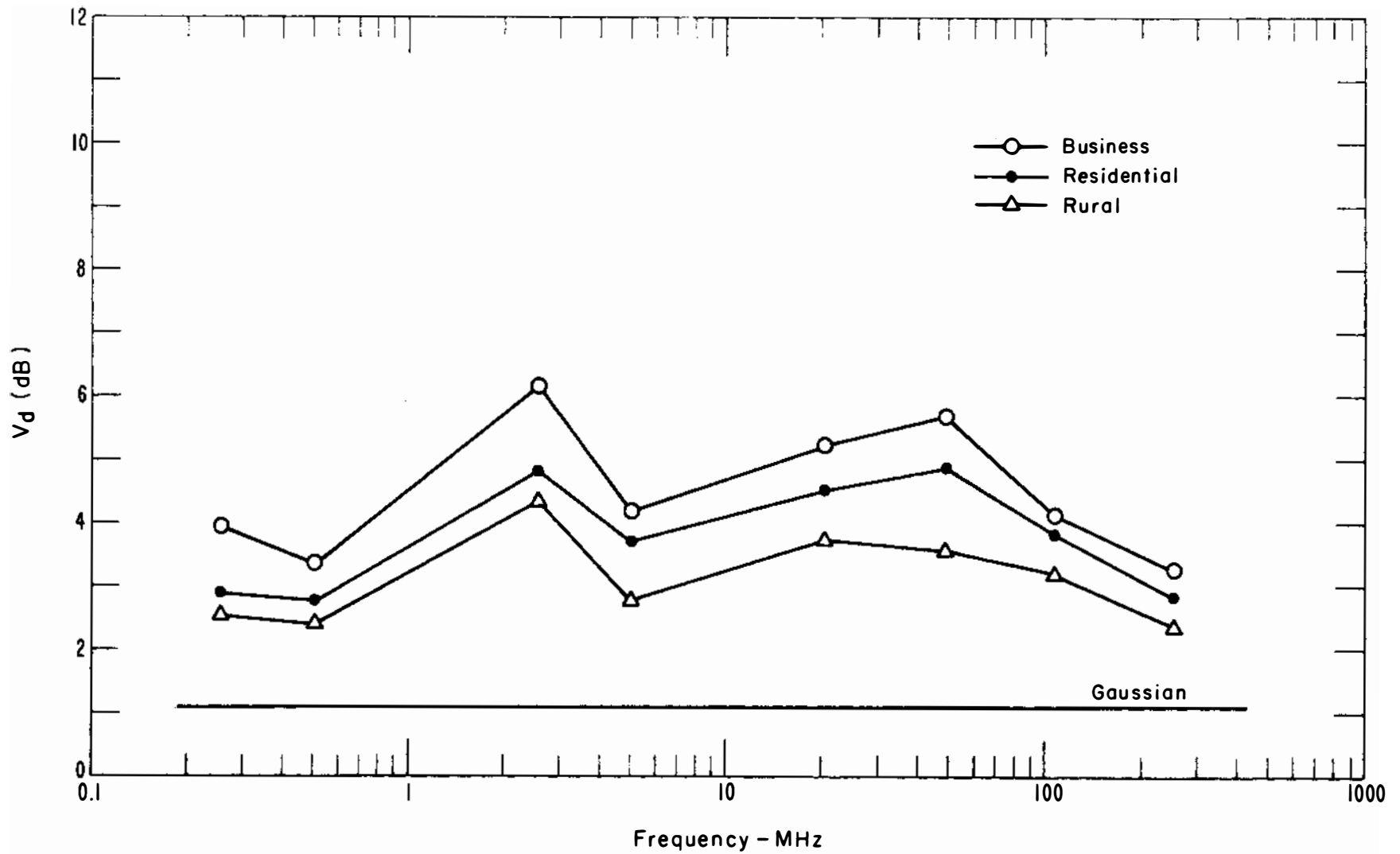


Figure 19. Mean of location median values of  $V_d$ , values measured in a 4-kHz bandwidth.

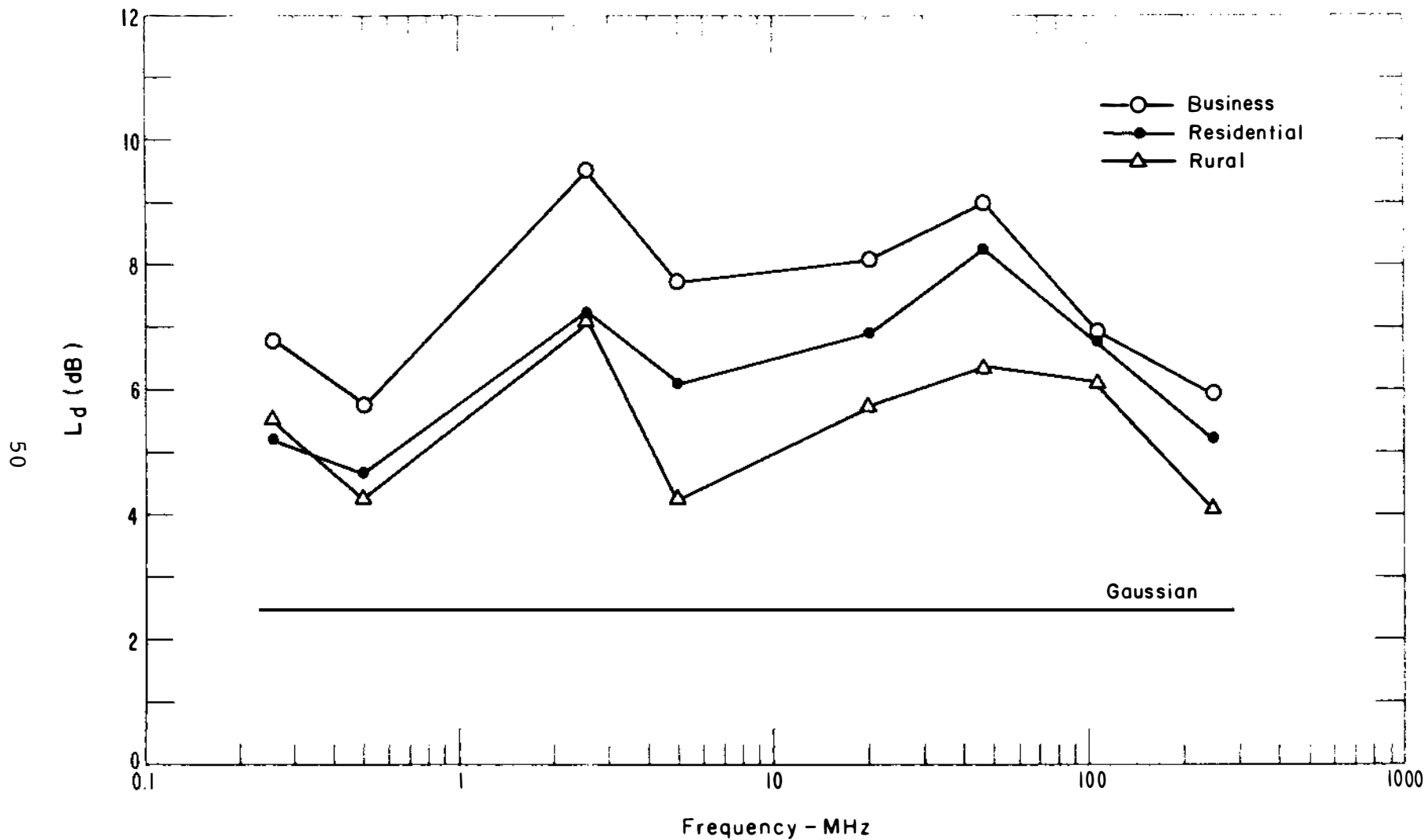


Figure 20. Mean of location median values of  $L_d$ , values measured in a 4-kHz bandwidth.

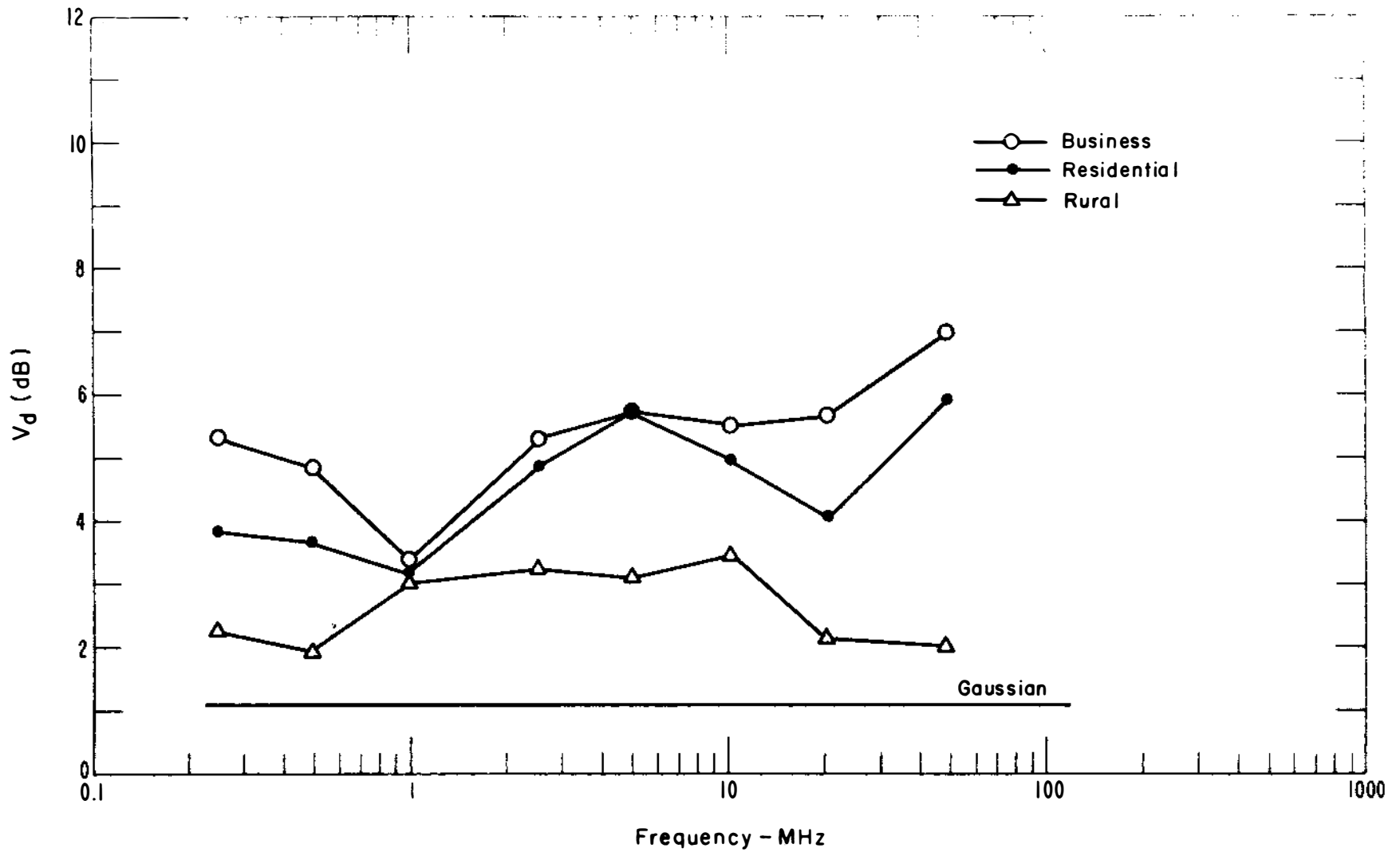


Figure 21. Mean of location median values of  $V_d$ , values measured in a 10-kHz bandwidth.

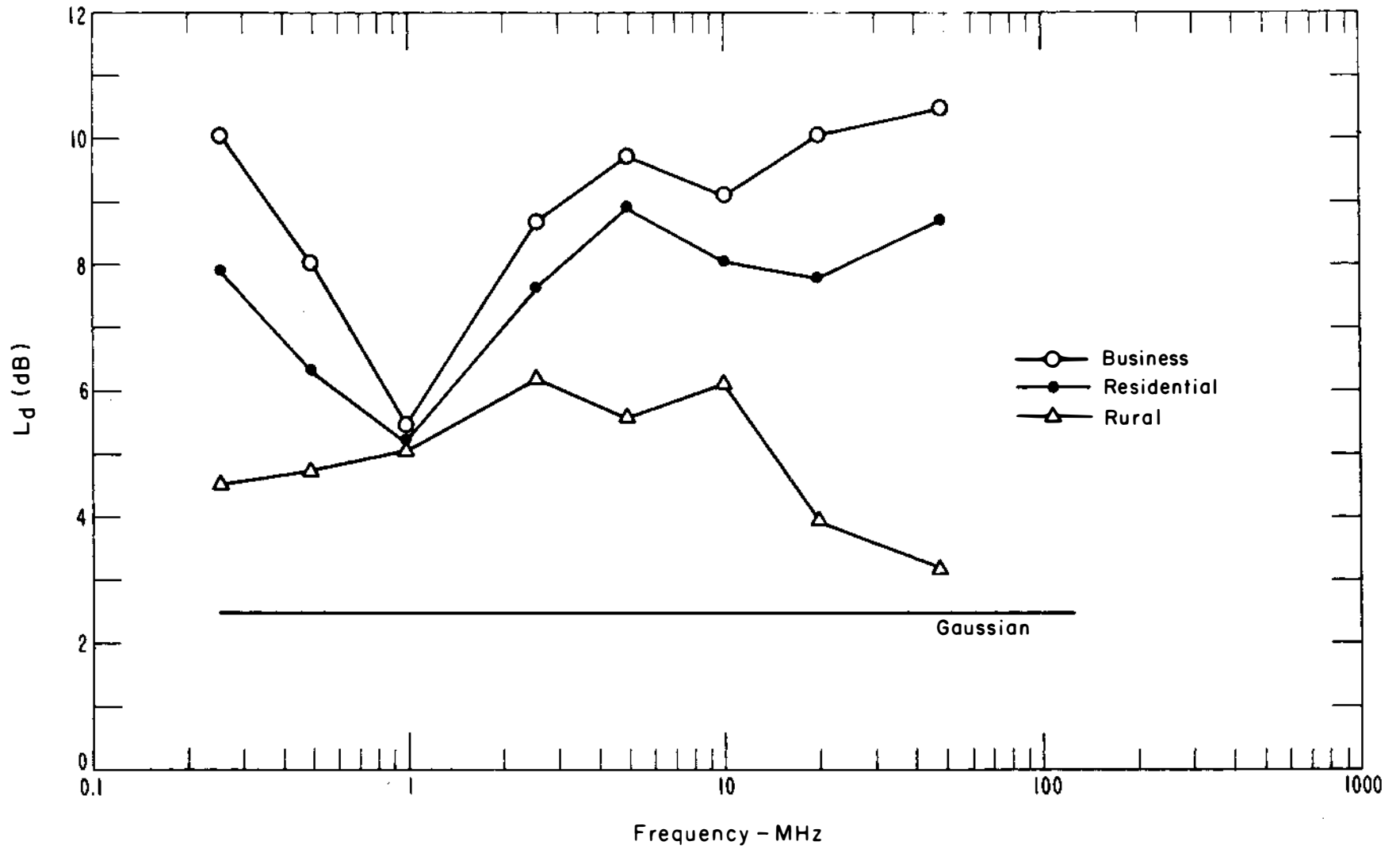


Figure 22. Mean of location median values of  $L_d$ , values measured in a 10-kHz bandwidth.

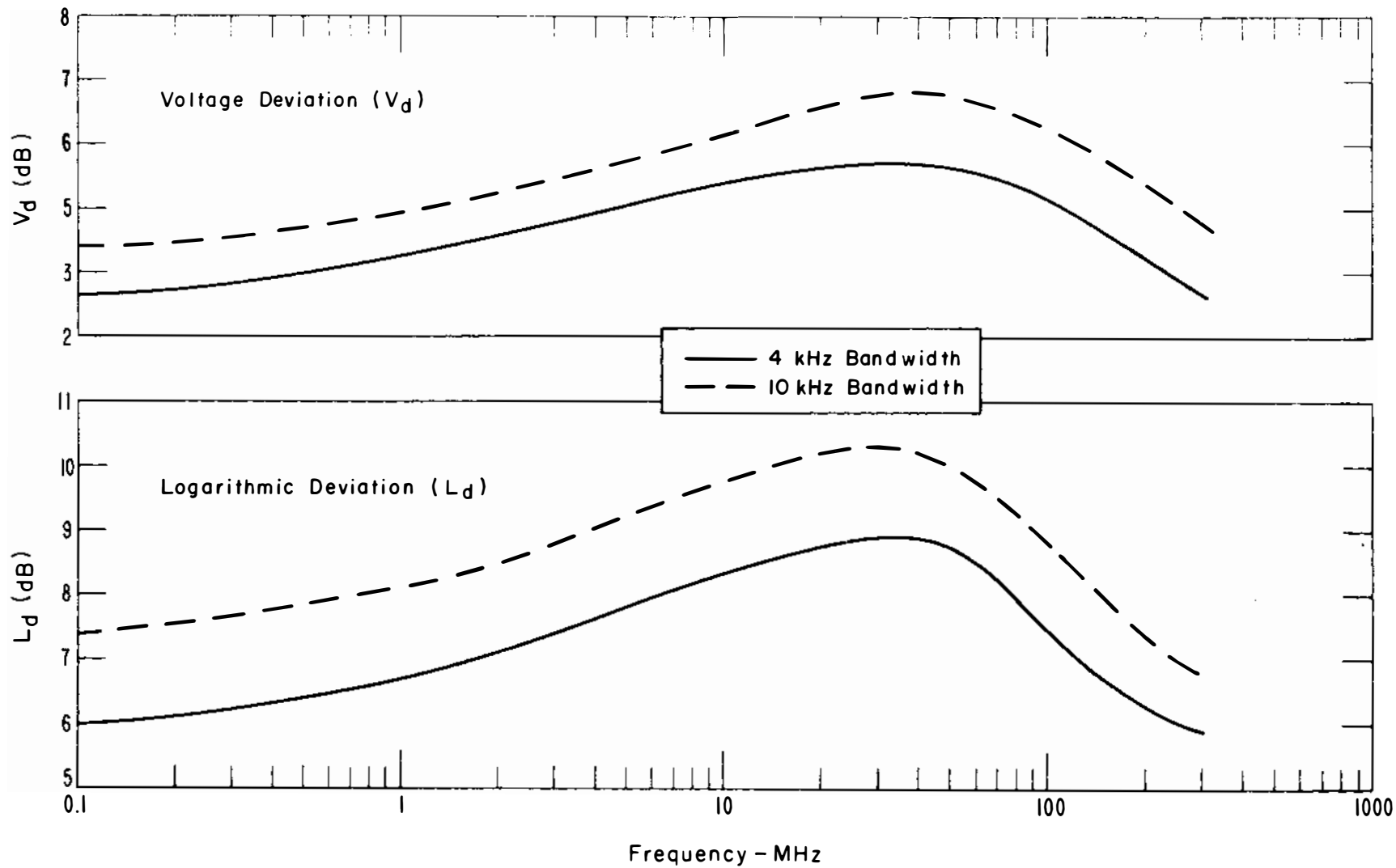


Figure 23. Expected median values of  $V_d$  and  $L_d$  for business areas.



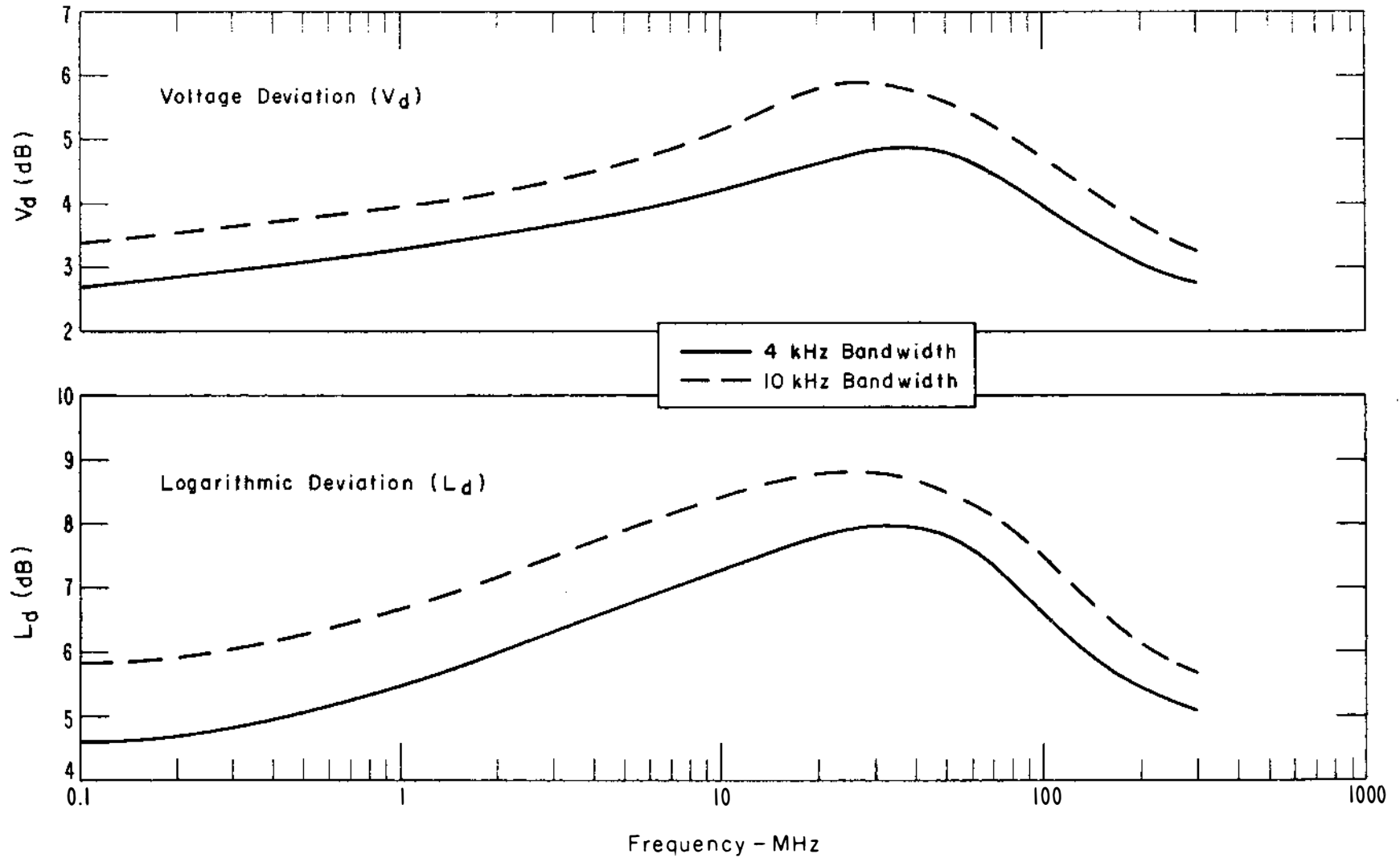


Figure 24. Expected median values of  $V_d$  and  $L_d$  for residential areas.

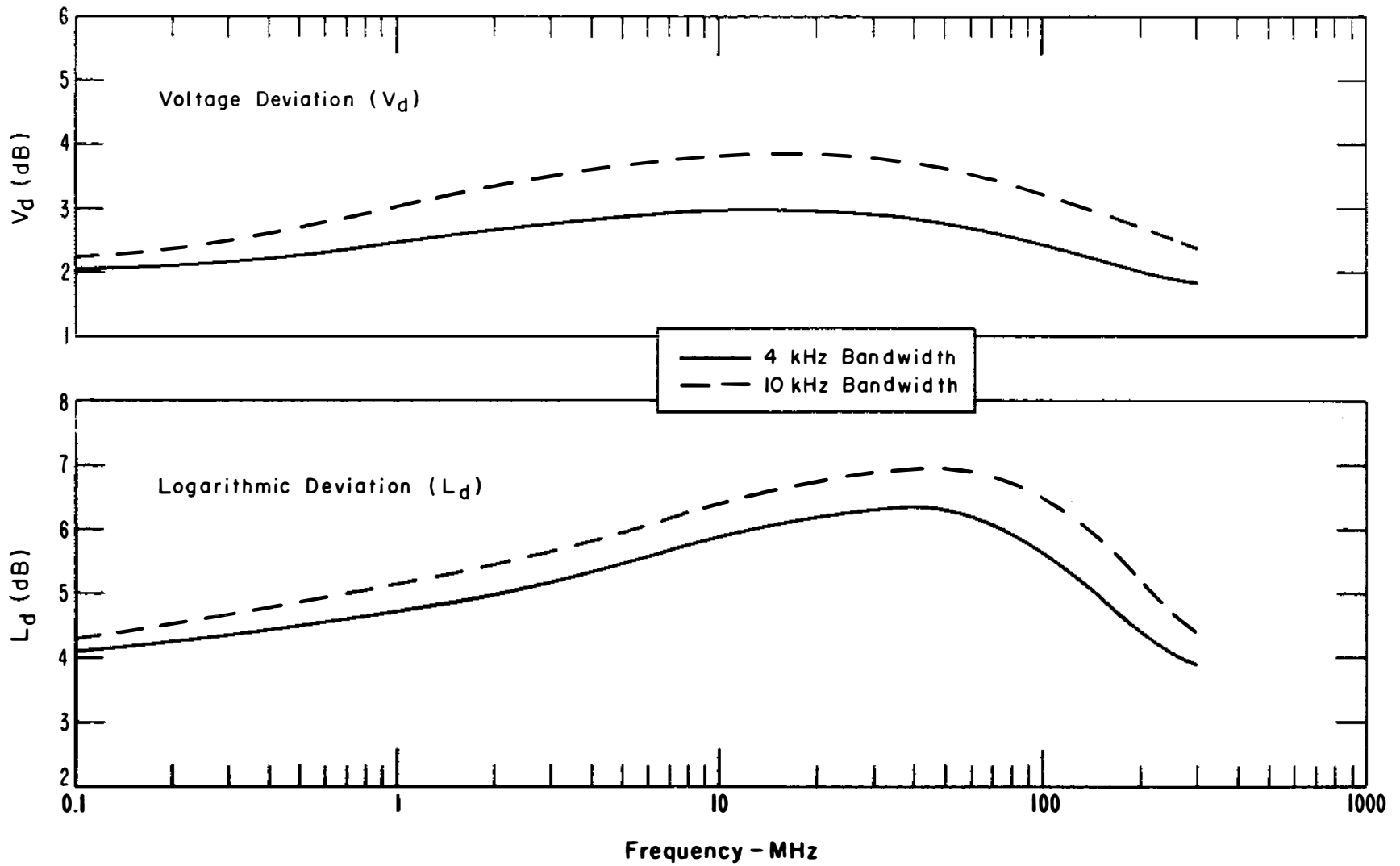


Figure 25. Expected median values of  $V_d$  and  $L_d$  for rural areas.

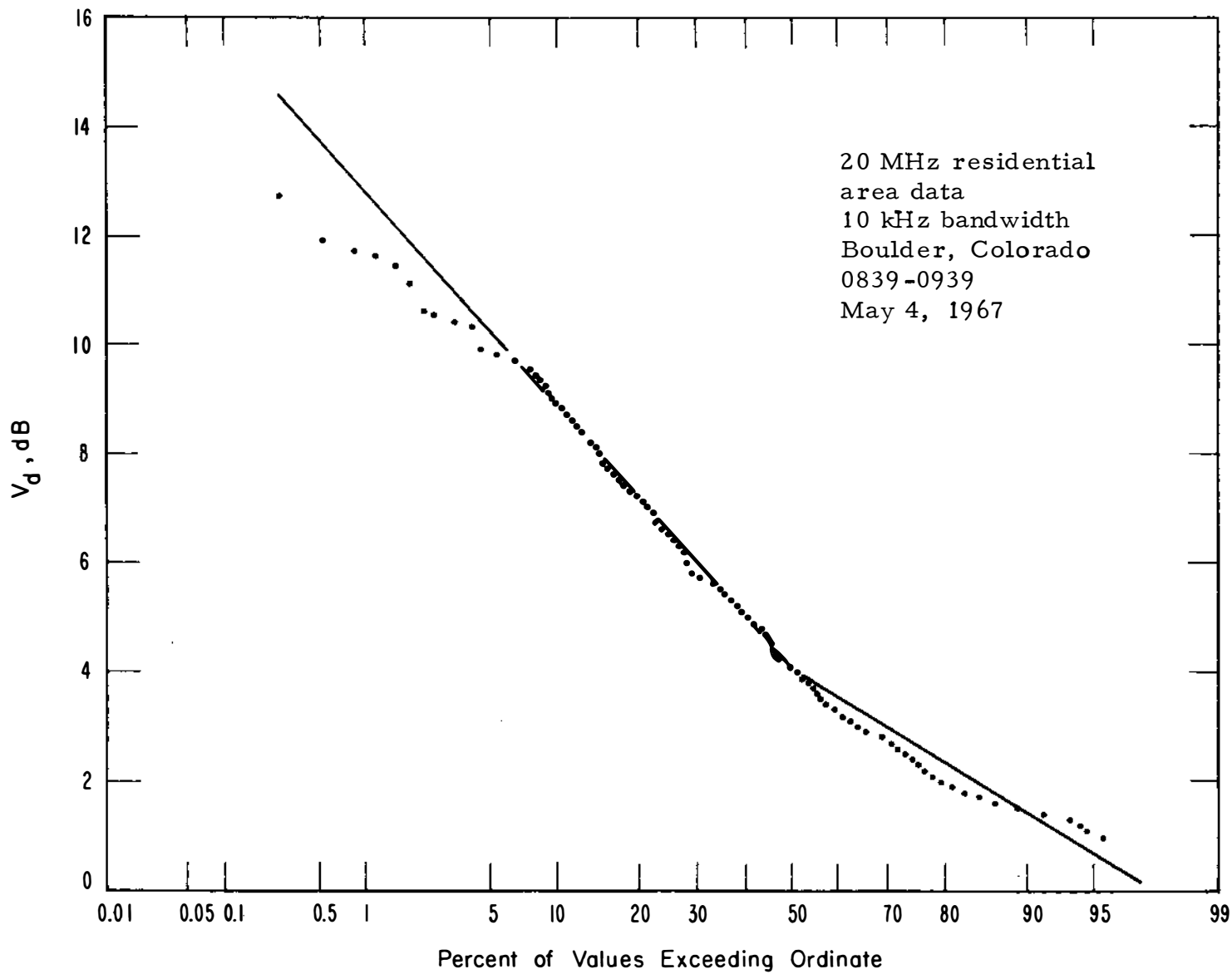


Figure 26. Distribution of  $V_d$  within an hour for a residential area.

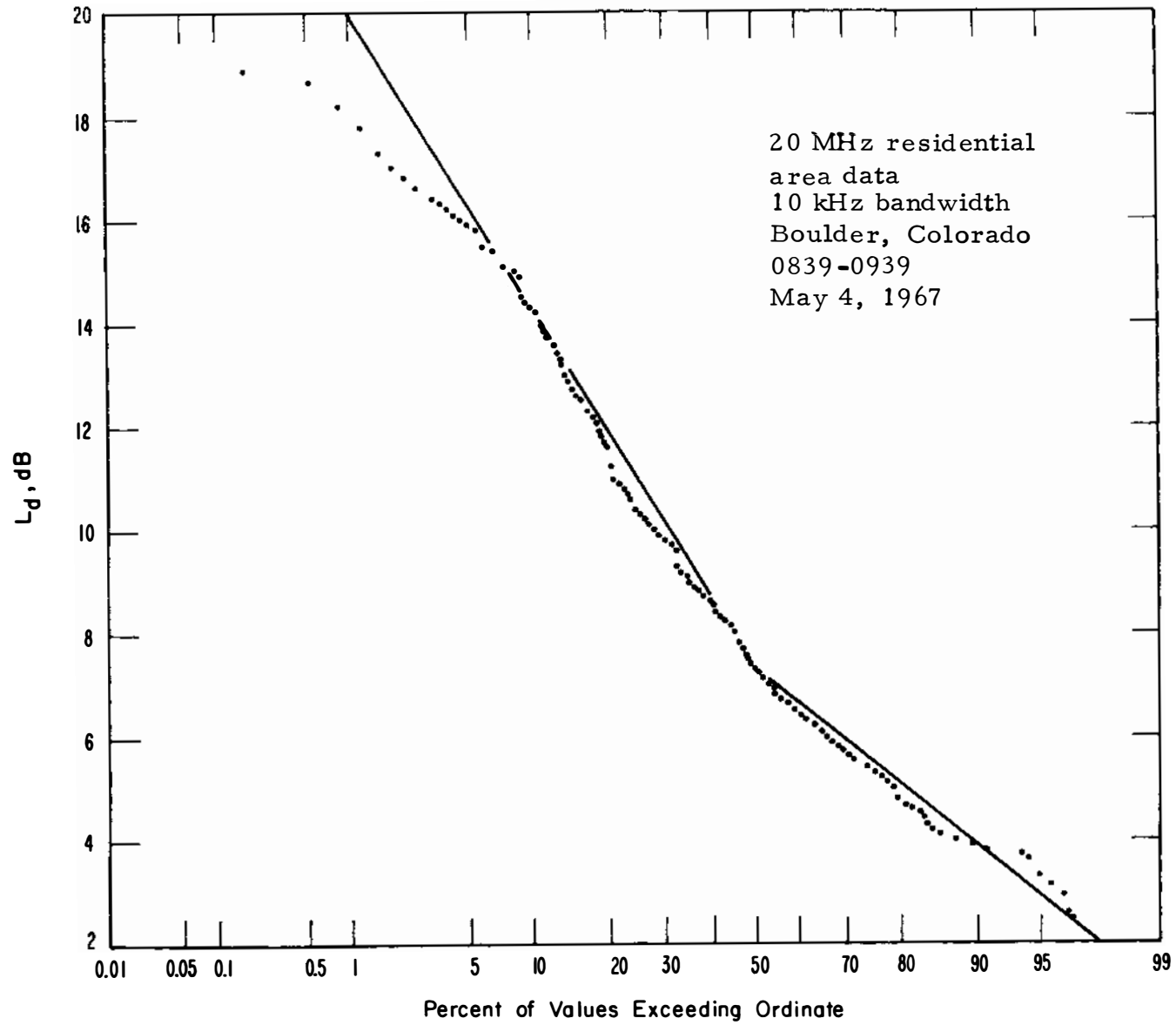


Figure 27. Distribution of  $L_d$  within an hour for a residential area.

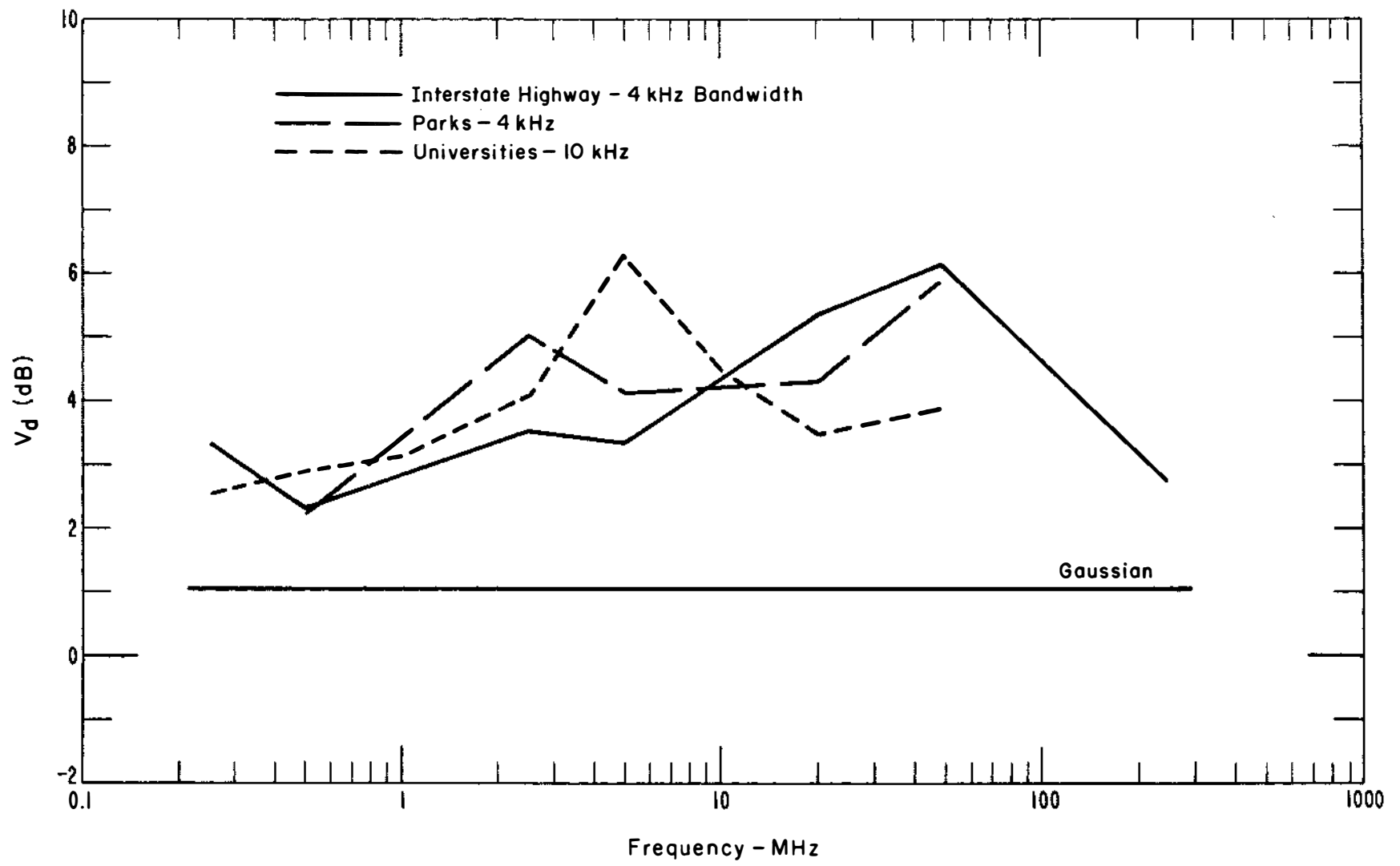


Figure 28. Median values of  $V_d$  measured along interstate highways, in parks, and on university campuses.

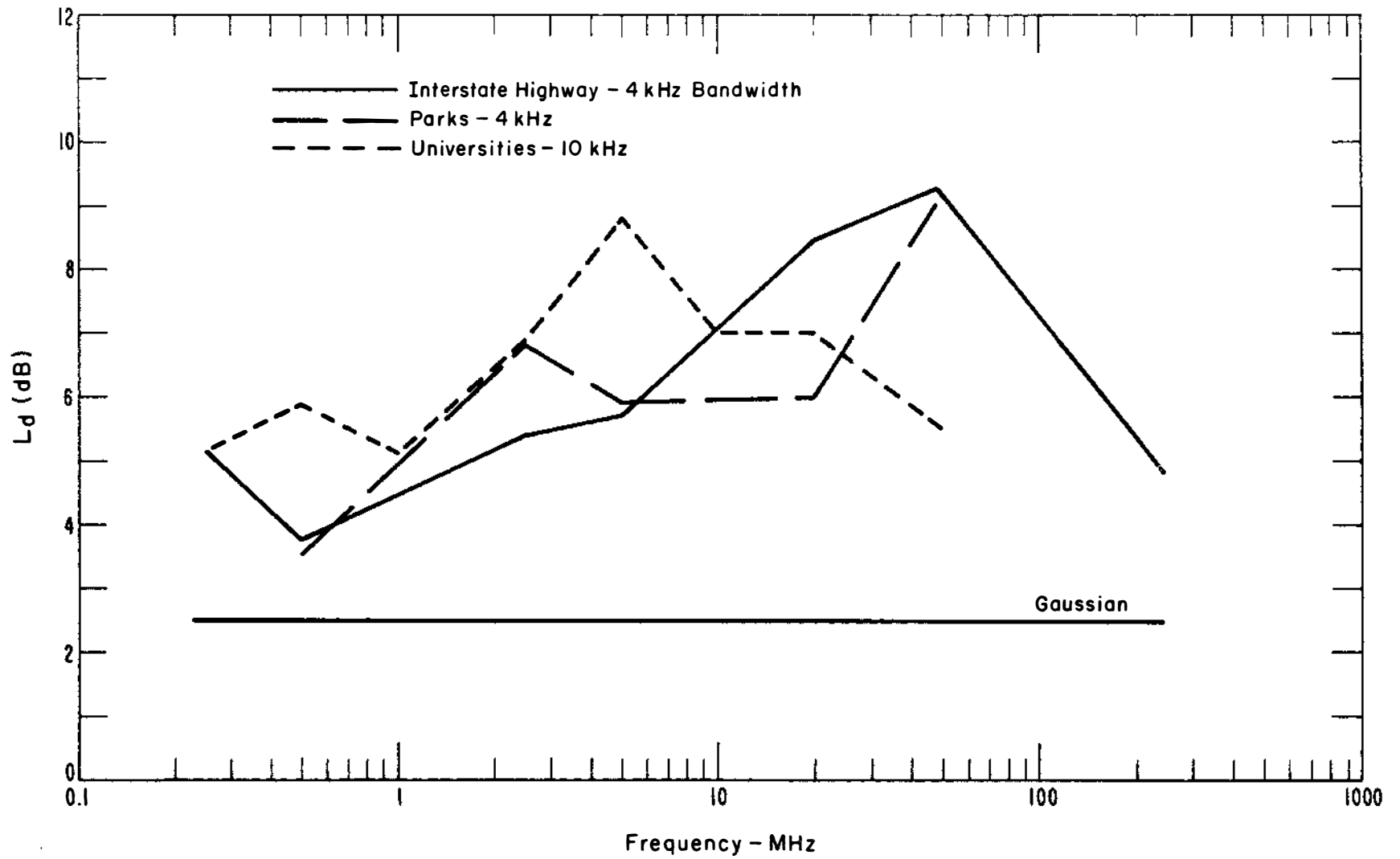


Figure 29. Median values of  $L_d$  measured along interstate highways, in parks, and on university campuses.

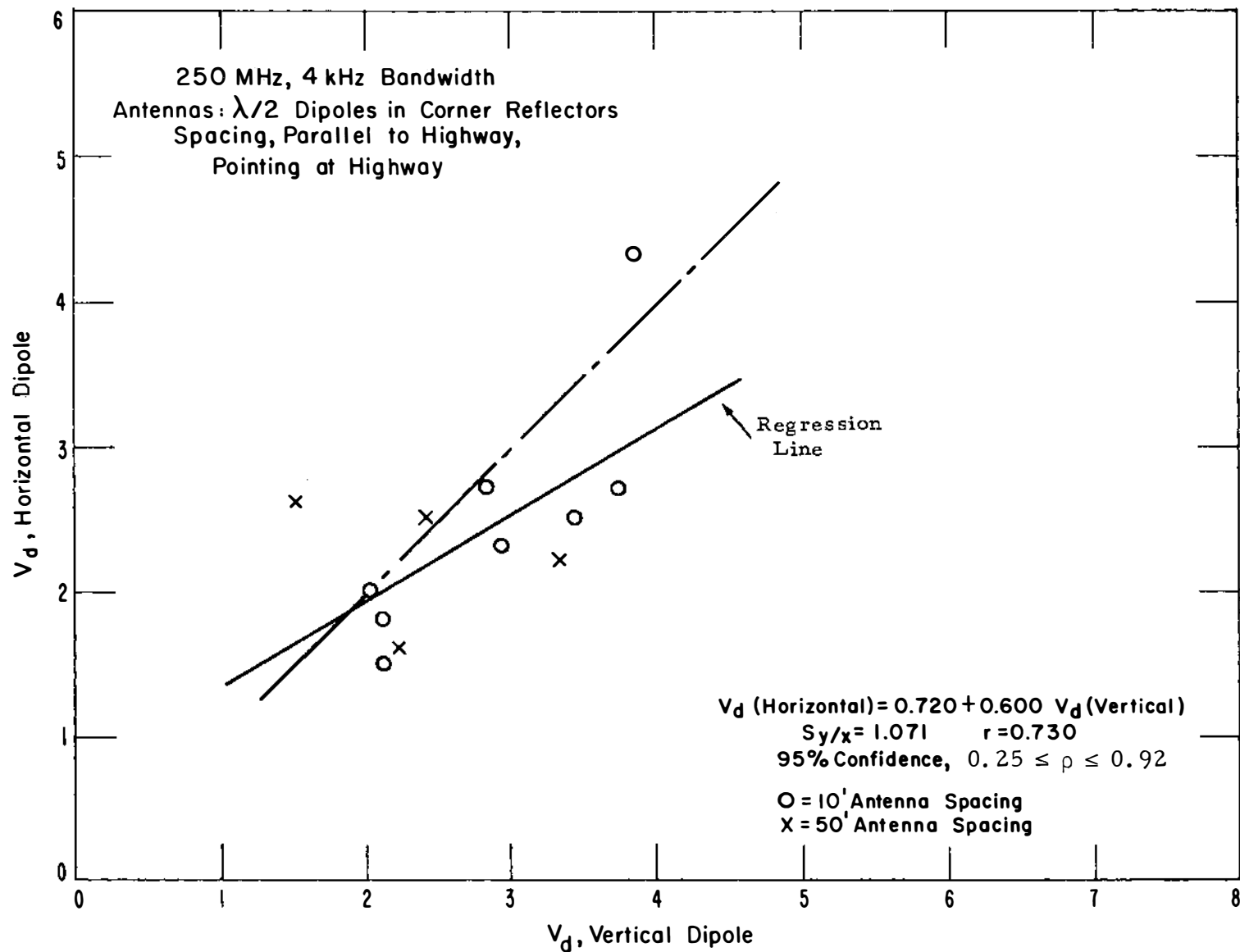


Figure 30.  $V_d$  for horizontal component of man-made noise versus  $V_d$  for vertical component.

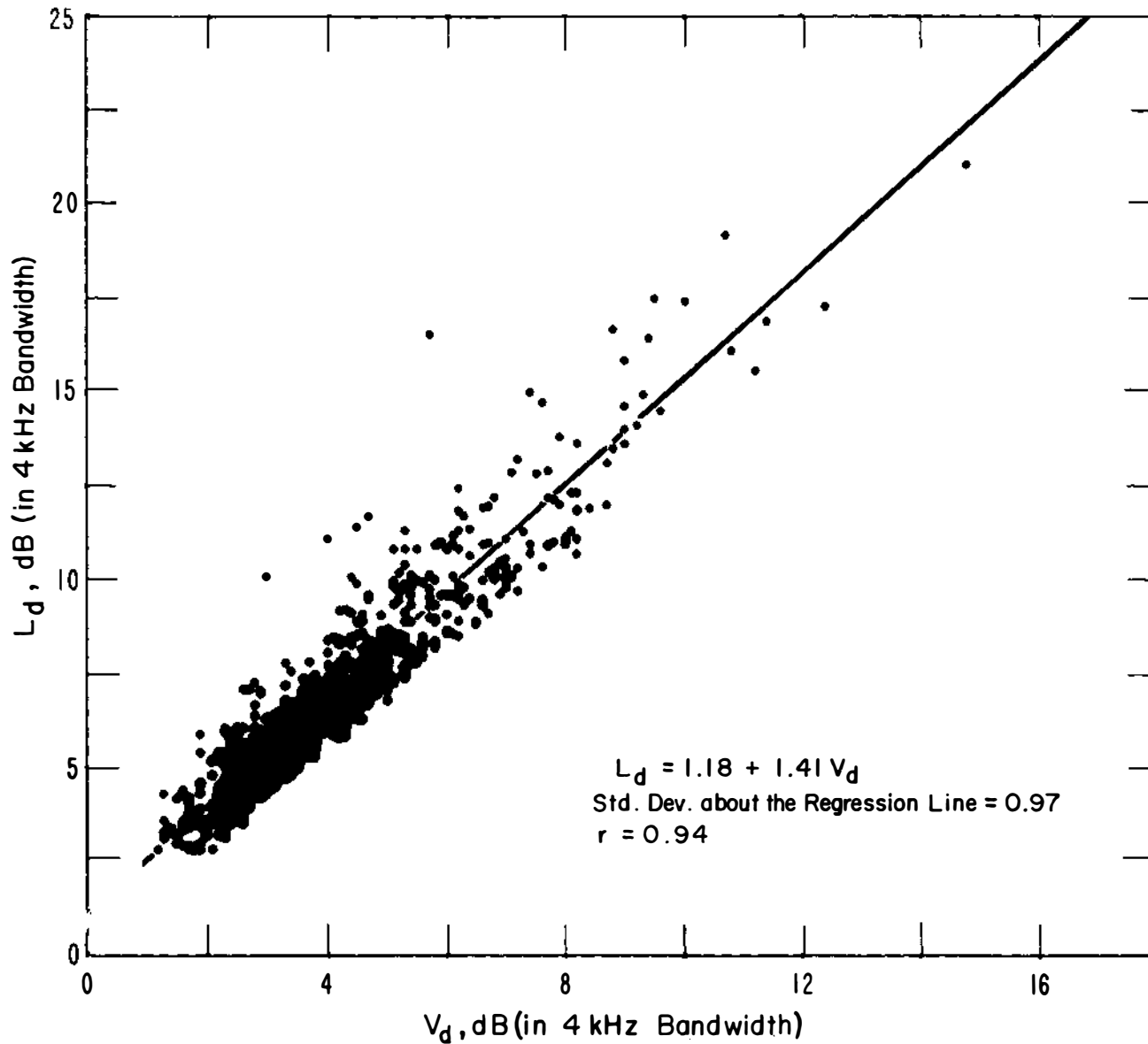


Figure 31. Correlation of  $V_d$  and  $L_d$  for man-made noise.



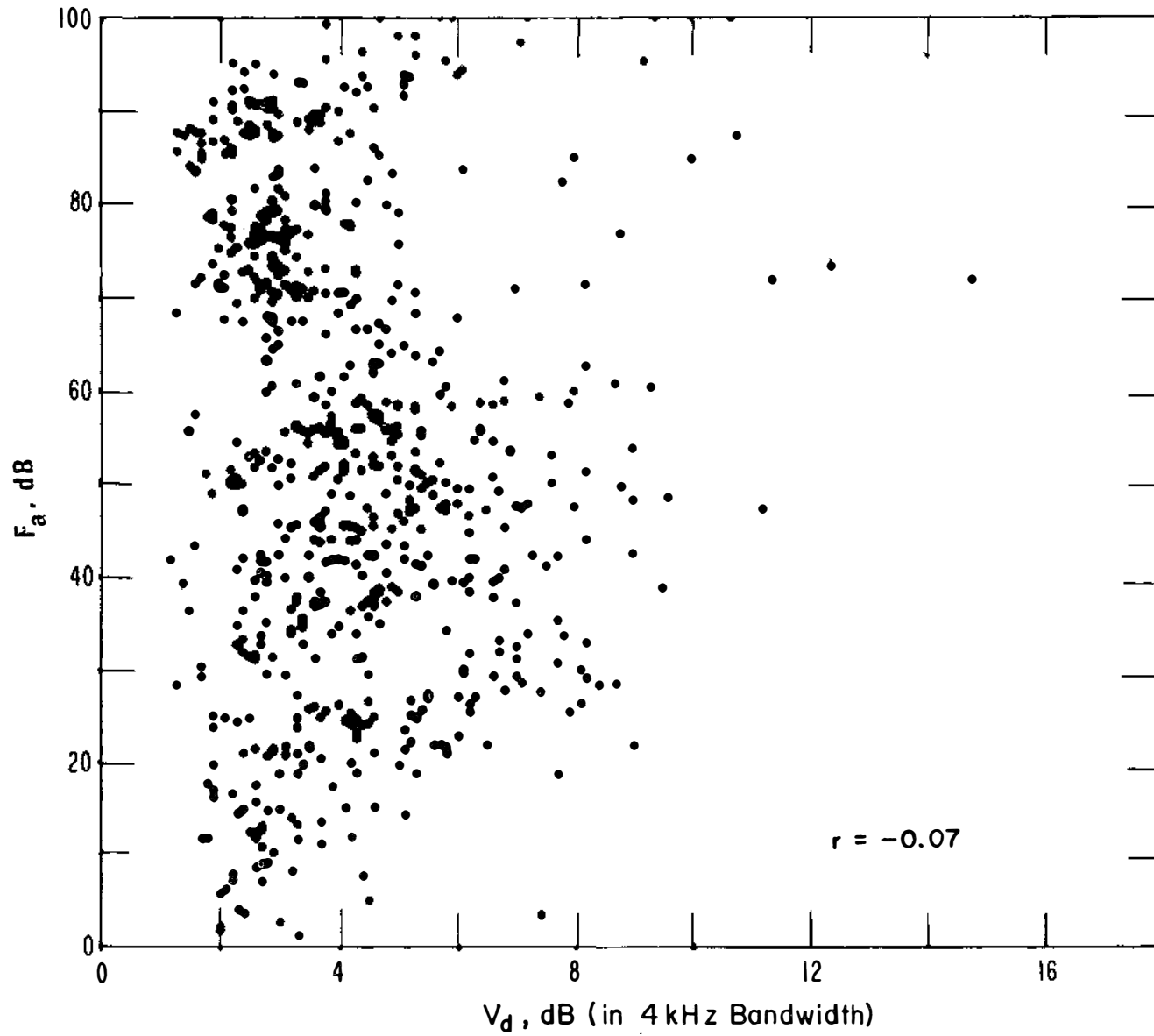


Figure 32. Lack of correlation of  $F_a$  and  $V_d$  for man-made noise.

### 4.3 Amplitude and Time Statistics

In order to determine system performance, more detailed statistical information about the received noise waveform is generally required than that given by  $F_a$ ,  $V_d$ , and  $L_d$ . Some examples of such detailed statistics of the received waveform are given in this section.

Examples of the noise envelope amplitude probability distribution are given on figures 33-37. The APD's shown are plotted relative to the power moment (in dB relative to the rms envelope voltage). The APD shown in figure 33 was measured in a 4 kHz bandwidth and at a center frequency of 48 MHz. The measurement covered a 5-min period and was made at the intersection of 28th Street and Arapahoe, Boulder, Colorado, during the evening rush hour (1655-1700 LST). The level, because of the high traffic density at the time, is quite high, having been measured at 43.5 dB above  $kT_o$ . This is approximately 1 dB higher than the estimated upper decile value for business areas. The value of  $V_d$  for this particular distribution is 5.4 dB. The APD's of the man-made radio noise measured at 102 MHz in a 4 kHz bandwidth at Grand Coulee Dam is shown on figure 34 and at Boulder, Colorado, on 30th Street between Walnut and Peak on figure 35. An APD measured in a rural area in the state of Washington is shown on figure 36. The absence of any nearby, high noise source precludes the occurrence of the very high noise spikes even at the 0.0001 percent point. The range of APD's given here for business areas (figs. 34 and 35) to rural (fig. 36) can be considered typical for this frequency and bandwidth.

The distributions measured along interstate 80 as shown on figure 37 exhibits considerably greater dynamic range than any of the other APD's shown. This principally is caused by the low rural background noise level with the high noise impulses from the traffic on the highway superimposed. This APD was measured at 48 MHz using a 10 kHz

bandwidth. The increase in bandwidth, 4 kHz to 10 kHz, will also increase the dynamic range of the noise envelope voltage.

The APD's are plotted on probability coordinates with an abscissa scale such that a Rayleigh distribution (the envelope distribution for a white Gaussian noise process) plots as a straight line with a slope of  $-1/2$ . The  $V_{\text{rms}}$  level of a Rayleigh distribution is approximately at the 36 percent point. A Rayleigh envelope distribution for Gaussian noise is also shown on figure 33. Note that the lower amplitude, higher percentage portions of all the APD's are Rayleigh in character. Even the most impulsive noise will be composed of this Gaussian background with the high noise pulses superimposed upon it. Typical APD's and their variations for residential areas for 2.5, 10, 20, and 48 MHz and a 10-kHz bandwidth have been given by Spaulding et al. (1971).

The radio noise generated internal to the receiving system (antenna circuit losses, receiver noise, etc.) is Gaussian in character and will combine with the external noise. For all the distributions shown, the receiving system noise was well below the man-made noise level. That is, the internally generated noise had no effect on the measured distributions.

A number of 6-min analog tape recordings (see Appendix A) of the pre-detection noise process have been made. The recordings were detected (to obtain the noise envelope), digitized, and computer analyzed to obtain detailed envelope statistics.

Two examples of the analysis of these analog recordings are shown on figures 38-43 and figures 44-51. The first example is for a noise sample recorded in a 4 kHz bandwidth at 250 MHz. The recording was made in a business area in Colorado Springs, Colorado, June 5, 1970, 0857-0903 MST. A randomly selected 200 msec portion of the digitized envelope is shown on figure 38, while figure 39 shows the autocovariance for this 200 msec sample. Note that for short periods of time ( $\tau < 100$  msec)

the noise appears to be uncorrelated. This is generally, but not always, the case. The APD for this 6-min recording is shown on figure 40. Also shown by the dashed Rayleigh distribution on figure 40 is the system (receiving, recording, playback, and digitizing) noise level. The average crossing rate characteristic (ACR) is shown on figure 41, while figures 42 and 43 show the pulse duration distributions (PDD) and the pulse spacing distributions (PSD), respectively.

The second example, also in a 4 kHz bandwidth, was recorded at 48 MHz in a Denver, Colorado, residential area. Two randomly selected 200 msec sample of the digitized envelope are shown on figures 44 and 46, and figures 45 and 47 give the corresponding autocovariance functions. Note the low level CW signal present on the second sample (figs. 46 and 47). The APD, ACR, PDD's, PSD's, for the 6-min recording are given on figures 48, 49, 50, and 51, respectively.

The average crossing rate, ACR, is the average number of positive crossings of given levels by the noise envelope. At the higher levels, a positive crossing of a level can be considered to correspond to the occurrence at the receiver input of a noise pulse of amplitude greater than that level. The maximum number of positive crossings depends on the receiver bandpass and noise characteristics. Additional ACR measurements have been given by ACLMRS (1966).

The pulse duration is the time that the noise pulse is above a particular envelope voltage level. That is, at a given level, it is the time between the positive crossing of the level and the next negative crossing. The curves on figures 42 and 50 show the percent (probability  $\times 100$ ) of pulses whose durations at the indicated level are equal to or greater than the time indicated by the ordinate.

The pulse spacing is the time from a negative crossing of a given level by the noise envelope to the next positive crossing of that level. The curves on figures 43 and 51 show the distribution of these times

for various levels. If man-made noise was composed of pulses occurring randomly according to a Poisson distribution, the pulse spacing distributions would be exponential at the higher envelope levels. An exponential distribution plots as a straight line of slope -1 on the coordinates used for figures 42, 43, 50, and 51. As can be seen from figures 43 and 51, the pulse spacing distributions at the higher levels and wider spacings are not exponential. This indicates correlation in the noise process for these longer time periods.

These samples of the various amplitude and time statistics given here are for guidance to provide some insight into the characteristics of the noise process. They are not, however, intended to be estimates of the statistics for all types of man-made radio noise. While these are examples of the statistics that will be found, they are not average values but strictly the results of the analysis of a few samples. The statistics for the various types of man-made radio noise encountered in the environment will vary with time, location, frequency, and the receiving system.

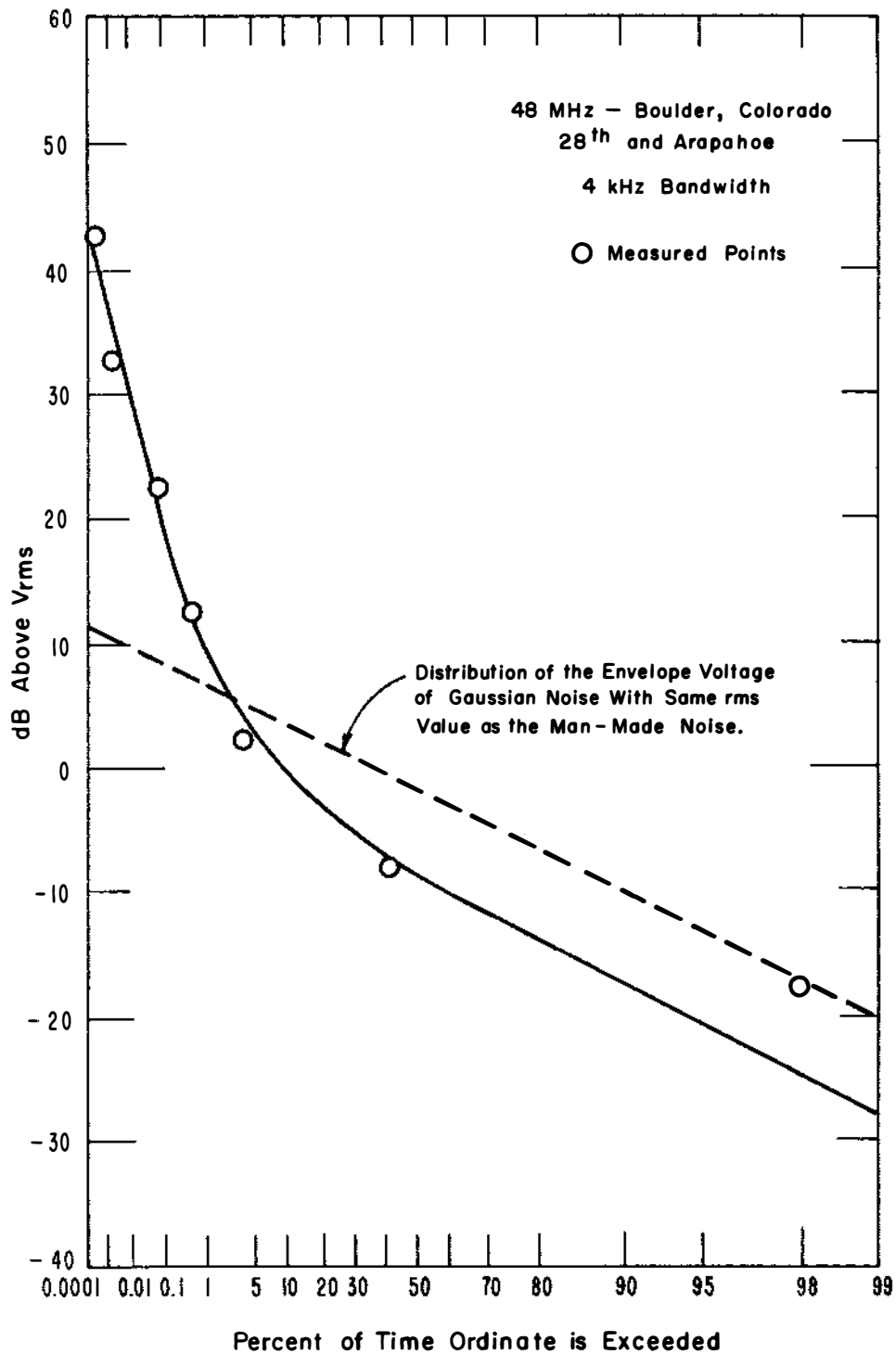


Figure 33. Amplitude probability distribution of envelope of man-made radio noise at 48 MHz.

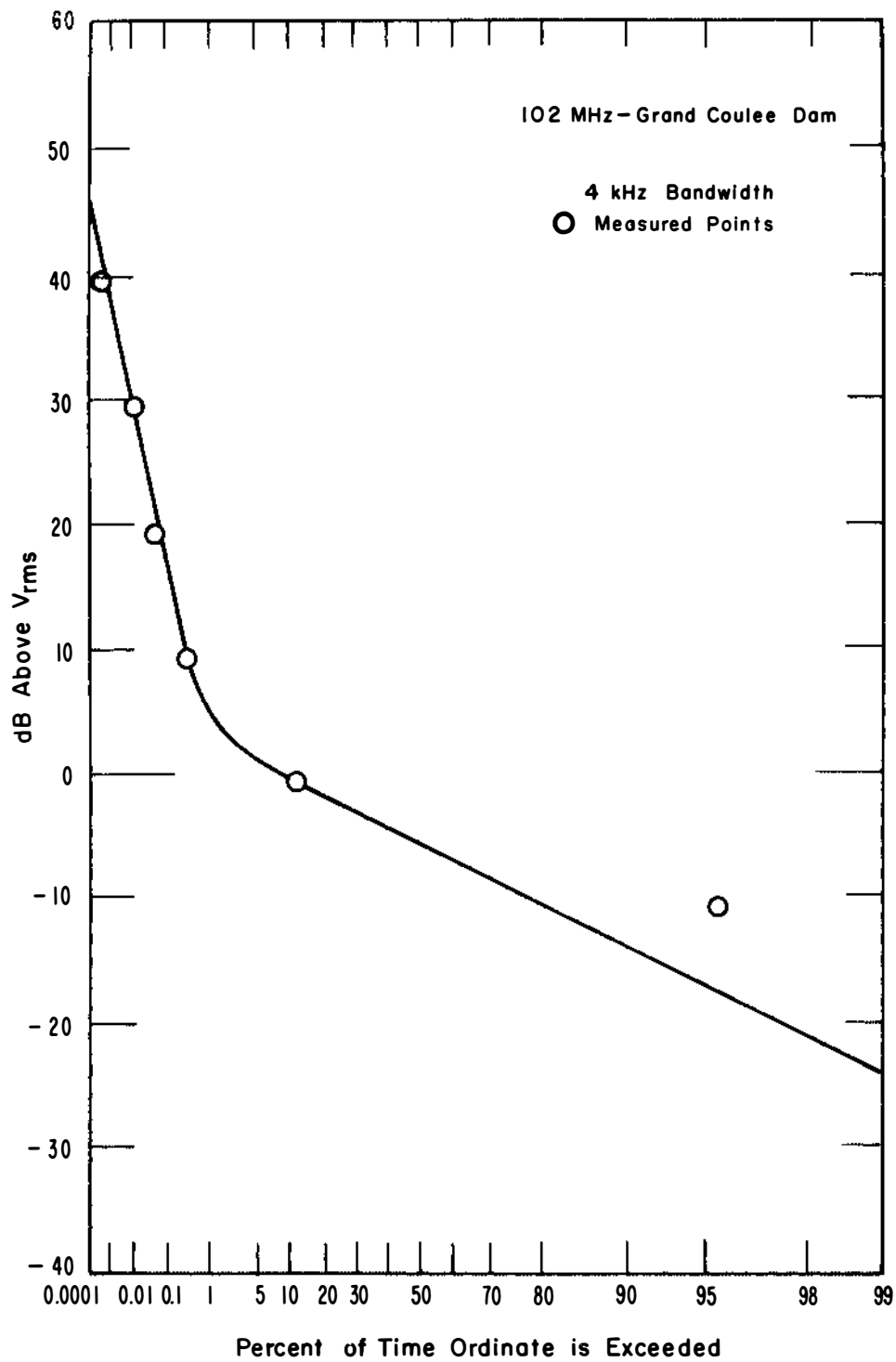


Figure 34. Amplitude probability distribution of man-made noise at 102 MHz.

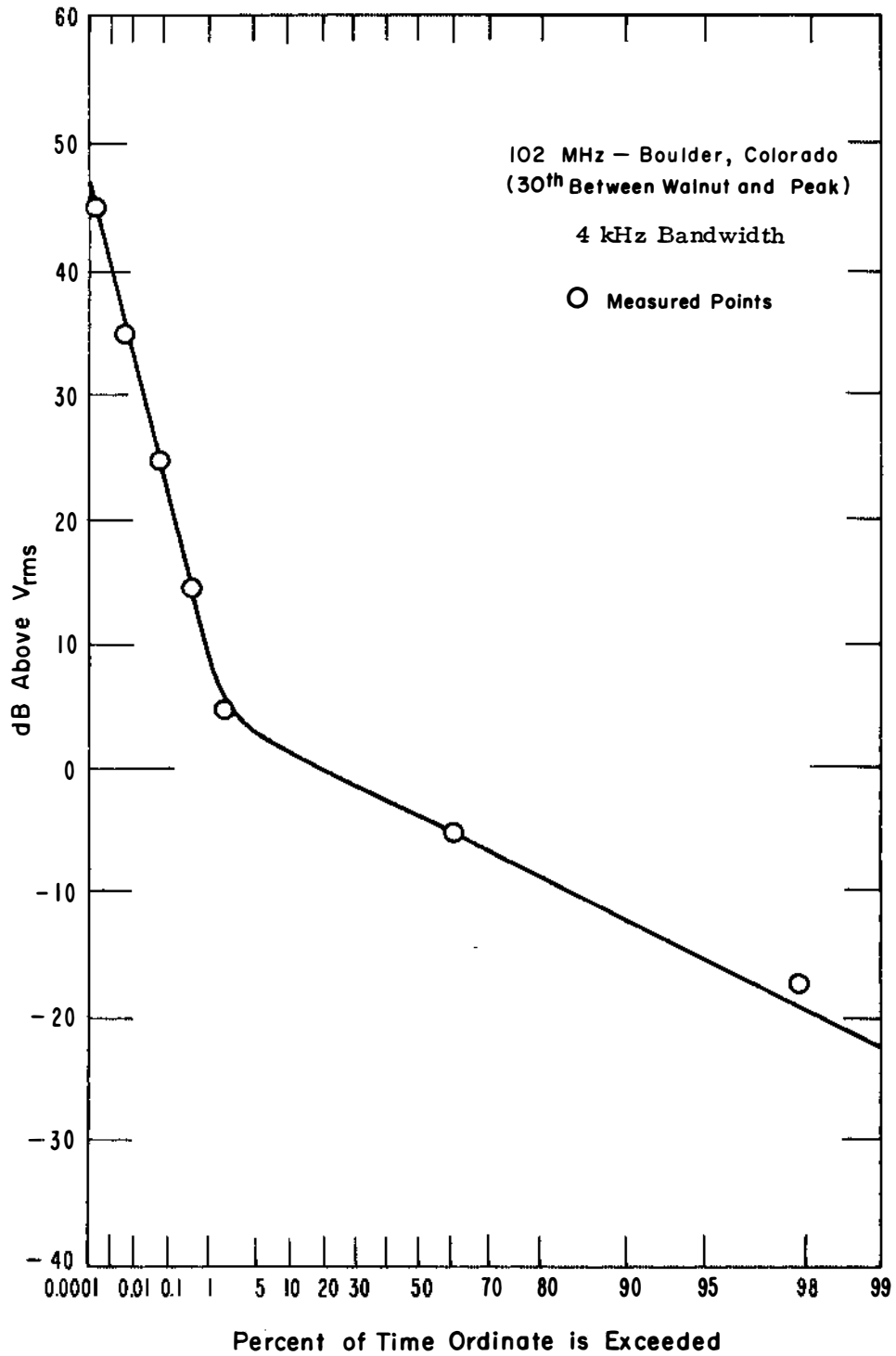


Figure 35. Amplitude probability distribution of man-made noise at 102 MHz.



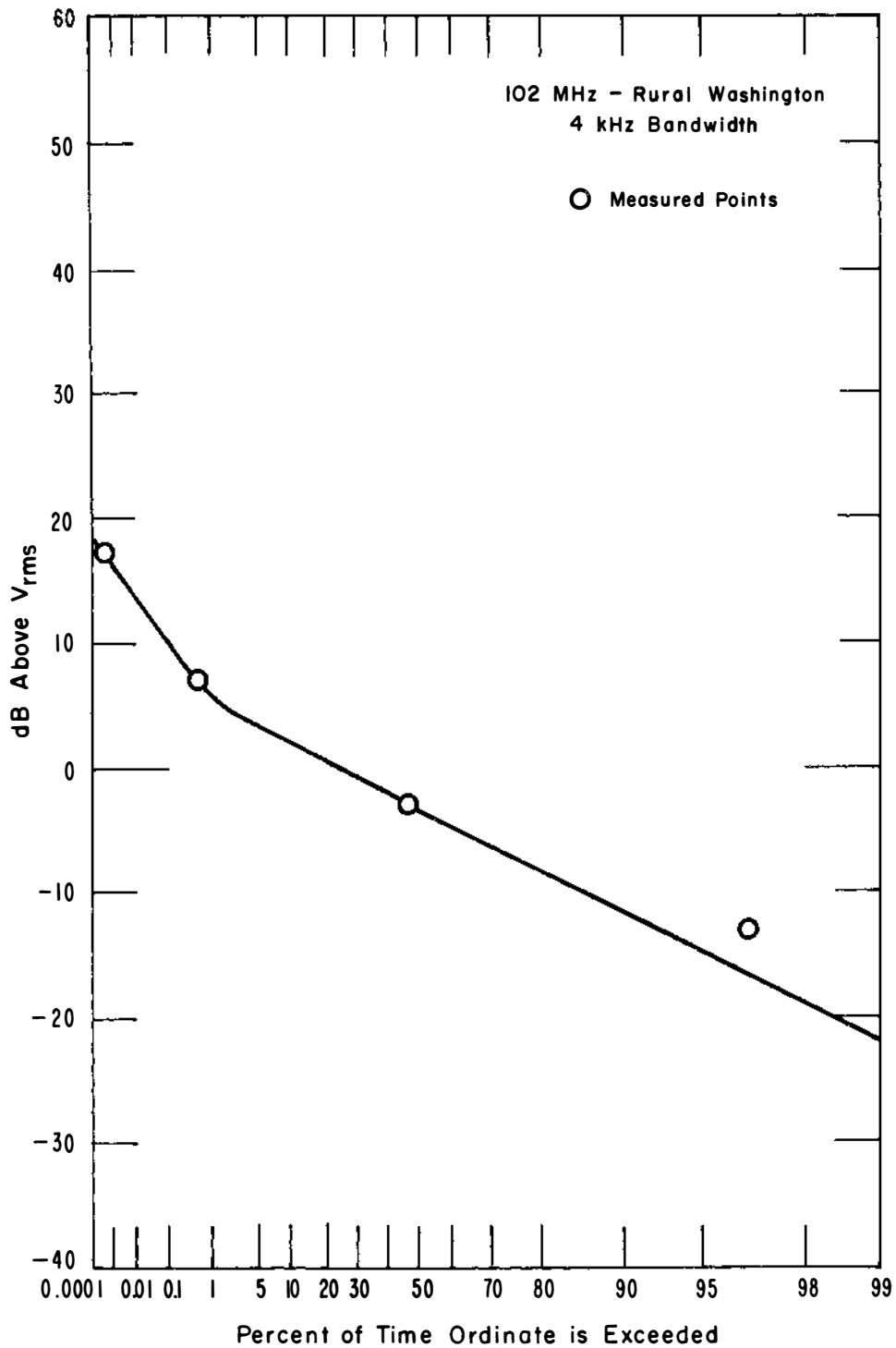


Figure 36. Amplitude probability distribution of man-made noise at 102 MHz.

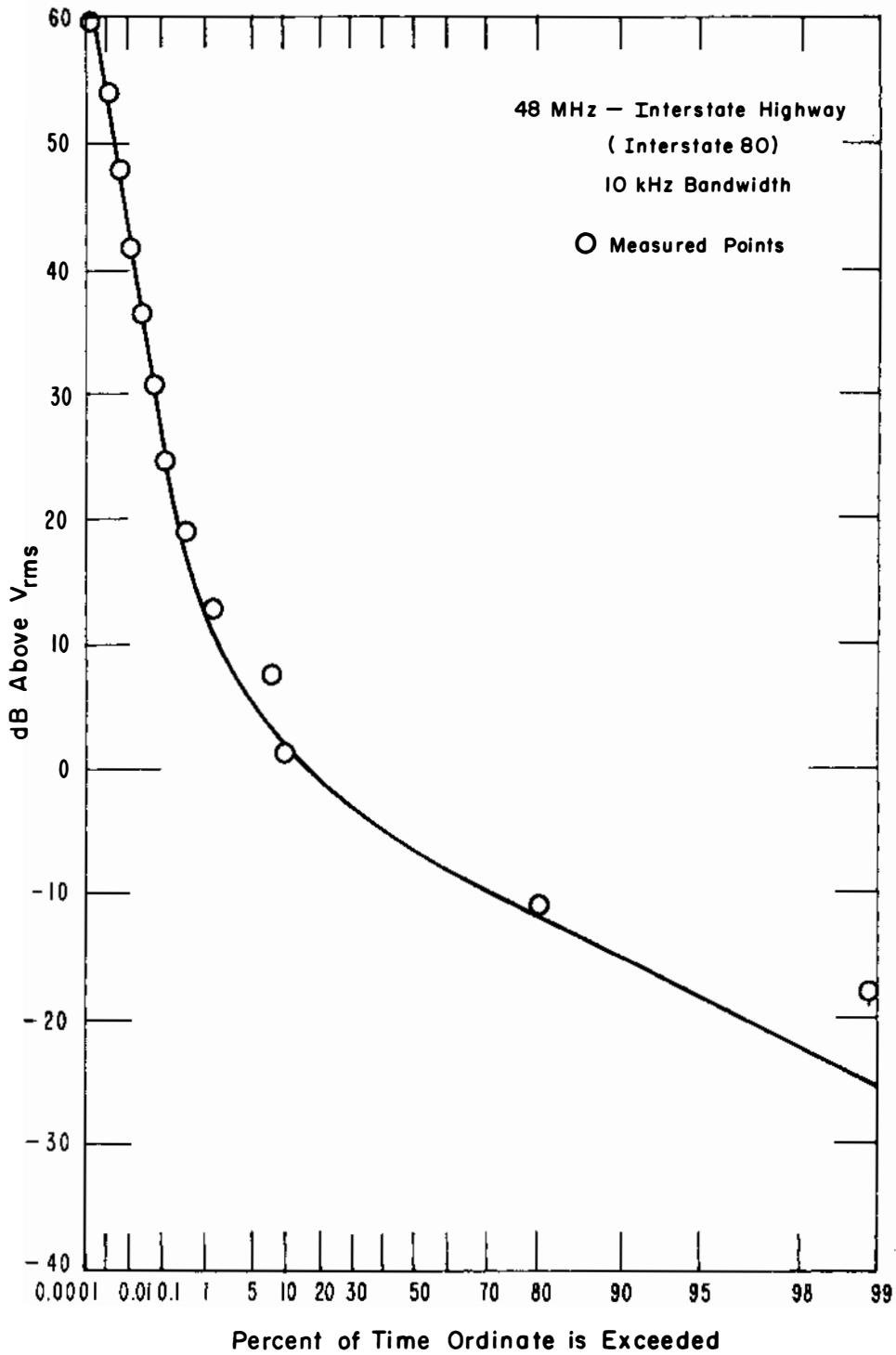


Figure 37. Amplitude probability distribution of man-made noise at 48 MHz, 10 kHz bandwidth.

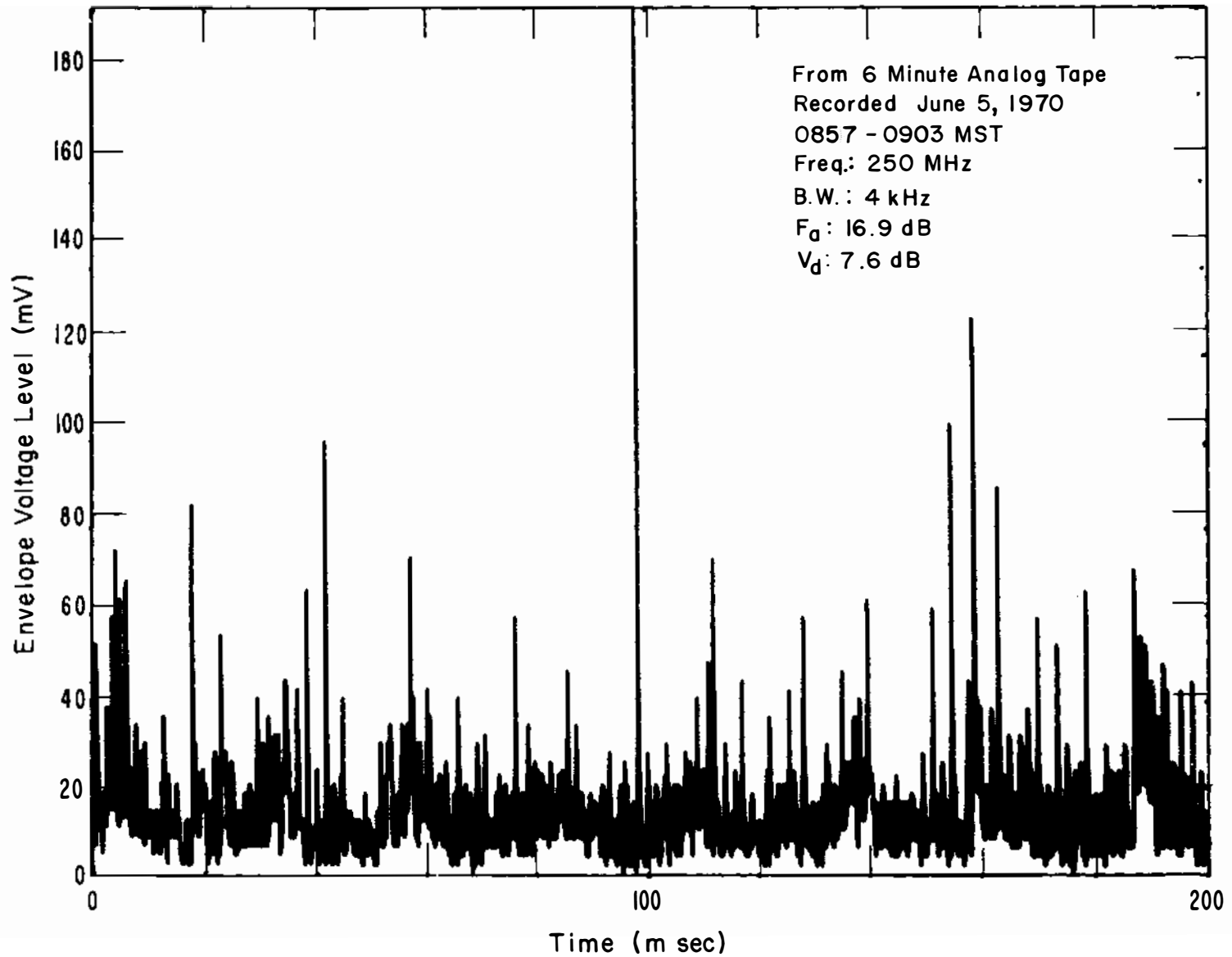


Figure 38. Randomly selected 200 ms sample of noise envelope from a 6-minute, 250 MHz central Colorado Springs recording.

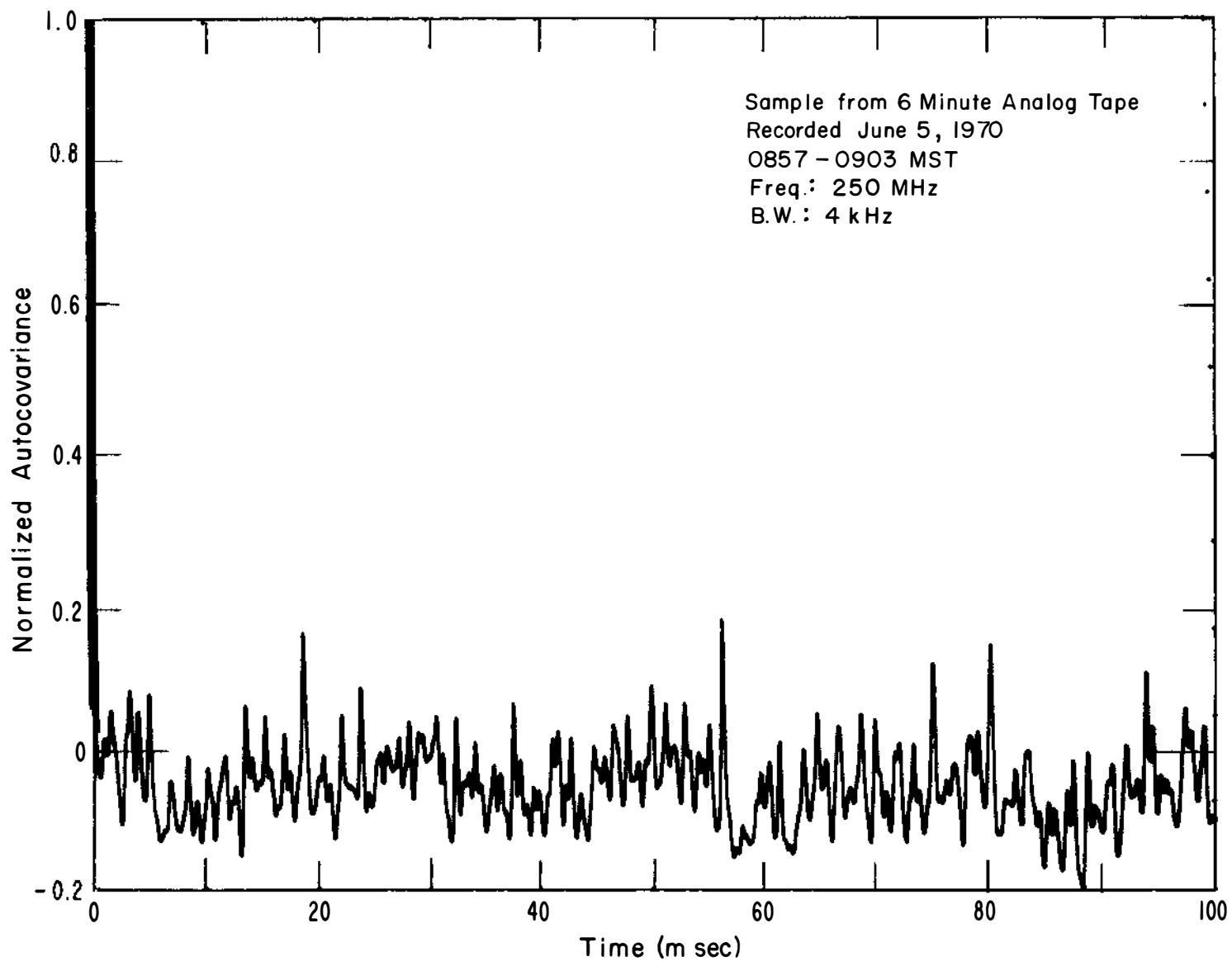


Figure 39. Normalized autocovariance for the noise sample of figure 38.

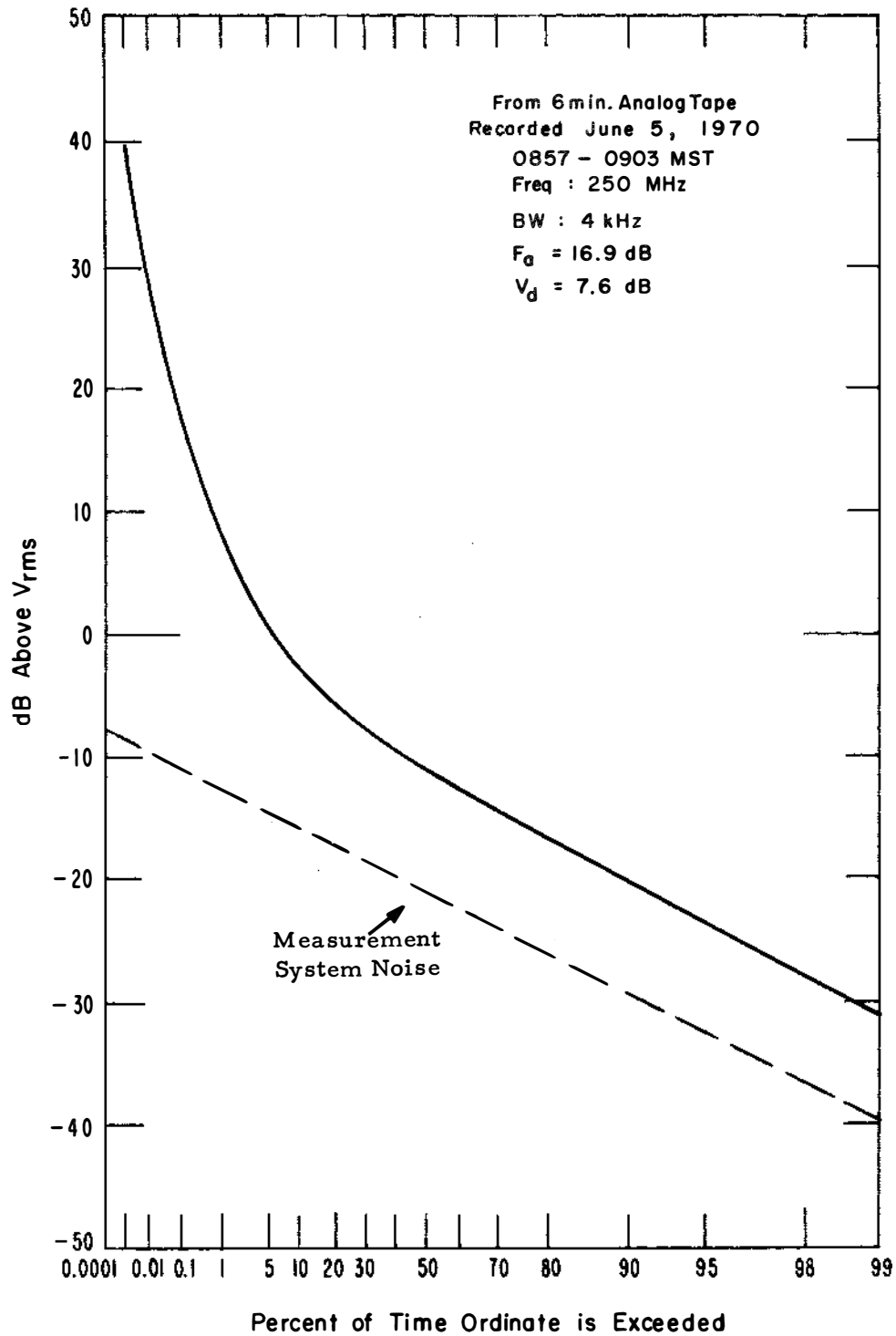


Figure 40. Amplitude probability distribution for a 6-minute sample of noise recorded in central Colorado Springs.

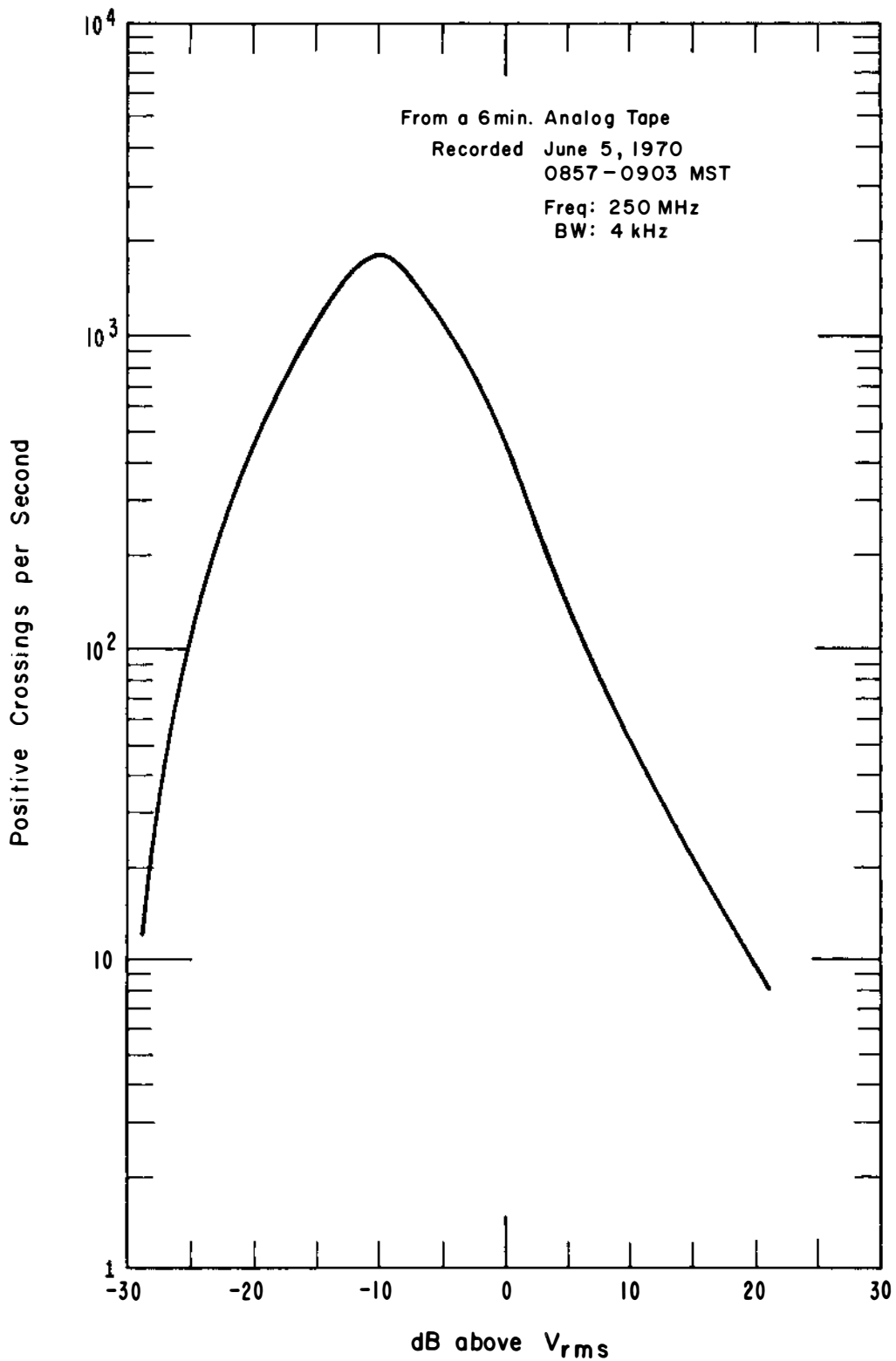


Figure 41. Average positive crossing rate characteristic for the sample of noise of figure 40.

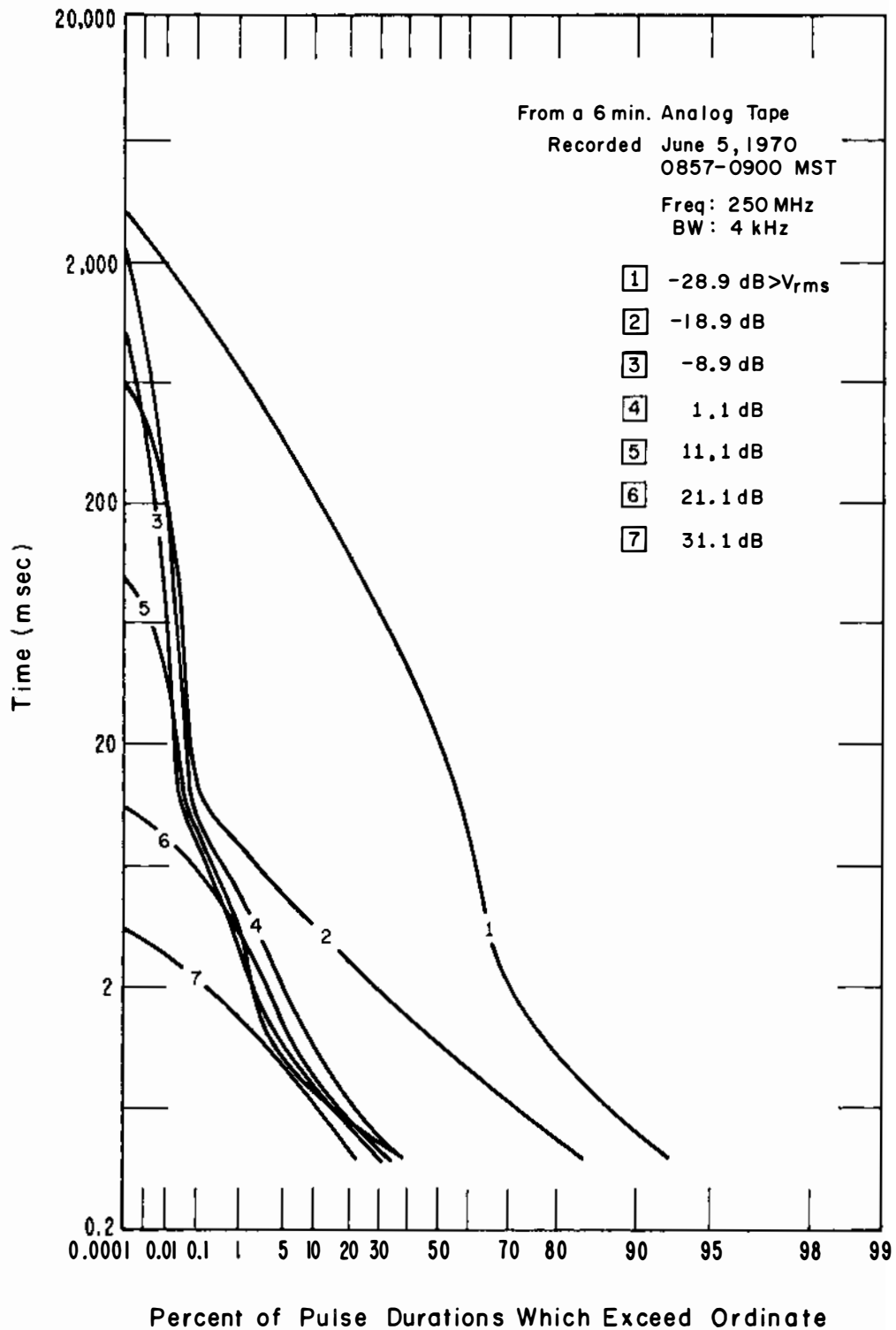


Figure 42. Pulse duration distributions for the sample of noise of figure 40.

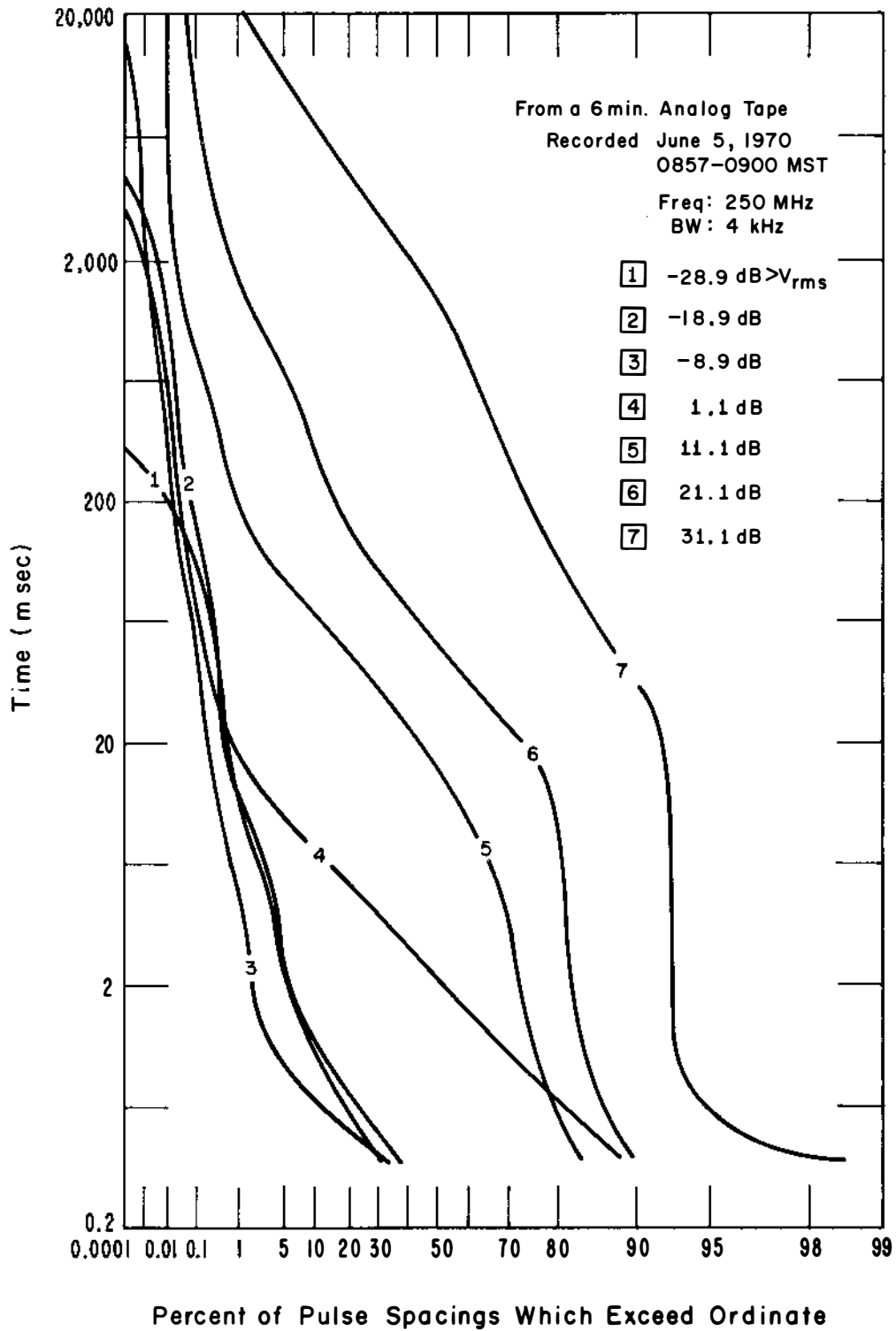


Figure 43. Pulse spacing distributions for the sample of noise of figure 40.



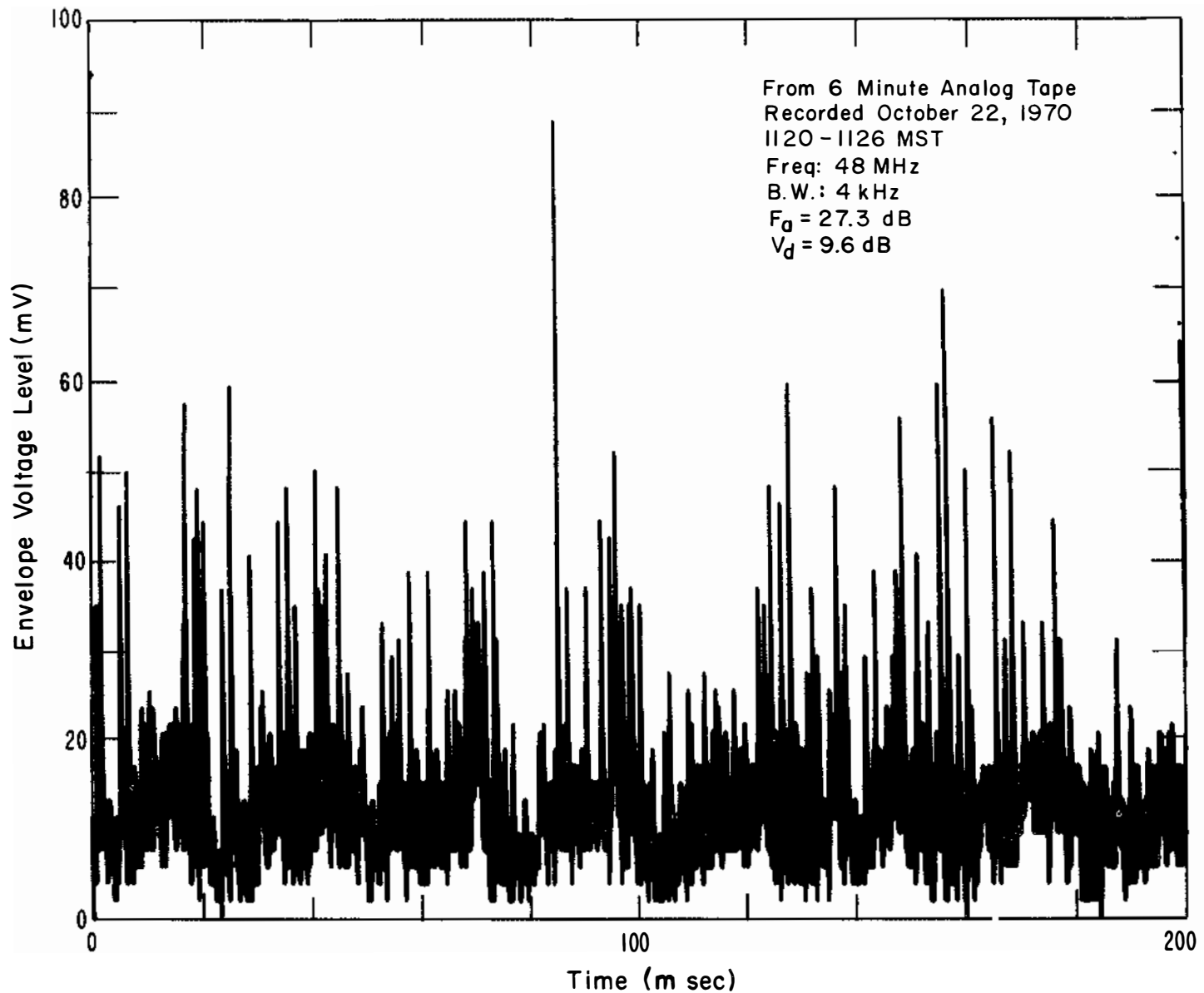


Figure 44. Randomly selected 200 ms sample of noise envelope from a 6-minute, 48 MHz, Denver, Colorado, residential area.

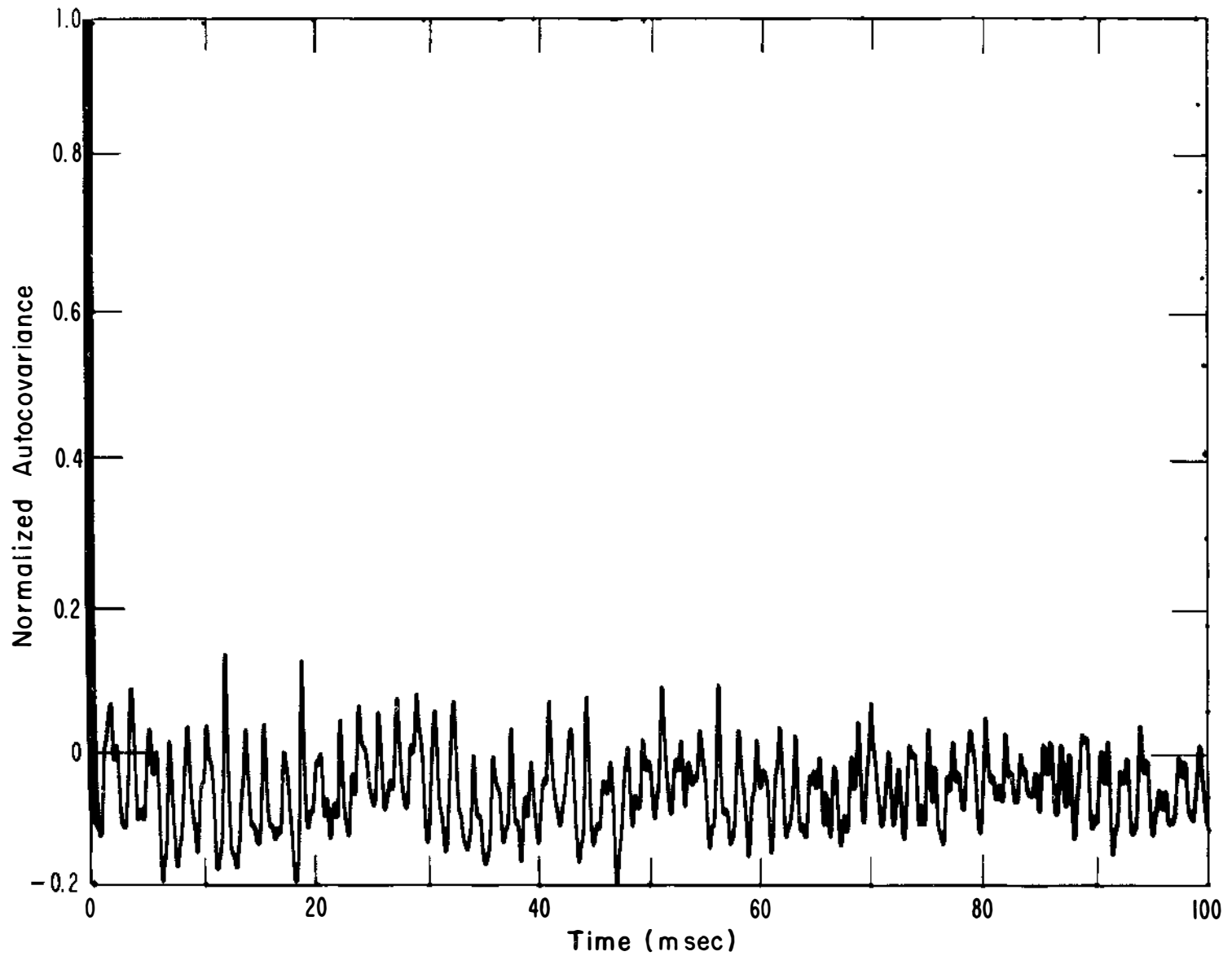


Figure 45. Normalized autocovariance for the noise sample of figure 44.

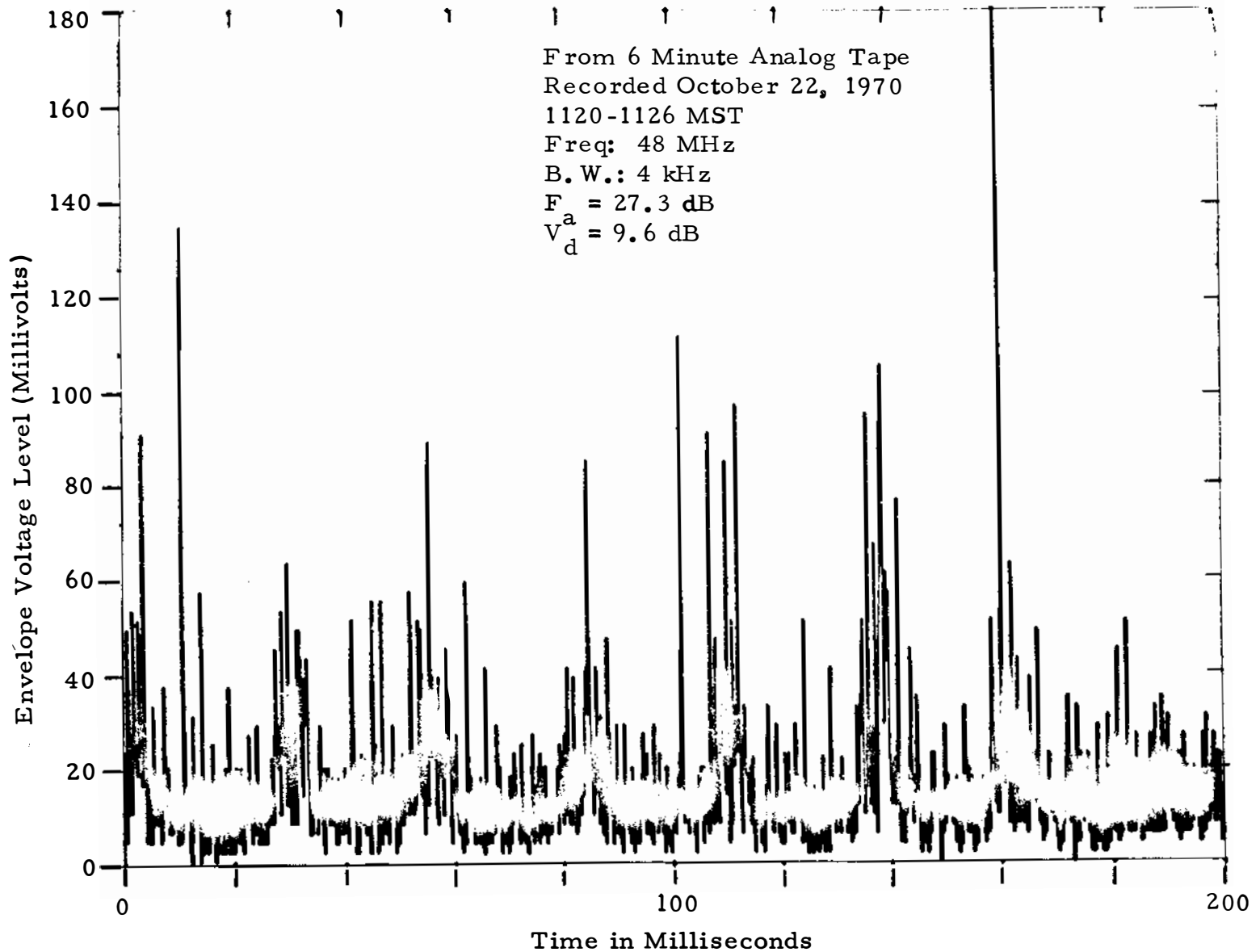


Figure 46. Randomly selected 200 ms sample of noise envelope from a 6-minute, 48 MHz, Denver, Colorado, residential area.

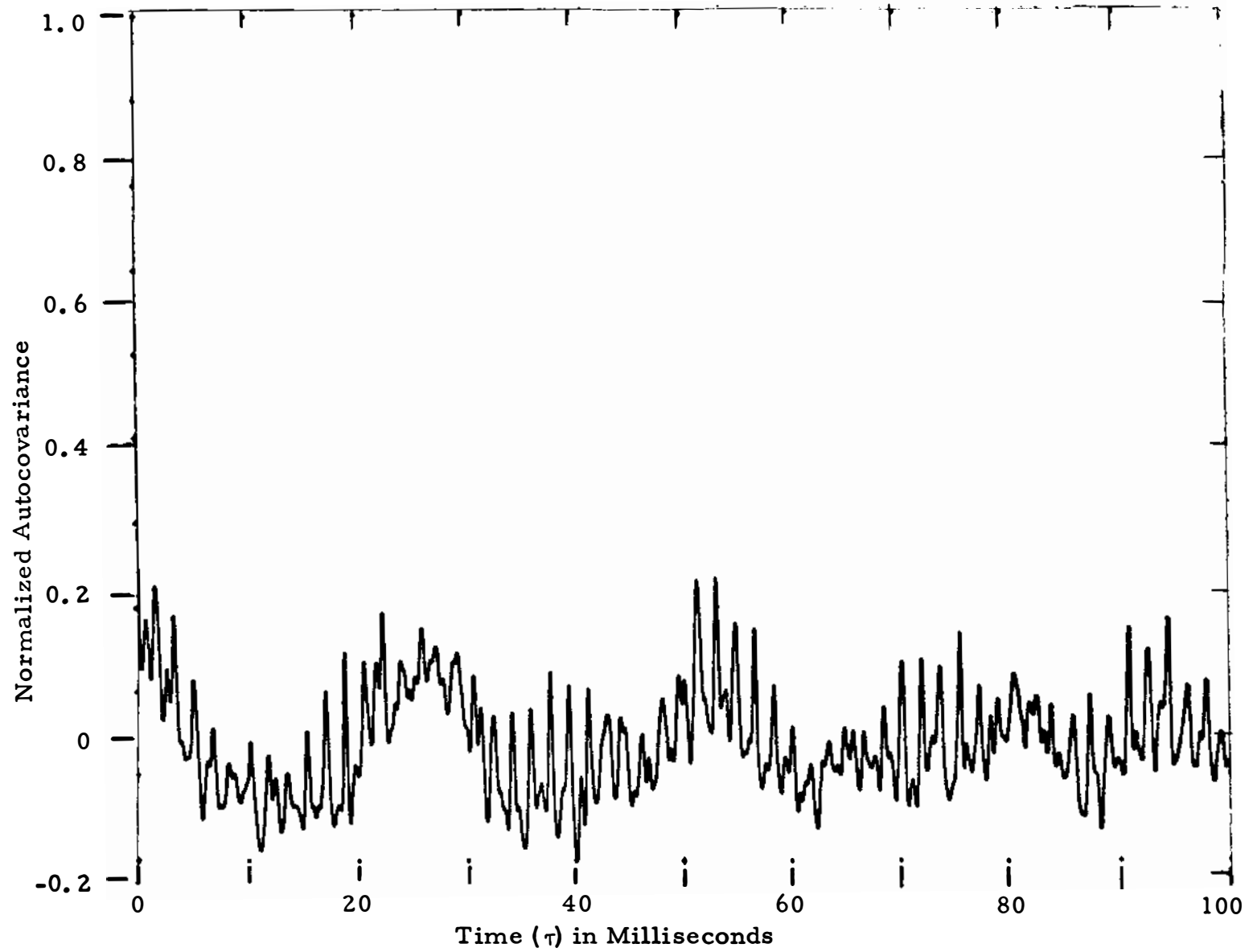


Figure 47. Normalized autocovariance for the noise sample of figure 46.

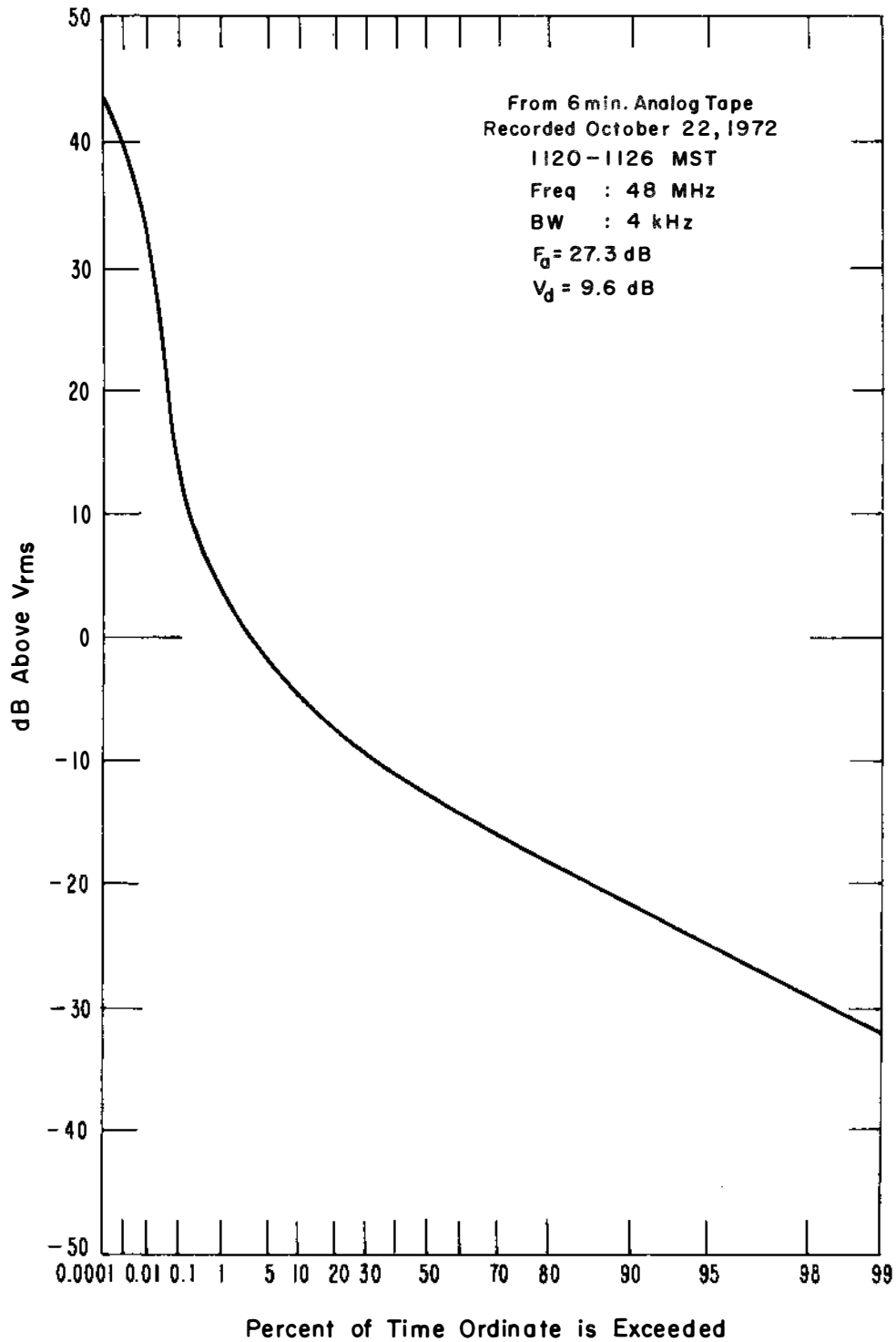


Figure 48. Amplitude probability distribution for a 6-minute sample of noise recorded in a residential area of Denver, Colorado.

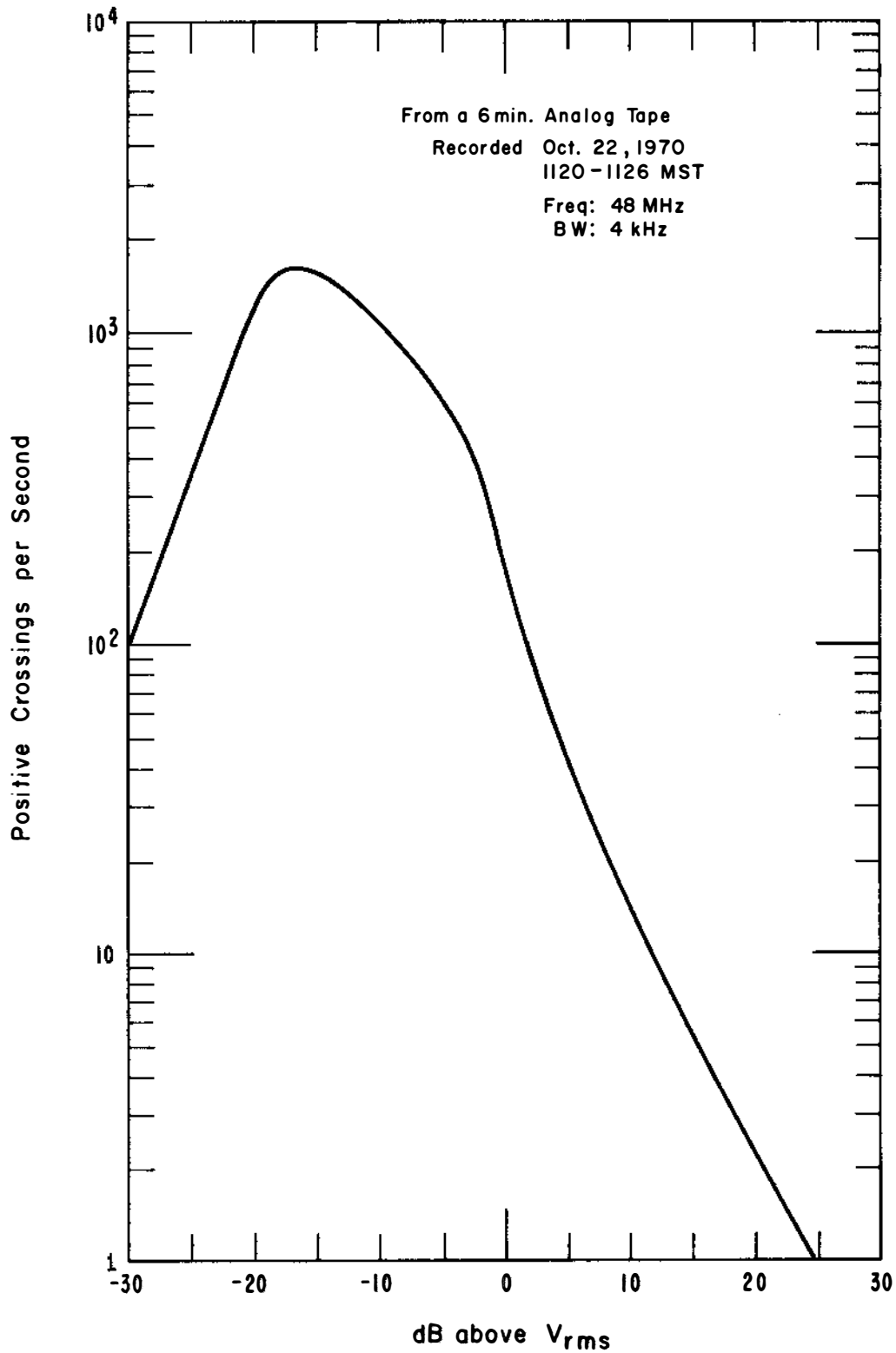


Figure 49. Average positive crossing rate characteristic for the sample of noise of figure 48.

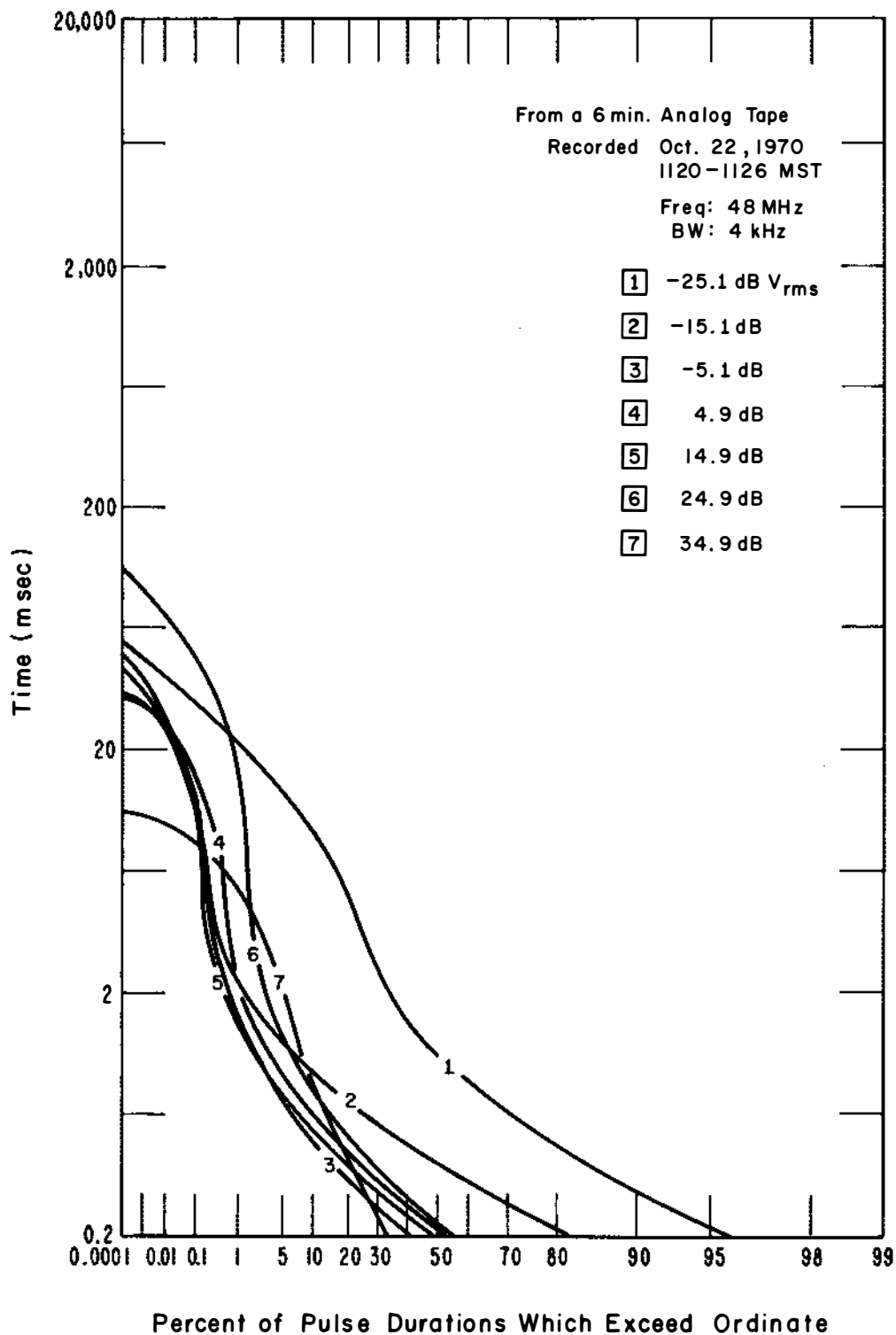


Figure 50. Pulse duration distributions for the sample of noise of figure 48.

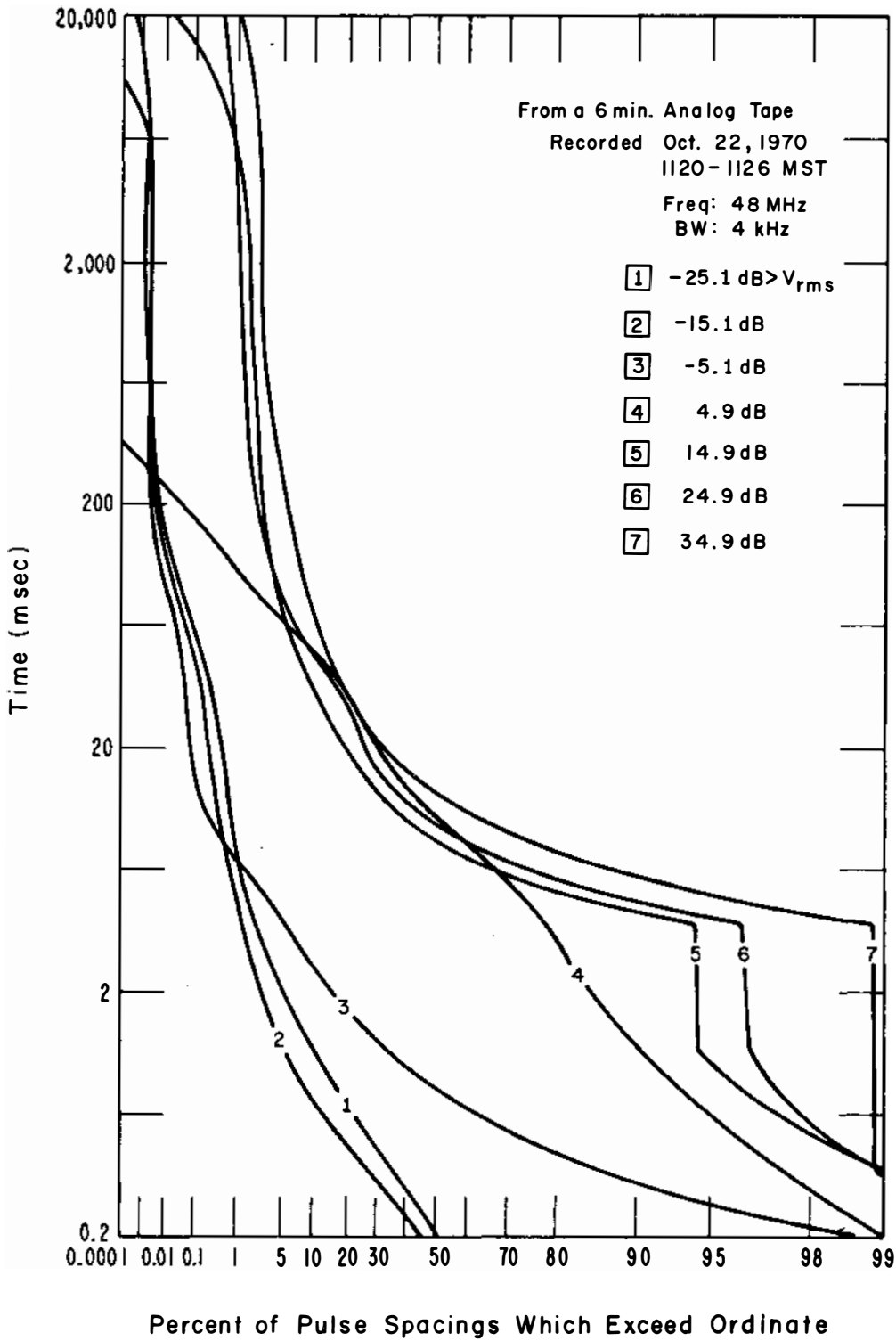


Figure 51. Pulse spacing distributions for the sample of noise of figure 48.



## 5. USE OF THE MAN-MADE NOISE ESTIMATES IN DETERMINING SYSTEM PERFORMANCE

The usefulness of the man-made radio noise predictions given here will be determined by the degree to which they are applicable to the solution of frequency management or system design problems. We now have a means of estimating the average power, the average envelope voltage, and the average log of the envelope voltage as a function of location, time, and frequency. The question of what can be done with these parameters to provide an estimate of the performance of a system that is going to operate in an environment described by the parameters must be considered.

The first determination that can be made is whether or not the system will be limited by this type of noise and, if so, for what percentage of time this is likely to be the case. There are several limitations that might prevent the system from operating satisfactorily. Let us first consider other types of noise external to the receiving system. At the lower frequencies, that is at HF and below, atmospheric radio noise often will be the limiting type of interference for a fairly large percentage of the time, especially in rural areas. A comparison of the predicted levels of atmospheric radio noise for a given location and for various times as given by CCIR (1964) with the expected man-made noise will determine the choice between these two types of external radio noise to use in the particular design calculations to be made. Since both types of noise have similar characteristics, i. e., impulsive noise spikes superimposed on a white Gaussian noise background, a comparison of the  $F_a$  values generally will provide sufficient information on the relative importance of the two. At the higher frequencies where distant sky-wave propagation will not be present, the atmospheric radio noise can almost always be neglected. Only the noise from local activity will interfere under these conditions. In some cases where

high reliability circuits are being considered, it may be necessary to determine the effect of local thunderstorm activity. In general, local activity will have the effect of disrupting the system for several milliseconds anywhere from two to three times a minute to once every 5 min over a period from 15 min to about 2 hrs. In areas of high thunderstorm activity, this intermittent interference may occur as much as 0.5 percent to 1 percent of the year. Since such circuits generally are designed to operate satisfactorily with a time availability of 0.95 (CCIR, 1966), the effect of local thunderstorm activity usually can be neglected at these higher frequencies.

The second type of noise to consider is galactic radio noise. At some locations, this may be the controlling type of noise for a large percentage of the time at any frequency above 20 MHz, but usually the man-made radio noise will be higher than the galactic noise up to some place between 100 to 300 MHz. The predicted curve of galactic radio noise received on a short vertical antenna is shown on figure 1 (from CCIR, 1964). While the variation of this type of noise will be only about  $\pm 2$  dB with location and time for this antenna (Crichlow et al., 1955), the level at the terminals of any narrow beam antenna can vary considerably, depending upon the part of the sky within the antenna beam. For an antenna pointing in a fixed direction relative to the earth, the variations of the galactic noise level, if this is the predominant noise, can be measured easily as various parts of the galaxy pass through the antenna beam. Once this pattern has been found for a one-year cycle, it generally will be repeated with only minor variations. The largest variation would be due to the sun passing through the antenna beam if a  $0.5^\circ$  (or less) beamwidth were used. If the galactic noise information is required prior to the installation of a highly directional antenna, the expected levels can be calculated using sky temperature charts and knowing the antenna characteristics. Galactic noise is Gaussian in

character, and this must be considered when comparing it with man-made radio noise. That is, even though the  $F_a$  value for the man-made noise may be below the  $F_a$  value for the galactic noise, the impulsive nature of the man-made noise can result in noise pulses greatly exceeding the galactic noise level.

If an omnidirectional antenna is used or any type of directional antenna used in a position where the ground is in the antenna beam, thermal noise from the ground, being at reference temperature, must also be considered. However, the only time that this contribution is of any consequence is when the external noise from all other sources is equal to or less than an  $F_a$  value of 6 dB. This type noise is also Gaussian in character, and, therefore, the APD is Rayleigh.

Consideration must also be given to the noise factor of the receiving system including antenna circuit losses, transmission line losses, and the noise figure of the receiver, including any preamplifiers or lossy circuits. In general, the receiving system noise figure does not need to be much lower than the expected external noise. If it is much higher than the expected external noise, redesign or improvement in the system noise figure generally will allow improvement in the performance of the communications system. Other factors (signal fading characteristics, intermodulation products, overload characteristics, etc.) may be the limiting factor in the system. If this is the case, equipment or system redesign may decrease these problems.

If it has been established that man-made radio noise will be the limitation to the operation of the system under consideration, the system performance in the predicted environment must be determined. In order to make this determination, a knowledge of how the system will operate in various noise environments is necessary. The required signal-to-noise ratio (SNR) will be dependent on the character of the

additive noise and the characteristics of the system under consideration. When the SNR required to give satisfactory service in the expected type of environment has been determined, the required signal power at the terminals of a lossless receiving antenna (assuming all circuits will affect the signal and noise in the same manner) can be found by

$$P_s = F_a + B + R - 204 \text{ dBW} ,$$

where  $P_s$  = the required signal power at the receiving antenna terminals and  $R$  = the signal-to-noise ratio, in dB, required for satisfactory service. The value of  $F_a$  used here can be the estimated value for some percentage of time based on the median predicted value for the location, the decile value given for that type of location, and an estimate of the expected diurnal variation. This will then provide an estimate of the percentage of time that the required signal-to-noise ratio (and satisfactory service) will be achieved. The difficult part, of course, is determining the required SNR. Some values of required SNR's for certain systems have been established by the International Radio Consultative Committee (CCIR), The Electronics Industries Association (EIA), the Federal Communications Commission (FCC), etc. These values often are given based on the assumption that the interfering noise is Gaussian. Impulsive noise will affect system performance quite differently, and this must be taken into account when using these SNR's. The dashed line on figure 33 is the envelope distribution for Gaussian noise with the same rms value as the impulsive man-made noise sample shown. If the SNR for satisfactory operation in a Gaussian noise environment is used when the actual environment is predominantly man-made noise, an error of several decibels in required signal power could be obtained. For example, consider a binary noncoherent frequency shift keying (NCFSK) system for which a bit error of  $10^{-4}$  or less is required.

For this system, the probability of bit error is given by one half the probability that the instantaneous noise envelope level exceeds the signal level (Montgomery, 1954). Therefore, from figure 33, the required SNR to achieve this performance is 9.5 dB for Gaussian noise, while for man-made impulsive noise (shown on fig. 33) a 29 dB SNR is required to achieve this same performance.

Two examples of methods used to find system performance in atmospheric radio noise are given in CCIR (1964). By using the values of  $F_a$ ,  $V_d$ , and  $L_d$  given here, the same type of analysis can be performed for man-made radio noise.

The application of the amplitude statistics of man-made radio noise in determining system performance (i.e., the required SNR) is well documented in Part II, Bibliography, of this report, especially for various types of digital communications systems. Examples of work in this area have been given by Shaver et al. (1972), Gilliland (1972), Bello and Esposito (1969, 1970), Akima et al. (1969), Omura (1969), Halton and Spaulding (1966), Bello (1965), Conda (1965), and Lindenlaub and Chen (1965). These references specify the determination of system performance in impulsive noise.

## 6. MATHEMATICAL MODELING OF THE NOISE PROCESS

A number of schemes have been developed in the past to improve the operation of various telecommunications systems operating in the presence of noise environments. In the design of optimum detection schemes, the noise usually has been assumed to be Gaussian for lack of a better model that could be handled mathematically. This was the case even though it has long been recognized that the Gaussian model is rarely found unless the limiting noise is due to noise internal to the receiving system or from galactic radio noise. Several methods have been devised for providing better operation in the presence of impulsive

noise. However, all of the more commonly used of these systems, e.g., wideband noise limiting or clipping, hole punching, smear-de-smear, etc., approached the problem by attempting to make the noise less impulsive or more Gaussian in character so that the available detection scheme would be operating in the type of noise for which it was optimized. While these methods do improve system operation under certain conditions, much greater improvement can be obtained by designing the system to match the noise.

For good system design and the determination of the optimum receiving system, more information about the noise is required than generally can be obtained from measurements. Therefore, a mathematical model for the random noise process (as seen by a receiver) must be developed. The problem is to develop a model for the noise that: (1) fits all the available measurements, (2) is physically meaningful when the noise sources, their spatial distribution, etc. are considered, and (3) is simple enough so that the required statistics can be obtained for solving the signal detection problem. In short, the problem is to do for the non-Gaussian man-made noise channel what statistical communications theory has achieved for the Gaussian channel.

Many attempts have been made in the past to model narrowband impulsive noise processes (Furutsu and Ishida, 1960; Bowen, 1963; Beckman, 1964; Galejs, 1966; for example). These models are essentially similar to each other in that they take the received noise to be composed of a sum of filtered impulses whose amplitude and occurrence in time follow various probability distributions. While the above forms are motivated well physically and can be made to fit measured first-order statistics (APD of the noise envelope and ACR, for example), they have several disadvantages as far as the signal detection problem is concerned. For example, these forms generally assume independence in the noise which is not always the case. They are not directly

relatable to the physical characteristics of the noise sources, and the resulting statistics are so mathematically complicated that no attempt has been made to apply them to signal detection problems.

Various empirical models have been developed and related to measurements of impulsive noise (especially for atmospheric noise). These models do not represent the noise process, but only the measured statistics of the process and, therefore, are not, in general, applicable to determining optimum systems for the particular noise under consideration. These models have been used to determine the performance of various suboptimum receivers. Reference to all the above work can be found in the Bibliography, Part II, of this report.

Hall (1968) has developed a different model for impulsive phenomena and applied it to signal detection problems considering LF atmospheric noise. This model, in modified form, also has been shown to be appropriate for HF atmospheric noise and some kinds of man-made noise (Disney and Spaulding, 1970). While optimum receiving structures have been derived and the performance obtained, the Hall model is not easy to relate to the physical environment. Therefore, the proper values of the parameters that specify the model are difficult to obtain. Also, the model has infinite variance for a physically appropriate range of values. Recently, Giordano and Haber (1972) developed an excellent model for atmospheric noise based on the distributions and characteristics of the noise sources, and their approach might be applicable to man-made radio noise problems.

Recent work at OT/ITS has led to the development of a statistical-physical model for man-made noise (Middleton, 1972, 1973, 1974). This model is based on the actual physical parameters of the interference environment (source distributions in space and time, source waveforms, propagation, etc.). Received waveform statistics have been derived for

this model, and they presently are being compared with measurements. Work on the analysis of system performance, deriving of optimal detection schemes, obtaining the performance of these optimal structures, waveform designs, etc. is in progress at OT/ITS using this basic statistical model.

## 7. CONCLUSIONS AND DISCUSSION

Estimates of the levels of man-made radio noise that will occur at locations and times in the future have been given. These estimates were obtained from the analysis of the OT data base of measurements made over the past several years. A method for obtaining the available noise power at a receiving location from the automotive traffic densities in the vicinity of this location has been developed. Also, measurements showing the noise power to be expected from high voltage transmission lines have been included. Some indication regarding the relationship between the horizontal and vertical components of the noise field has also been given.

Estimates of the average and average logarithm of the noise envelope voltage are given for two bandwidths, 10 kHz and 4 kHz. It has been shown that the parameters  $V_d$  and  $L_d$  are highly correlated, but that the noise level,  $F_a$ , is uncorrelated with the noise impulsiveness (as characterized by  $V_d$ ). In addition, examples of detailed amplitude and time statistics of the received noise process have been shown.

While the OT/ITS data base is undoubtedly the largest single source of noise data available, it is still a relatively small sample considering the few areas actually investigated. One can ask if the results given are typical of all cities since most of the business and residential area measurements were made in medium or small size metropolitan areas. There appears to be no really good way of relating the man-made noise data to what would be found in a large metropolitan area



such as New York City or Los Angeles until compatible measurements in this type of area are available for comparison. However, the following reasons seem to indicate that, with care, the estimates given here will be applicable: In general, the noise in the business and residential areas seems to be principally due to the noise sources within a fairly short distance of the receiving location. This is evidenced by the substantial changes in noise level that take place within a block when mobile measurements are being taken (Spaulding et al., 1971). A small area within a business area, as large as it is homogeneous, should not have too different characteristics, whether it is in Boulder, Colorado, or New York City. As long as traffic densities, power distribution systems, and other man-made radio noise sources are comparable and the general character of the areas is the same, the number of additional noise sources in the larger population area cannot be increased greatly per block. The only exception might possible be the presence of numerous high-rise office buildings, such as exist in some New York City business areas. In an area where freeways must carry large numbers of vehicles moving at a relatively high speed, the amount of traffic could be considerable higher, as might be the case when comparing Denver with, say, Los Angeles. However, when considering the business areas of these two locations, the street widths and speed limits are comparable; thus, traffic density cannot vary by a large amount, since traffic congestion is found at both places. From these considerations, it seems reasonable to expect the noise estimates to be as valid for New York City as for, say, Albuquerque, New Mexico, even though there is a twenty-to-one population difference.

Most of the rural data were taken in the sparsely populated areas of the western United States. Comparison with data from the few rural areas measured in the eastern United States does not seem to show

significant differences, since these values were within the range of variations found from place to place in the western areas. The presence of nearby power lines, however, should be considered in all areas but especially in rural areas and at frequencies below about 20 MHz.

The analysis in this report indicates that the noise power decreases with increasing frequency at a rate of 27.7 dB/decade. Whether this same trend continues at frequencies above 250 MHz is unknown; in fact the 250 MHz values would suggest that the noise power might not decrease as rapidly, or even decrease at all, with increasing frequency for frequencies above about 100 MHz. There are some contentions that the man-made radio noise from ignition systems will show a peak between 300 and 500 MHz. However, the AMA peak measurements on individual cars do not bear this out, although peak values cannot be related to the received noise power. Also, the 250 MHz OT/ITS values may be high because of the editing process necessitated by the recording system noise factor at this frequency.

The results given in this report can only give estimates of the man-made noise at average or typical locations and at ground level. Any strictly local unusual effects must also be considered. For example, OT/ITS personnel found strong elevator control noise at 1.7 GHz to be the predominant source of interference at the top of an 18-story building, noise from computers and peripheral equipment to be even higher than traffic noise on the highway near the buildings at the old NBS site in Washington, D.C., and that the highest noise source at Pow Main, Alaska, was a beacon light on top of a 200-ft tower.

In 1967 the authors of this report prepared an estimate of the man-made radio noise expected in urban, suburban, and rural locations for JTAC (1968). Since the present estimates show as much as a 10 dB difference from the previous JTAC estimates and since the JTAC estimates have been widely used, a comparison of the two sets of

estimates is in order here and is shown in figure 52. Note the scale change for the three types of areas on this figure to provide separation of the sets of curves. The first noticeable difference is in the shape of the JTAC curves with a break between 10 and 20 MHz. This occurred when data were combined from measurements made by various investigators at different times, locations, and frequencies, with no one set of data covering the whole frequency range. The break seemed not unlikely at the time since between 10 and 20 MHz the predominant noise sources change from those associated with power lines to automotive ignition systems. It appears now, though, that the real cause was due to the time and location variation, the incomplete frequency coverage of the measurements, and the attempt to relate dissimilar parameters.

The next obvious difference is in the nomenclature used to describe the types of areas. The designations of business, residential, and rural were chosen in place of urban, suburban, and rural, since the latter are based more on political divisions than on the uses of the area. For example, urban is within the limits of a city, while suburban is considered to be a fairly populous area surrounding a city but outside the city limits. However, the man-made radio noise is similar for residential areas or for business areas (shopping centers, manufacturing and service locations), whether they are within the political boundaries of a city or in a suburban area. Therefore, the new designations are more definitive and can be better identified and described without the ambiguities arising from using the previous designations.

The analysis of additional data has decreased the difference between the average values for the three types of areas. A good part of this difference results from the fact that the JTAC rural curve below 20 MHz was greatly influenced by the inclusion of the CCIR man-made rural noise data (CCIR, 1964). In the present analysis, these data were not included in the general rural area estimates since the data

were from locations carefully selected in each case to be as free of man-made radio noise as possible. In addition, the data base from these locations far exceeded the amount of data collected at all other rural locations and would give undue influence to an estimate utilizing all rural data in one group. Altogether, a much better estimate of the man-made radio noise and its location and temporal variations should be obtained from the present estimates than from the JTAC values.

#### 8. ACKNOWLEDGMENTS

The authors wish to thank the personnel taking the data in the field and doing the data reduction and preliminary analysis without whose conscientious efforts this report would not be possible. The efforts of Don Zacharisen of ITS, who performed the computer programming and data analysis, and Larry Schultz, who advised in the proper mathematical analysis of the data, are especially appreciated. Special thanks are given to George Hagn of Stanford Research Institute, Ed Skomal of Aerospace Corporation, and A. G. Hubbard of the Department of Defense for their invaluable discussions, comments, and suggestions after reading the first draft.

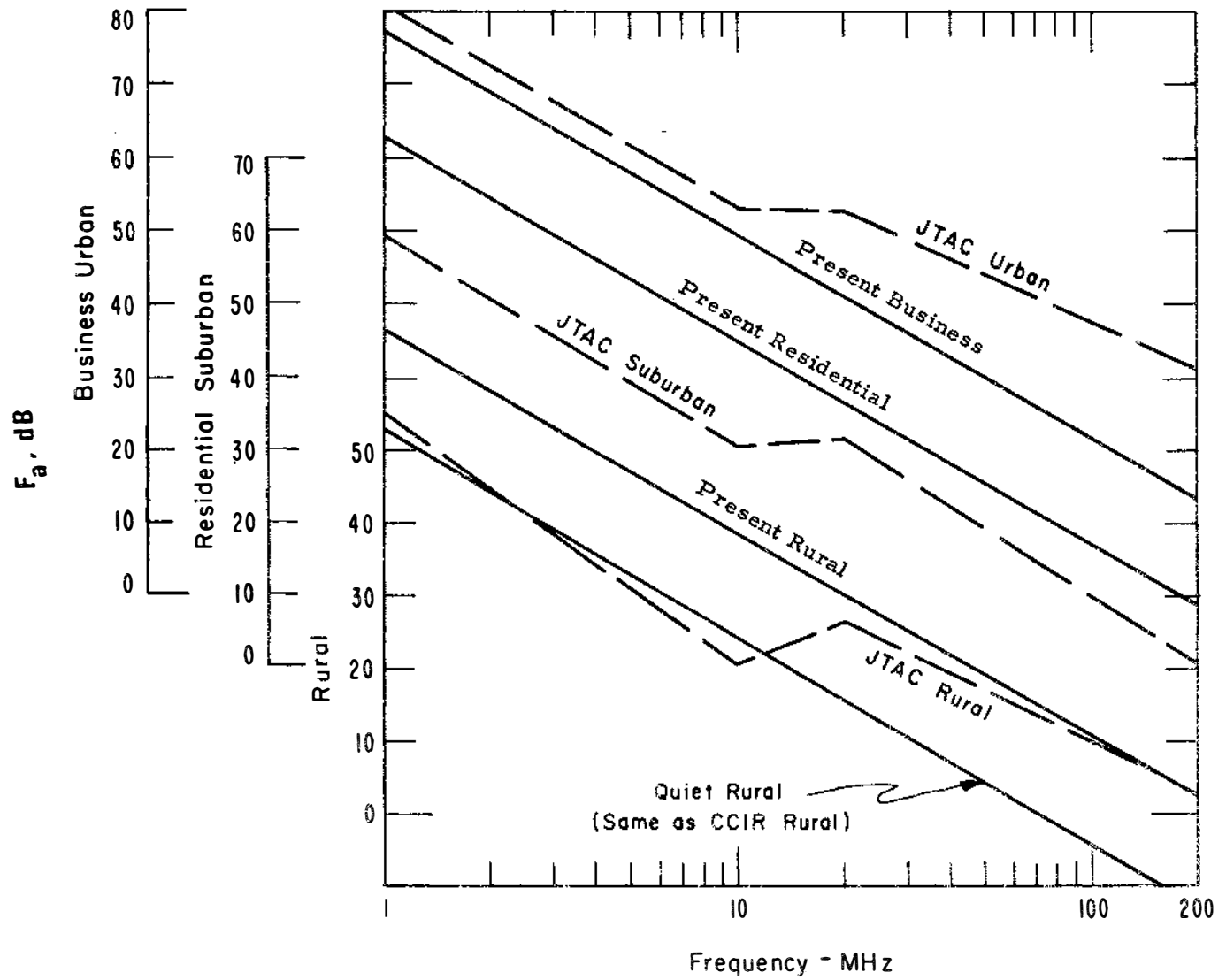


Figure 52. Comparison of present estimates with JTAC (1968) estimates.

## 9. REFERENCES

- ACLMRS (1966), Man-made noise, Report to the Technical Committee of the Advisory Committee for Land Mobile Radio Services from Working Group 3 (Jules Deitz Chairman), (U. S. Government Printing Office).
- Automobile Manufacturers Association (1971), Data package, Radio Interference Tests, South Lyon, Michigan, June 1417, Automobile Manufacturers Association Inc., Detroit, Michigan.
- Akima, H., G. G. Ax, and W. M. Beery (1969), Required signal-to-noise ratios for HF communications systems, ESSA Technical Report ERL 313-ITS92.
- Beckman, P. (1964), Amplitude probability distributions of atmospheric radio noise, Radio Science, Vol. 68D, No. 6, pp. 723-736.
- Bello, P. A. (1965), Error probabilities due to atmospheric noise and flat fading in HF ionospheric communications systems, IEEE Trans. on Comm. Tech. Vol. 13, No. 3, pp. 266-279.
- Bello, P. A., and R. Esposito (1969), A new method for calculating probabilities of errors due to impulsive noise, IEEE Trans. Communications Technology, Vol. COM-17, pp. 368-379.
- Bello, P. A., and R. Esposito (1970), Error probabilities due to impulsive noise in linear and hard limited DPSK systems, Technical Memorandum No. T-857, Raytheon Co., Research Div., Waltham, Massachusetts.
- Bowen, B. A. (1963), Some analytical techniques for a class of non-Gaussian processes, Queens University Research Report No. 63-3.
- CCIR (1957), Revision of atmospheric radio noise data, Documents of the VIII Plenary Assembly, Report 65, International Telecommunication Union (ITU), Geneva, Switzerland.
- CCIR (1964), World distributions and characteristics of atmospheric radio noise, Documents of the Xth Plenary Assembly, Report 322, ITU, Geneva, Switzerland.

- CCIR (1966), Operating noise-threshold of a radio receiving system, Documents of the XIth Plenary Assembly, Report 413, Oslo, Reports by the International Working Party III/1, ITU, Geneva, Switzerland.
- Crichlow, W. Q., D. F. Smith, R. N. Norton, and W. R. Corliss (1955), Worldwide radio noise levels expected in the frequency band 10 kilocycles to 100 megacycles, National Bureau of Standards Circular 557.
- Crichlow, W. Q., A. D. Spaulding, C. J. Roubique, and R. T. Disney (1960), Amplitude probability distributions for atmospheric radio noise, National Bureau of Standards, Monograph 23.
- Crippen, L. J., O. D. Stewart, and J. W. Engles (1970), Program for controlling the effects of radio noise and improving telecommunications system effectiveness: Bibliography: Statistical parameters of radio noise, Naval Security Engineering Facility, 3801 Nebraska Ave., N.W., Washington, D.C.
- Crippen, L. J. (1971), Investigation of radio frequency interference at Edgell, Scotland, Final Report, Naval Electronic Systems, Test and Evaluation Facility, Project No. 70-157, Serial No. 3, March 13, 1971, Washington, D.C.
- Conda, A. M. (1965), The effect of atmospheric noise on the probability of error for a NCFSK system, IEEE Trans. Communications Technology, Vol. COM-13, pp. 280-283.
- Disney, R. T., and A. D. Spaulding (1970), Amplitude and time statistics of atmospheric and man-made radio noise, ESSA Tech. Report ERL 150-ITS98, ESSA Research Laboratories, Boulder, Colorado.
- Doty, A. C., Jr. (1971), A progress report on the Detroit electromagnetic survey, Automotive Engineering Congress, Detroit, Michigan, January 11-15, 1971, Paper No. 710031, Society of Automotive Engineers.
- Friis, H. T. (1944), Noise figure of radio receivers, Proc. IRE, 32, 419.
- Furutsu, K., and T. Ishida (1960), On the theory of amplitude distributions of impulsive random noise and its application to the atmospheric noise, J. Radio Res. Labs. Japan, Vol. 7, No. 32, pp. 279-307, July.

- Galejs, J. (1966), Amplitude distributions of radio noise at ELF and VLF, *J. Geophys. Res.*, 71, pp. 201-216.
- Gilliland, K. E. (1972), Models of nondiversity digital receiver performance in general noise, No. ESD-TR-72-295, Electromagnetic Compatibility Analysis Center, North Severn, Annapolis, Md.
- Giordano, A. A., and F. Haber (1972), Modeling of atmospheric noise, *Radio Science*, Vol. 7. No. 11, pp. 1011-1023.
- Hall, H. M. (1966), A new model for "impulsive" phenomena: application to atmospheric noise communication channels, Stanford Electronics Laboratories Technical Report No. 3412-8 and No. 7050-7.
- Halton, J. H., and A. D. Spaulding (1966), Error rates in differentially coherent phase systems in non-Gaussian noise, *IEEE Trans. Communications Technology*, Vol. COM-14, pp. 594-601.
- JTAC (1968), Man-made radio noise, Report of Joint Technical Advisory Committee, Subcommittee 63.1.3 (Unintended Radiation), Supplement 9, Spectrum Engineering, the Key to Progress, published by IEEE.
- Lindenlaub, J. C., and K. A. Chen (1965), Performance of matched filter receivers in non-Gaussian noise environments, *IEEE Trans. on Comm. Tech.* Vol. 13, No. 4, pp. 545-547.
- Middleton, D. (1960), Introduction to Statistical Communications Theory (McGraw-Hill Book Co., Inc., New York, N. Y.)
- Middleton, D. (1972), Statistical-physical models of urban radio noise environments - Part I: Foundations, *IEEE Trans. EMC*, Vol. EMC-14, No. 2, pp. 36-56.
- Middleton, D. (1973), Man-made noise in urban environments and transportation systems: Models and measurements, *IEEE Trans. on Communications*, Vol. COM-21, No. 11, pp. 1232-1241.
- Middleton, D. (1974), Statistical-physical models of man-made radio noise, Part I: First-order probability models of instantaneous amplitude (to be published as OT Report).



- Montgomery, G. F. (1954), Comparison of amplitude and angle modulation for narrow-band communication of binary-coded messages in fluctuation noise, Proc. IRE, Vol. 42, pp. 447-454.
- Norton, K. A. (1953), Transmission loss in radio propagation, Proc. IRE, 41, 146.
- Office of Telecommunications Policy (1970), Manual of Regulations and Procedures for Radio Frequency Management, Basic parameter for measurement of radio noise, Chapter 5, pp. 5-35 (sect. 5.8).
- Omura, J. K. (1969), Statistical analysis of LF/VLF communications modems, Special Technical Report 1, SRI project 7045, Stanford Research Institute, Menlo Park, California.
- Shaver, H. N., V. E. Hatfield, and G. H. Hagn (1972), Man-made radio noise parameter identification task, Final Report, SRI Project 1022-2, Stanford Research Institute, Menlo Park, California.
- Spaulding, A. D., W. H. Ahlbeck, and L. R. Espeland (1971), Urban residential man-made radio noise analysis and predictions, OT/ITS Telecommunications Research and Engineering Report 14.
- Spaulding, A. D. (1971), Amplitude and time statistics of urban man made noise, IEEE International Conference on Communications, Conference Record, IEEE Cat. No. 71C28-COM.
- Watt, A. D., R. M. Coon, E. L. Maxwell, and R. W. Plush (1958), Performance of some radio systems in the presence of thermal and atmospheric noise, Proc. IRE, Vol. 46, pp. 1914-1923.
- Wozencraft, J. M., and I. M. Jacobs (1965), Principles of Communications Engineering (New York, Wiley).

## APPENDIX A

### MEASUREMENT METHODS USED TO OBTAIN THE DATA BASE

Data used in this report were obtained using the OT/ITS mobile radio noise lab. The exclusion of other data was felt justified, not on the basis of the validity of the other data, but because of lack of compatibility with data used in this report. In many instances parameters have been measured (e.g., peak or quasi peak) which by themselves do not provide sufficient information for frequency management or system design considerations and, without further information about the noise process from which the measurements were obtained, cannot be related to other parameters of the radio noise. In general, other measurements provided information at only one or two frequencies, and attempting to combine these measurements with others proved futile since frequency, time, and location statistics were hopelessly intermixed.

Since the entire data base used here came from measurements taken with the OT/ITS mobile radio noise lab, a description of the noise lab and the equipment involved, as well as some information on measurement techniques, may prove helpful in providing a better understanding of the predictions. This appendix is principally a description of this facility and its advantages and limitations for use in obtaining an adequate man-made radio noise data base. The mobile laboratory consists of a tractor and van. The tractor utilizes a full diesel engine and was purchased under the MIL-specifications for a quiet vehicle. Additional noise suppression was added after delivery; e.g., suppression on windshield wiper motor, alternator and controls, wheel bearings, etc. A diesel generator set was installed between the cab and the fifth wheel to provide power for mobile or remote operation. A low-boy type semitrailer van is used so that a two-meter-high vertical antenna on the van roof

will clear power and telephone lines that might be encountered during mobile measurements. The van has an exterior aluminum skin with the roof acting as the ground plane for the receiving antennas. The van is heated and air-conditioned for temperature stability, thus providing for measurement stability after approximately a half-hour equipment warm-up period.

The measuring-recording system is shown in the block diagram figure A1. Any eight of the ten nominal recording frequencies can be used simultaneously. The ten frequencies were chosen with approximately octave spacings between 250 kHz and 250 MHz. As shown on figure A1, these frequencies are 250 and 500 kHz, 1, 2.5, 5, 10, 20, 50, 100, and 250 MHz. Relatively clear channels were used when possible, e. g., the WWV guard bands. Limited frequency adjustment about the nominal frequencies is provided to assist in tuning away from signals in the recording channels. Two receiving antennas are used, 2 meter and 0.5 meter vertical whip antennas. The eight lower frequencies are recorded from the 2-meter antenna, and the two higher frequencies are recorded from the 0.5 meter antenna. Each antenna is connected to a passive coupling unit which provides some preselection and gives 50  $\Omega$  outputs for the preamplifiers.

The basic data source in the van is the set of eight noise receivers and metering strips. Each of these measures the rms envelope voltage, the ratio between the rms and the average voltage ( $V_d$ ), the ratio between the rms and the average of the logarithm of the voltage ( $L_d$ ), and the ratio between quasi-peak voltage and rms voltage ( $Q_d$ ). The quasi-peak detector uses a 1 ms charging time constant and a 160 ms discharge time constant. Currently the receivers are modified general purpose superhetrodyne communications receivers, and the metering strips are of a running average type with time constants in the

50-100 sec range. The receivers, as modified, operate with a 4 kHz effective noise bandwidth (the original noise bandwidth was 10 kHz). All channels have preamplifiers such that the system noise figure (excluding antenna losses) is less than 5 dB. The instantaneous dynamic range is approximately 85 dB, 50 dB above and 35 dB below the rms voltage. The recording ranges of the averaged values are 70 dB for the rms voltage, 20 dB for  $V_d$ , 30 dB for  $L_d$ , and 30 dB for  $Q_d$ .

The data recording system consists of an analog multiplexer, an A-D converter, a digital multiplexer, and an IBM-compatible incremental digital tape recorder. Each of the 32 averaged detector outputs (rms,  $V_d$ ,  $L_d$ , and  $Q_d$  on each of eight channels) are sampled every 10 sec, and the values are recorded. Time, location, and channel status are also recorded at the 10-sec intervals.

Other equipment available includes a distribution meter (DM-2) which can be used to obtain the APD or the ACR, giving more detailed noise information on any one of the 8 channels. The DM-2 utilizes 15 level detectors spaced at 6 dB intervals. Counters at each level accumulate the time the noise was above each level when measuring the APD or the number of positive crossings at each level when measuring the ACR. When used with the data recording system, the counters are read every 10 sec, and the results are recorded on the incremental tape recorder. The 15 levels can be divided so that part of the 15 channels can be used to obtain APD information and the balance can be used to obtain ACR information. The DM-2 will operate on the output of any of the receivers, but can be used on only one frequency channel at a time. The DM-2 contains built-in calibrators and power supplies, as well as direct visual readouts, and is often used separately in a manual mode for obtaining the APD or ACR for radio noise samples obtained by other recording means.

An FM tape recorder is used with special associated circuitry to provide analog recordings of the predetection noise process. The analog tape system (ATS) is designed to record accurately wide dynamic range electromagnetic noise signals. Up to three noise channels can be recorded simultaneously. The system has a bandwidth of 4 kHz and a dynamic range of 90 dB. The wide dynamic range is achieved by taking the logarithm of the higher levels, thus decreasing the dynamic range of the signal recorded on tape. The lower 30 dB of the dynamic range is handled linearly throughout the system, while the upper 60 dB is log-compressed into an effective 10 dB range. Consequently, the signal recorded on the tape will require only a 40 dB dynamic range. The tape recorder, operating in its FM mode at 60 ips, will adequately handle a 40 dB dynamic range, and most of its accuracy is in the upper part of the dynamic range where it is needed to recover accurately the log-compressed portion of the signal.

The noise to be recorded is obtained from the IF output of a receiver, with a 4 kHz bandwidth, tuned to the desired frequency. The noise signal is translated to zero frequency by two balanced mixers, with local oscillators supplying the sine and cosine components of the IF. This results in two outputs, each of which will have components in the range of d-c to 2 kHz. This mixing scheme gives a bandwidth whose lower limit is d-c, without losing phase information (i. e., without detecting). These outputs are compressed and recorded.

The recorded outputs can be recovered using complimentary circuits (providing the antilog of the log-compressed portion) to obtain the original 90 dB dynamic range of the noise. These two outputs (one created by mixing with the sine component and the other with the cosine component) are mixed with a sine and cosine local oscillator, respectively, and added together. This gives the original noise centered on an IF, which may or may not be the same as the original IF.

The recording and playback system consists of the tape recorder, the auxiliary recording electronics (mixers, local oscillators, log compressors, etc.), and the auxiliary playback electronics (antilog expanders, mixers, local oscillators, etc.). Figure A2 shows a block diagram of the analog recording system.

The advantage of such a system are considerable. Enough dynamic range is available to make accurate recordings of the high amplitude impulses which occur relatively infrequently but still contain most of the energy in the noise process. The noise can be played back at any desired center frequency, with the original phase information retained. This makes it useful for system simulation studies and detailed analysis by computer data systems too large or expensive to be carried in the van. Software has been developed which obtains all of the above-mentioned (section 2) amplitude and time statistics from such recordings. The use of a well-analyzed noise sample in system simulation studies provides an accurate means of comparing theoretical performance with actual performance.

Another available piece of equipment measures the correlation coefficient between two noise envelopes. This equipment has been used to obtain information on spatial and directional correlation, and the correlation between the vertical and horizontal components of the noise. The correlator is a wide dynamic range device with inputs at 455 kHz. It not only provides the product of the two channels, but measures the average voltage and rms voltage in each channel, which is necessary to obtain the correlation coefficient and permits combining 10-sec correlation data to calculate the correlation coefficient for larger time intervals. This equipment accurately handles noise information over a 70 dB instantaneous dynamic range. Automatic gain control and integrate-and-dump circuitry are responsible for the wide dynamic range

performance of this device. The correlation coefficient  $C_{12}$  between the two received noise waveforms is

$$C_{12} = \frac{\langle v_1 v_2 \rangle - \langle v_1 \rangle \langle v_2 \rangle}{(\langle v_1^2 \rangle - \langle v_1 \rangle^2)^{\frac{1}{2}} (\langle v_2^2 \rangle - \langle v_2 \rangle^2)^{\frac{1}{2}}}, \quad (A1)$$

where  $v_1$  and  $v_2$  are the detected inputs to the two channels and  $\langle \cdot \rangle$  denotes the time average. Many commercial correlators provide only the first term of the numerator. If the noise process is stationary over the proper time period (or if one has a means of continually replaying the same noise samples), the denominator can be measured and system gains set to make the denominator = 1. If the signals are also zero-mean signals, then the correlation coefficient does reduce to one term,  $\langle v_1 v_2 \rangle$ . Unfortunately, a radio noise envelope is neither zero-mean nor stationary over the proper time period, necessitating measurement of all of the quantities necessary to calculate (A1).

Equation (A1) may be rewritten as

$$C_{12} = \frac{\left( \frac{\langle v_1 v_2 \rangle}{\langle v_1^2 \rangle^{\frac{1}{2}} \langle v_2^2 \rangle^{\frac{1}{2}}} \right) \left( \frac{\langle v_1^2 \rangle^{\frac{1}{2}} \langle v_2^2 \rangle^{\frac{1}{2}}}{\langle v_1 \rangle \langle v_2 \rangle} \right) - 1}{\left( \frac{\langle v_1^2 \rangle}{\langle v_1 \rangle^2} - 1 \right)^{\frac{1}{2}} \left( \frac{\langle v_2^2 \rangle}{\langle v_2 \rangle^2} - 1 \right)^{\frac{1}{2}}}. \quad (A2)$$

Putting this more explicitly in terms of the quantities which the correlator measures (fig. A3), we have

$$C_{12} = \frac{ACE - 1}{[(A^2 - 1)(E^2 - 1)]^{\frac{1}{2}}} = \frac{BCD - BD/AE}{[(B^2 - B^2/A^2)(D^2 - D^2/E^2)]^{\frac{1}{2}}}, \quad (A3)$$

where

$$A = v_{d1} = \frac{\langle v_1^2 \rangle^{\frac{1}{2}}}{\langle v_1 \rangle} ,$$

$$B = v_{rms1} = \langle v_1^2 \rangle^{\frac{1}{2}} ,$$

$$C = \frac{\langle v_1 v_2 \rangle}{v_{rms1} v_{rms2}} , \quad (A4)$$

$$D = v_{rms2} = \langle v_2^2 \rangle^{\frac{1}{2}} ,$$

$$E = v_{d2} = \frac{\langle v_2^2 \rangle^{\frac{1}{2}}}{\langle v_2 \rangle} .$$

Equation (A3) gives the correlation coefficient for a single 10-sec period, based on the quantities measured in that period. The correlation coefficient for any longer time period can be computed from the five values recorded each 10 sec in the following manner. The correlation coefficient,  $C_{12T}$ , for some time period, T, consisting of n 10-sec periods is

$$C_{12T} = \frac{\sum_{i=1}^n B_i C_i D_i - \frac{1}{n} \sum_{i=1}^n \frac{B_i}{A_i} \sum_{i=1}^n \frac{D_i}{E_i}}{\left( \left[ \sum_{i=1}^n B_i^2 - \frac{1}{n} \left( \sum_{i=1}^n \frac{B_i}{A_i} \right)^2 \right] \left[ \sum_{i=1}^n D_i^2 - \frac{1}{n} \left( \sum_{i=1}^n \frac{D_i}{E_i} \right)^2 \right] \right)^{\frac{1}{2}}} . \quad (A5)$$

The calibration equipment completes the normal van installation. The primary calibration relates the rms output to  $F_a$ , the equivalent



noise power spectral density available from a short, lossless antenna. All other calibrations are maintained relative to this value. The basic calibration for the rms channels consists of two steps. One step is the calibration of the system from the preamp input to the recorded output by means of a known input from a noise diode. This provides a relationship between the recorded voltage level and  $F_a$ , required at the preamp input to give the output reading. Since both the noise process and the calibration source are broad-band phenomena, the calibration with the noise diode eliminates any bandwidth problems in obtaining an accurate calibration. The second step in the basic calibration procedure is to determine the antenna circuit losses up to the preamp. This is accomplished by using a CW generator connected first to a permanently installed calibration stub antenna and then connected to the preamplifier input, where the noise diode calibration signal is injected. By knowing the relation between the two CW inputs, the self-impedance of the antenna and the calibration stub, and the mutual impedance between the two, the antenna circuit losses can be determined (Ahlbeck et al., 1958, "Instruction Book for ARN-2 Radio Noise Recorder," NBS Report 5545). The calibration of the other three moments is accomplished by setting the gains such that, for a CW signal,  $V_d$ ,  $L_d$ , and  $Q_d$  are all equal to zero. The DM-2 is calibrated by relating one of the 15 levels relative to a given rms value, which in turn can be related to the available power from a lossless antenna. The same type of calibration is used on the analog tape recording system by recording a CW reference level on the tape which is related to the noise rms level.

Calibration measurements are made at the beginning and end of each run. While the recording equipment has been stabilized as much as possible, some variation in gain may occur over the measurement period. The two calibrations are averaged to find the calibration factors to be used for a block of data.

The accuracy of the recorded data will depend on the precision of the measuring/recording equipment and the calibration accuracy. The overall accuracy of the system is within  $\pm 2$  dB for the basic available power measurement. The accuracy of the other measurements is within  $\pm 0.5$  dB relative to the power measurement.

The design criteria used in establishing the sensitivity of the recording equipment was based on natural noise levels expected and the lowest values of man-made radio noise expected. A comparison of the system noise factor achieved at each frequency with the design criteria is shown on figure A4. The lowest atmospheric radio noise expected in the United States (CCIR, 1964) occurs during the winter 0800-1200 time block. This is the atmospheric noise curve shown. Also from CCIR (1964), the Galactic radio noise curve and the quiet rural curve for man-made radio noise are shown. Since we obtained this man-made noise curve from data recorded at our world-wide network of atmospheric radio noise recording stations, where each site was carefully chosen to be as free of man-made radio noise as possible, lower levels were not expected to be encountered when using the mobile noise lab. The design criteria, therefore, was the highest of these three curves at each nominal recording frequency. This was fairly well achieved except at 250 MHz, where a 7 dB noise factor was obtained. In some rural areas, the 250 MHz external man-made radio noise was found to be equal to or even less than the system noise factor.

The present radio noise measuring capability is limited in frequency range, with 250 MHz being the highest available channel. Some measurements of man-made radio noise have been made at frequencies up to 2.5 GHz (Automobile Manufacturers Association, 1969, 1970, and 1971; Anzic, 1970). A great deal of information about the various required amplitude and time statistics is needed at these higher frequencies. To

date, even the most basic parameters (such as power spectral density) are little known as to variation with time and location.

Present measurement bandwidths are limited to 4 kHz by the IF band limiting in the receivers. This probably is adequate for frequencies up through the HF band. For measurements at VHF and higher frequencies, considerably wider bandwidths should be used. While the effect of bandwidth reduction on some of the noise statistics can be estimated (Spaulding et al., 1962), extrapolating radio noise statistics measured in a narrower bandwidth to those that would have been present in a wider bandwidth can be questionable since some information on the noise process is lost in bandlimiting. Therefore, bandwidths approximately equal to the widest expected bandwidth used in the various frequency ranges generally should be used for recording the radio noise information. Except for use with the correlator, only vertical monopole antennas have been used. Additional antenna configurations should be employed to obtain direction and polarization information.

Most of the data taken with the radio noise laboratory has been under mobile operating conditions. After selection of an area to be measured, a route was layed out in business or residential areas to include all streets or highways in the area if the whole area was homogeneous. If not, an attempt was made to separate the different types of areas. Once the route was layed out, at least two runs were made, if possible, with the noise laboratory going in opposite directions on the two runs. In some areas this was not possible due to the presence of one-way streets. In the rural areas, only one run was generally made over a given route.

Fixed-location measurements have been made using either self-contained power or commercial power for equipment operation. Additional precautions have been necessary when using commercial power

to insure that the temporary power line is not a source of the recorded noise. When fixed-location measurements are made, the analysis of these data is separated from the analysis of the mobile data.

The choice of frequencies to be used for any given set of measurements and the choice of recordings to be made will depend upon the primary purpose of the measurements. A full set of eight frequencies is used for each measurement run unless a channel is used for the analog tape recorder or the distribution meter recordings which generally will leave only seven channels for the moment measurements. The moments always are measured simultaneously on the channel with the tape recordings or distribution recordings.

## REFERENCES, APPENDIX A

- Automobile Manufacturers Association (1969), Ambient electromagnetic survey, Detroit, Michigan, Engineering Report 69-15, Radio Committee, AMA, Detroit, Michigan.
- Automobile Manufacturers Association (1970), Microwave (1-2.5 GHz) radiation from motor vehicles, Engineering Report, Radio Committee, AMA, Detroit, Michigan.
- Automobile Manufacturers Association (1971), Data Package, Radio Interference Tests, South Lyon, Michigan, June 14-17, 1971, AMA, Detroit, Michigan.
- Anzic, G. (1970), Measurements and analysis of radio frequency indigenous noise, IEEE Electromagnetic Compatibility Symposium Record, pp. 183-195.
- CCIR (1964), World distributions and characteristics of atmospheric radio noise, Documents of the Xth Plenary Assembly, Report 322, International Telecommunication Union, Geneva, Switzerland.
- Spaulding, A. D., C. J. Roubique, and W. Q. Crichlow (1962), Conversion of the amplitude probability distribution function for atmospheric radio noise from one bandwidth to another, J. Res. NBS, Vol. 66D, pp. 713-720.

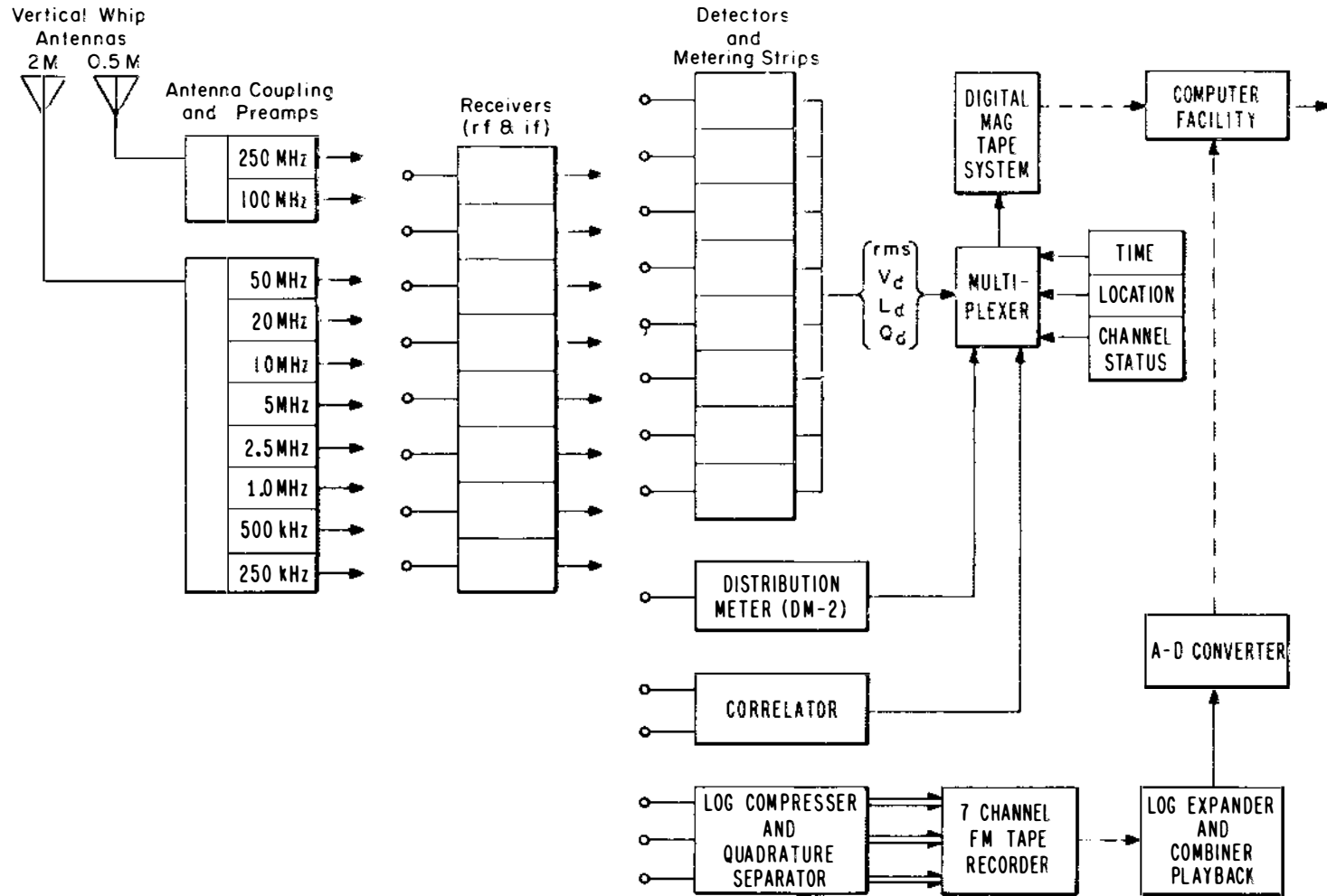


Figure A1. Block diagram of the measuring and recording facilities in the OT/ITS mobile radio noise lab.

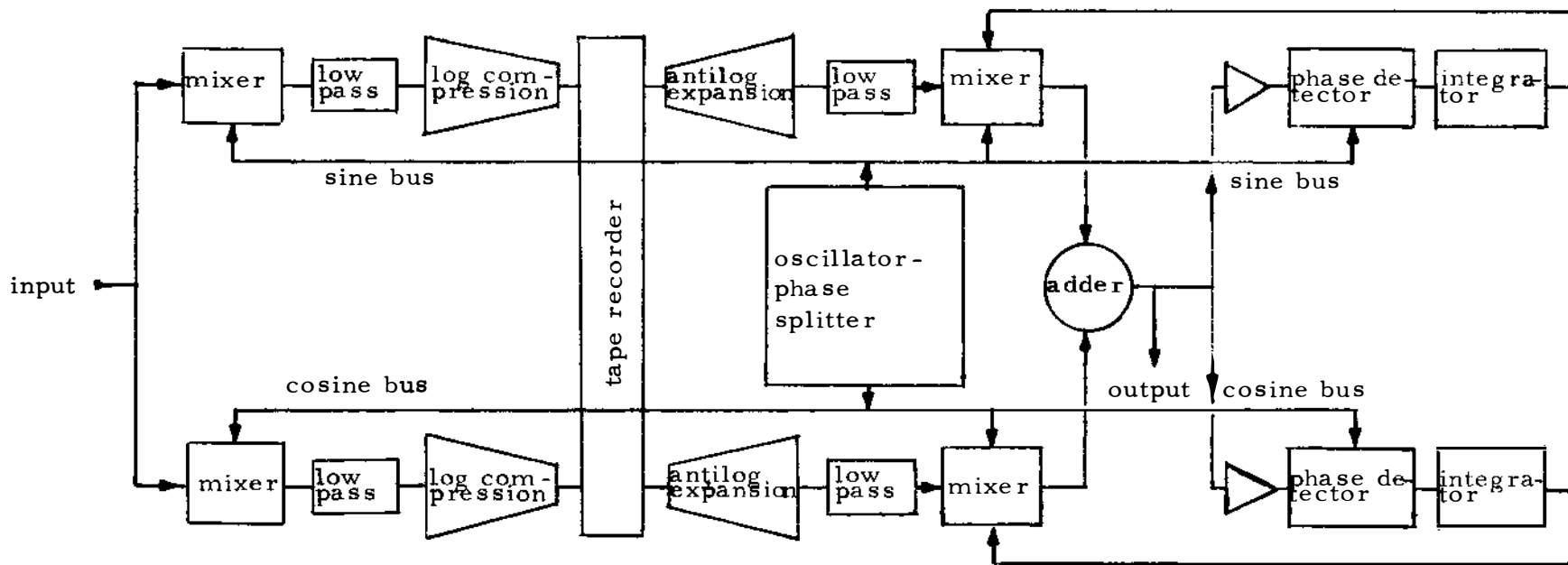


Figure A2. Block diagram of the analog recording-playback system.

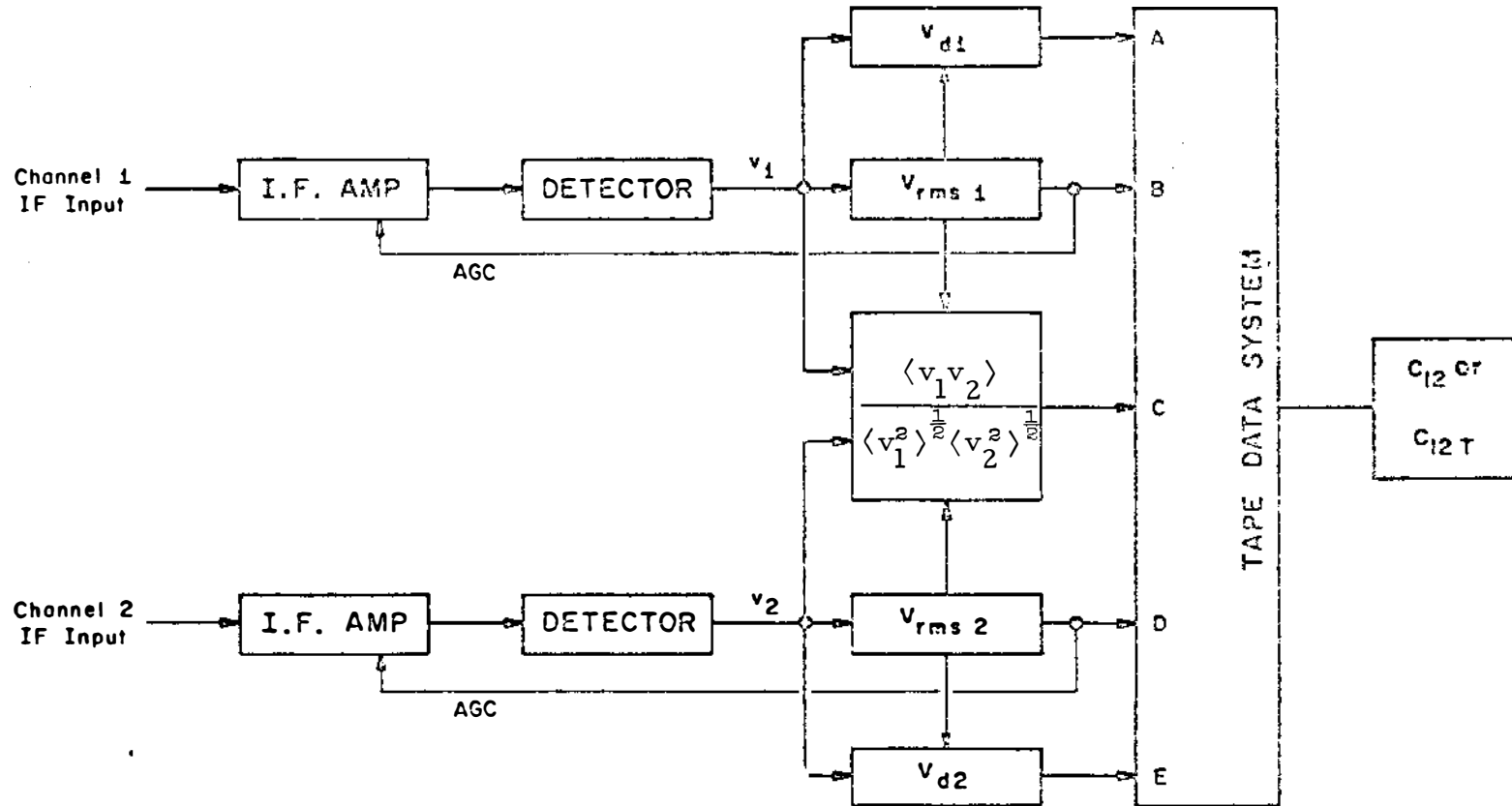


Figure A3. Block diagram of the correlation measurement system.



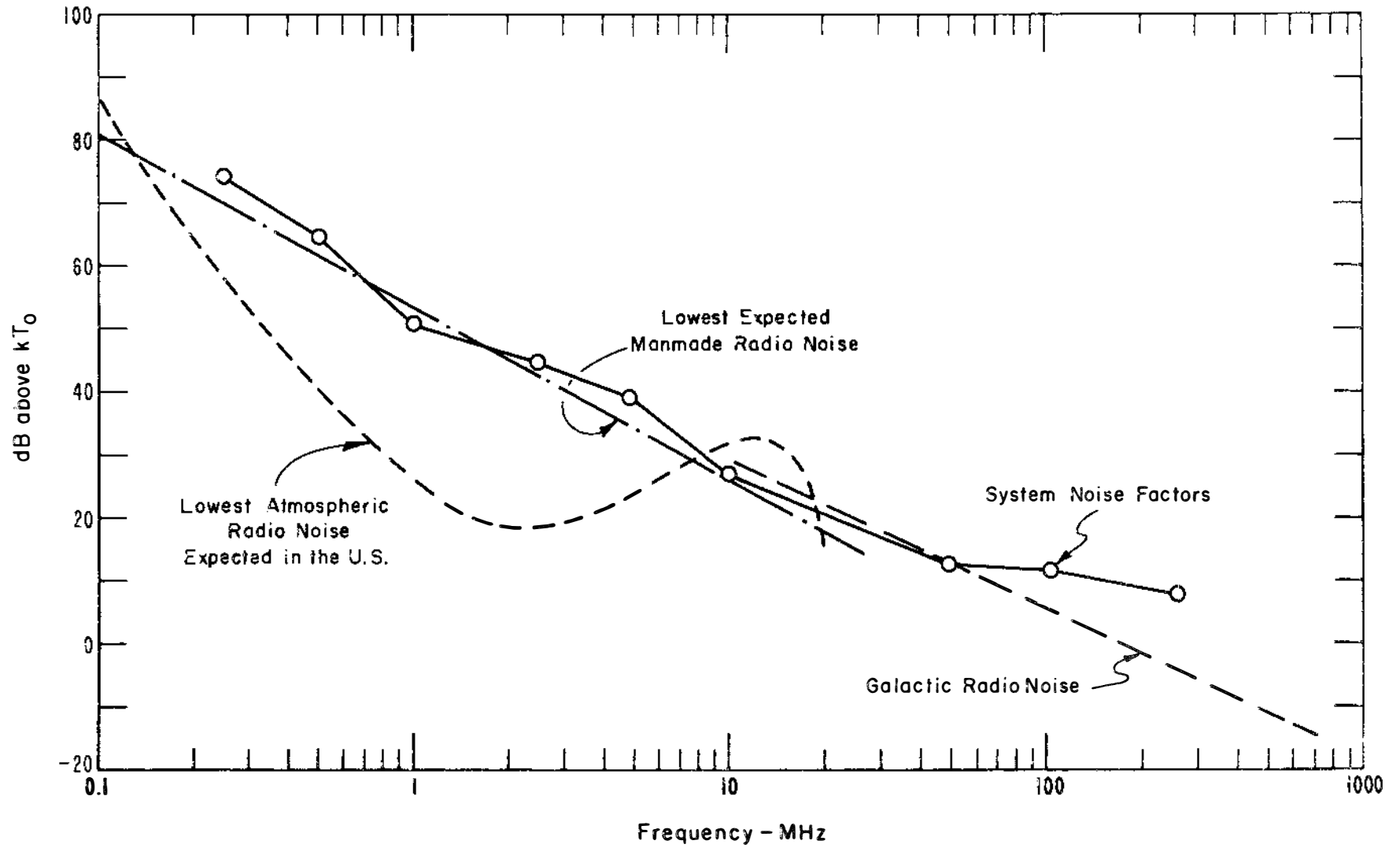


Figure A4. OT/ITS mobile radio-noise lab system noise factors.

APPENDIX B  
THE USE OF TRAFFIC DENSITY INFORMATION AS A  
NOISE PREDICTOR

The levels and other characteristics of man-made radio noise, as has been seen, are quite variable with location and time. It is not feasible to make long-term measurements at all possible locations, and therefore some prediction of the noise is needed for locations where receiving terminals of various communications systems are planned. As has been shown, a general estimate of the noise environment can be obtained by assuming that the characteristics of the noise will be the same as those measured at another place similar in nature to the particular area of interest. If additional information is available for the receiving terminal location on distribution of noise sources and the amount of radiation from these sources, a much better estimate of the radio noise environment could be obtained. Going one step further, a valid estimate of future changes in these sources would give a good estimate of the expected future environment. It is not generally possible to actually catalog all noise sources in a given area that would affect a given system.

In 1968 the Institute for Telecommunication Sciences completed a detailed noise measurement program in San Antonio, Texas. The noise measurements were made under mobile conditions on most of the thoroughfares within specified areas called SLA's (standard location area). The SLA's are areas defined by the Census Bureau for counting population and generally vary between 1 and 5 square miles in area. Various SLA's were chosen to give as wide a range of population density as possible. Figure B1 shows, as an example, the lack of correlation at 5 MHz between the average noise level,  $F_{a\mu}$ , within an SLA and the population density of that SLA. The  $F_{a\mu}$  is the mean of

all  $F_a$  values measured within an SLA. Similar results were obtained at the other frequencies of measurement (250 kHz to 48 MHz). Figure B2 shows the linear regression of  $F_{a\mu}$  at 48 MHz for 26 thoroughfares with the average hourly traffic count. Here,  $F_{a\mu}$  denotes the mean of all  $F_a$  values measured along the thoroughfare. The traffic count was obtained by averaging the traffic counts at various locations along the thoroughfares. These counts were obtained from past traffic records. Figure B3 shows the correlation coefficient and its 95 percent confidence bound as a function of frequency for  $F_{a\mu}$  versus the average vehicular density for all the measurements taken (Spaulding et al., 1971). More recent measurements have shown the same high correlation at 102 and 250 MHz. Figure B4 also shows the correlation of noise level with traffic density. This figure shows three days of continuous measurements taken 100 ft from the center of Broadway. Broadway is the highway directly to the east of the Department of Commerce, Boulder, Laboratories. Comparing the traffic count (10 log vehicles/hr) with the received noise power, one sees obvious correlation at 20 and 48 MHz and an obvious lack of correlation at 10 MHz. At 10 MHz, the noise is primarily due to power lines in the area. Figure B4 shows the "instantaneous" correlation for a given highway, that is, the traffic density was measured simultaneously with the noise measurements. Figure B3, on the other hand, shows the correlation of the average measured  $F_a$ 's along a large number of thoroughfares with the average traffic density on these thoroughfares (for the time of day for which the measurements were taken) obtained from past traffic studies.

Traffic counts for most highways generally are available from traffic or highway engineering departments. Also the expected growth and change in traffic patterns are used for highway planning and are available. Using this information, an estimate of the man-made noise

levels can be obtained for present traffic conditions and for changes due to expected changes in traffic density.

We can make use of the additivity of power to calculate the received noise at a distance,  $d$ , from a highway. If many highways, or many lanes of one highway are involved, the total power spectral density can be obtained by adding the contributions from each. Therefore, without loss of generality, we will consider a single highway, straight and infinite in extent. Of course, the automobiles far away (along the highway) from the receiving point of interest contribute negligible power to the total.

To calculate the received noise power spectral density at a distance,  $d$ , from a highway, let  $x$  be the power spectral density radiated from a single automobile as measured at some distance,  $d_m$ . Figures B5 and B6 show the distribution of the radiated power spectral density,  $F_a$ , from 958 individual automobiles measured by OT/ITS at 50 ft for frequencies of 20 and 48 MHz. A log normal distribution (dB values normally distributed) is a good approximation for the distribution of  $x$ , and figures B5 and B6 show the best fit normal distribution, along with its mean,  $\mu$ (dB), and standard deviation,  $\sigma$ (dB).

The distribution of  $y$ ,  $y = 10 \log x$ , is

$$p(y) = \frac{1}{\sqrt{2\pi}\sigma} \exp \left[ -\frac{(y - \mu)^2}{2\sigma^2} \right], \quad -\infty \leq y \leq \infty . \quad (B1)$$

Therefore, the distribution of  $x$  is

$$p(x) = \frac{4.343}{x\sigma\sqrt{2\pi}} \exp \left[ -\frac{1}{2} \left( \frac{10 \log x - \mu}{\sigma} \right)^2 \right], \quad 0 \leq x \leq \infty , \quad (B2)$$

and the mean value of  $x$ ,  $\bar{x}$ , and the variance of  $x$ ,  $\text{Var}[x]$ , are given by

$$\bar{x} = 10^{0.1\mu + 0.0115\sigma^2}, \quad (B3)$$

and

$$\text{Var}[x] = \left(10^{0.2\mu + 0.023\sigma^2}\right) \left(10^{0.023\sigma^2} - 1\right) . \quad (\text{B4})$$

Since, for surface wave propagation and for distances and frequencies of primary interest here (above 20 MHz), the received power falls off essentially as distance to the fourth power (Norton, 1959), the power,  $p_i$ , received from the  $i^{\text{th}}$  car along the highway is

$$p_i = \frac{x_i d_m^4}{\left(d^2 + s_i^2\right)^2} , \quad (\text{B5})$$

where  $d$  is the perpendicular distance from the point of interest to the highway,  $d_m$  is the distance (outside the induction field) at which  $x$  was measured, and  $s_i$  is the distance along the highway to the  $i^{\text{th}}$  car.

At lower frequencies, the power will fall off as distance squared (Norton, 1959), at least for the closer cars which contribute most of the power. We will, therefore, consider the total receiver power,  $p_T$ , to be given by

$$p_T = \sum_{i=-\infty}^{\infty} p_i = \sum_{i=-\infty}^{\infty} x_i \left( \frac{d_m^2}{d^2 + s_i^2} \right)^\ell , \quad (\text{B6})$$

where  $\ell = 1$  or  $2$  and the  $x_i$  are log normally distributed. Depending on the situation (i.e., car density, distance of interest, etc.), we might expect the total power,  $p_T$ , to be approximately normally distributed via the central limit theorem. This approximation will be valid for values of  $p_T$  around the mean value of  $p_T$ , but obviously cannot be correct very far out on the tails of the actual distribution of  $p_T$ . In any case, we want to calculate the mean and variance of  $p_T$ .

The spacing between cars will have some distribution. In traffic studies, the car spacings are taken usually to be either equal or exponentially distributed. Which car spacing assumption is best will

depend on the particular traffic situations. We will evaluate the mean and variance of  $p_T$  (B6) for both cases, starting with equal car spacing,  $s$ ; i.e.,  $s_i = is$ .

The mean and variance of  $p_T$  are, therefore, given by

$$\bar{p}_T = \bar{x} \sum_{i=-\infty}^{\infty} \left( \frac{d^2}{d^2 + (is)^2} \right)^{\ell} \quad (B7)$$

and

$$\text{Var}[p_T] = \text{Var}[x] \sum_{i=-\infty}^{\infty} \left( \frac{d^2}{d^2 + (is)^2} \right)^{2\ell} . \quad (B8)$$

For  $\ell = 1$  and 2, the above summations can be evaluated in closed form by the standard methods of contour integration and successive differentiation (see also Wheelon, 1954). The results are

$$\sum_{i=-\infty}^{\infty} \frac{d^2}{d^2 + (is)^2} = \frac{\pi d}{s} \coth\left(\frac{\pi d}{s}\right), \quad (B9)$$

$$\sum_{i=-\infty}^{\infty} \left( \frac{d^2}{d^2 + (is)^2} \right)^2 = \frac{\pi d}{2s} \coth\left(\frac{\pi d}{s}\right) + \frac{\pi^2 d}{2s^2} \text{csch}^2\left(\frac{\pi d}{s}\right), \quad (B10)$$

$$\begin{aligned} \sum_{i=-\infty}^{\infty} \left( \frac{d^2}{d^2 + (is)^2} \right)^3 &= \frac{3\pi d}{8s} \coth\left(\frac{\pi d}{s}\right) + \frac{3\pi^2 d}{8s^2} \text{csch}^2\left(\frac{\pi d}{s}\right) \\ &+ \frac{\pi^3 d}{4s^3} \text{csch}^4\left(\frac{\pi d}{s}\right), \end{aligned} \quad (B11)$$

and

$$\begin{aligned}
\sum_{i=-\infty}^{\infty} \left( \frac{d^2 m^2}{d^2 + (i s)^2} \right)^4 &= \frac{5\pi d^8 m^8}{16s d^7} \coth\left(\frac{\pi d}{s}\right) + \frac{5\pi^2 d^8 m^8}{16s^2 d^6} \operatorname{csch}^2\left(\frac{\pi d}{s}\right) \\
&+ \frac{\pi^3 d^8 m^8}{4s^3 d^5} \operatorname{csch}^2\left(\frac{\pi d}{s}\right) \coth\left(\frac{\pi d}{s}\right) \\
&+ \frac{\pi^4 d^8 m^8}{24s^4 d^4} \left[ \operatorname{csch}^4\left(\frac{\pi d}{s}\right) \right. \\
&\left. + \operatorname{csch}^2\left(\frac{\pi d}{s}\right) \coth^2\left(\frac{\pi d}{s}\right) \right]. \tag{B12}
\end{aligned}$$

Note, now, that for  $d/s > 1$ ,  $\coth(\pi d/s) \approx 1$  and  $\operatorname{csch}(\pi d/s) \approx 2 \exp(-\pi d/s) \approx 0$ , so we obtain the simple results (for the case  $d/s > 1$ ) for (B9):

$$\sum \cong \frac{\pi d^2 m^2}{s d};$$

for (B10):

$$\sum \cong \frac{\pi d^4 m^4}{2s d^3};$$

for (B11):

$$\sum \cong \frac{3\pi d^6 m^6}{8s d^5};$$

and for (B12):

$$\sum \cong \frac{5\pi d^8 m^8}{16s d^7}. \tag{B13}$$

We can now easily compute  $\bar{p}_T$  and  $\operatorname{Var}[p_T]$  from the distribution of power radiated from individual vehicles for whichever propagation law ( $l = 1, 2$ ) is appropriate.

As an example during quiet hours, consider (fig. B4) 48 MHz at 0300, Thursday. The traffic count was about 31.6 vehicles per hour. The speed limit on Broadway, where the measurements were taken, is 35 mph; therefore,

$$s = \frac{5280 \times 35}{31.6} = 5850 \text{ ft/vehicle} .$$

Since the distance at which the measurements were made (100 ft) is less than  $s$ , we cannot use the approximation (B13) and must use (B10). From figure 6 we have, for 48 MHz,  $\mu = 20.2$  dB and  $\sigma = 10.8$  dB. So from (B3),

$$\bar{x} = 10^{3.36} = 2170 \text{ kT}_o \left( 1 \text{ kT}_o = 3.97 \times 10^{-21} \frac{\text{watts}}{\text{Hz}} \right) .$$

From (A10), with  $d = 100$  ft,  $d_m = 50$  ft,  $s = 5850$  ft, we obtain

$$\sum_{i=-\infty}^{\infty} \left( \frac{d_m^2}{d^2 + (i s)^2} \right)^2 = 0.0627 .$$

Therefore,

$$\bar{P}_T = 2170 \times 0.0627 = 136 \text{ kT}_o$$

$$\bar{P}_T = 21.3 \text{ dB} > \text{kT}_o .$$

The actual measured value was 18 dB  $>$   $\text{kT}_o$ . Likewise, at 0300, Thursday, for 20 MHz, we obtain  $\bar{P}_T = 30.6$  dB  $>$   $\text{kT}_o$ , while the measured value was 31 dB  $>$   $\text{kT}_o$ .

If we now consider 48 MHz, 0800, Thursday, we obtain from (B10) (with  $\bar{x} = 2170 \text{ kT}_o$ ,  $d = 100$  ft,  $d_m = 50$  ft,  $s = 185$  ft) that  $\bar{P}_T = 21.8$  dB  $>$   $\text{kT}_o$ , while the measured value was 26.5 dB. The  $\bar{P}_T$  plus one standard deviation [from (B12)] is 28.5 dB.



In general, the lower measured values are matched quite well by the calculated values, but the calculated values are substantially lower (up to 8 dB) than the measured values during the busiest portions of the day. This is due, in part at least, to noise contributions from the many noise sources other than the automobile present on the laboratory grounds during the working day. There are also many other considerations which we will discuss later.

We will now evaluate the mean of  $p_T$  (B6) when the car spacings are exponentially distributed. The distribution of  $s_i$  is (Parzen, 1962)

$$p(s_i) = \frac{s_i^{i-1}}{s^i (i-1)!} e^{-s_i/s}, \quad (\text{B14})$$

and the mean value of  $s_i$  is given by  $i s$ . Then, with  $E$  denoting the mean value operation,

$$\begin{aligned} \bar{p}_T &= E[p_T] = E \left[ \sum_{i=-\infty}^{\infty} x_i \left( \frac{d^2}{d^2 + s_i} \right)^\ell \right] \\ &= d_m^{2\ell} E[x] \left\{ \frac{1}{d^{2\ell}} + 2 \sum_{i=1}^{\infty} E \left[ \left( \frac{1}{d^2 + s_i} \right)^\ell \right] \right\}. \quad (\text{B15}) \end{aligned}$$

Now

$$\sum_{i=1}^{\infty} E \left[ \left( \frac{1}{d^2 + s_i} \right)^\ell \right] = \sum_{i=1}^{\infty} \int_0^{\infty} \frac{1}{(d^2 + z^2)^\ell} \frac{z^{i-1}}{s^i (i-1)!} e^{-z/s} dz. \quad (\text{B16})$$

Interchanging summation and integration, we obtain the general result from (B15) and (B16),

$$\bar{p}_T = \bar{x} \left[ \frac{d^{2\ell}}{d^{2\ell}} + \frac{d^{2\ell} (2\ell - 2)! \pi}{s^{2\ell - 2} (\ell - 1)! (\ell - 1)! d^{2\ell - 1}} \right]. \quad (\text{B17})$$

Note, that, with the exception of the term  $d_m^{2\ell}/d^{2\ell}$ , (B17) is identical to (B13). The term  $d_m^{2\ell}/d^{2\ell}$ , however, as we will discuss later, often dominates. While the above (B17) gives the mean value of  $p_T$ , the variance appears to be much more difficult to calculate and is not done here.

On figure B4, again, equation B17, with  $\ell = 2$ , gives an average value of  $F_a$  of 21.5 dB compared with the previous value of 21.3 dB  $> kT_o$  for 0300, Thursday, 48 MHz. Likewise, (B17) gives 30.8 dB  $> kT_o$  compared with the previous 30.6 dB for 0300, Thursday, 20 MHz. For 48 MHz, 0800, Thursday, (B17) gives 24 dB  $> kT_o$  compared with the previous 21.8 dB. With the very limited measurements available, it would appear that (B17) gives a somewhat more accurate prediction of the mean value of  $p_T$  for high traffic density.

In the above analysis, there are a number of points to consider. First, we note that the results are heavily dependent on the propagation. Results have been given for  $\ell = 1$  and 2, i. e., inverse distance squared and inverse distance to the fourth power. We would expect  $\ell = 1$  to apply for low frequencies and  $\ell = 2$  to apply at the higher frequencies for the distances of interest, but recent measurements (Shafer et al., 1972) at 900 MHz by RCA have indicated that, in an urban area,  $\ell$  can vary anywhere between 0.75 and 2.25 for the distances of interest. Once one decides what propagation law fits his situation, good approximations probably can be made by interpolating between the results given here for integer values of  $\ell$ .

In spite of the close fit between the lowest measured noise values and the predicted values, the results are based on the assumption that there is essentially always one automobile at a distance,  $d$ , from the receiver. This is the  $d_m^{2\ell}/d^{2\ell}$  terms in (B17) and is also inherent in (B9) through (B12). The result is that this term dominates, giving

essentially the same  $\bar{p}_T$  for any traffic density between 10 and 200 vehicles/hour (at normal speeds). For proper consideration of very low traffic densities, this assumption would need to be modified. The analysis gives results [(B13) and (B17)] which should be valid for relatively high traffic densities.

In order to use the above results, knowledge of the power radiated from individual automobiles is required. From (B3) the mean and standard deviations of  $F_a$  are required for any particular frequency of interest. There appears to be very little such information (other than that given here) available. Measurements of individual automobiles have been made by the Automobile Manufacturers Association (AMA, 1969, 1970, 1971), but, in general, parameters other than power were measured; in any case, a very limited number of individual vehicles were measured. Detailed measurements of individual vehicles were recently made by Stanford Research Institute (Shepherd et al., 1973). References to some earlier measurements can be found in the bibliographies (Part II of this report and Thompson, 1971).

In general, the simple results given here can be used to obtain good approximations of the noise at a receiver site due to automotive traffic in the area. As with any such prediction method, however, the proper input statistics must be available. Here, the requirement is for only the mean and variance of the power spectral density (in dB at some measurement distance) radiated from individual vehicles for the frequency of interest. The traffic density (cars/hr) and the average speed must, of course, also be known.

Finally, it should be noted that all the measurements referred to here were made with vertical monopole antennas. For other antennas the basic expression (B6) can be modified by the antenna gain pattern. When this is done, the analysis can be carried through exactly as before, but, except for special cases, the resulting summations (and integrations) require numerical evaluation.

## REFERENCES, APPENDIX B

- Automobile Manufacturers Association (1969), Ambient electromagnetic survey, Detroit, Michigan, Engineering Report 69-15, Radio Committee, AMA, Detroit, Michigan.
- Automobile Manufacturers Association (1970), Microwave (1-2.5 GHz) radiation from motor vehicles, Engineering Report, Radio Committee, AMA, Detroit, Michigan.
- Automobile Manufacturers Association (1971), Data Package, Radio Interference Tests, South Lyon, Michigan, June 14-17, 1971, AMA, Detroit, Michigan.
- Norton, K. A. (1959), Transmission loss in radio propagation II, National Bureau of Standards Technical Note 12.
- Parzen, E. (1962), Stochastic Processes, Holden-Day, Inc., p. 134.
- Shafer, J., C. S. Haplan, and S. N. Honicknan (1972), Mobile radio propagation statistics at 900 MHz in New York City, RCA Laboratories, Princeton, N.J. -- talk given at the Microwave Mobile Radio Symposium, Department of Commerce Laboratories, Boulder, Colorado, March 1-3, 1972.
- Shepherd, R. A., J. C. Gaddie, V. E. Hatfield, and G. H. Hagn (1973), Measurement of automobile ignition noise at HF, Final Report, Contract No. 0039-71-A-0223, Delivery Order 0003, Stanford Research Institute, Menlo Park, California 94025.
- Spaulding, A. D., W. H. Ahlbeck, and L. R. Espeland (1971), Urban residential man-made radio noise analysis and predictions, OT/ITS Telecommunications Research and Engineering Report 14.
- Thompson, W. I., III (1971), Bibliography on ground vehicle communications and control: A KWIC index, Urban Mass Transportation Administration, U.S. Department of Transportation, Washington, D.C., Report No. DOT-UMTA-71-3.
- Wheelon, A. D. (1954), A short table of summable series, The Ramo-Wooldridge Corporation, Los Angeles, California.

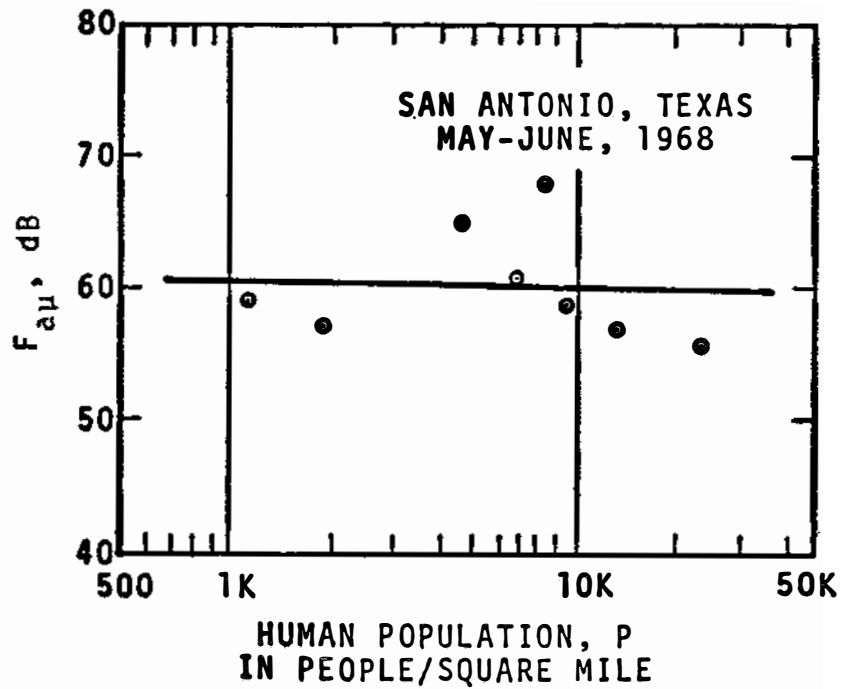


Figure B1. Regression of 5.0 MHz  $F_{a\mu}$  with log population density of SLA's.

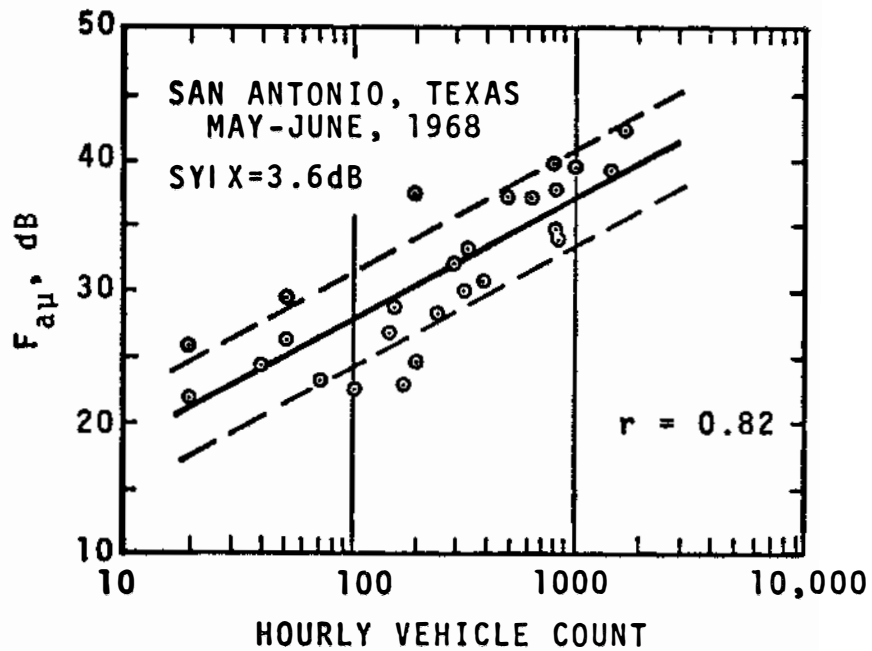


Figure B2. Linear regression of  $F_{a\mu}$  vs. log hourly traffic count along 26 thoroughfares at 48 MHz.

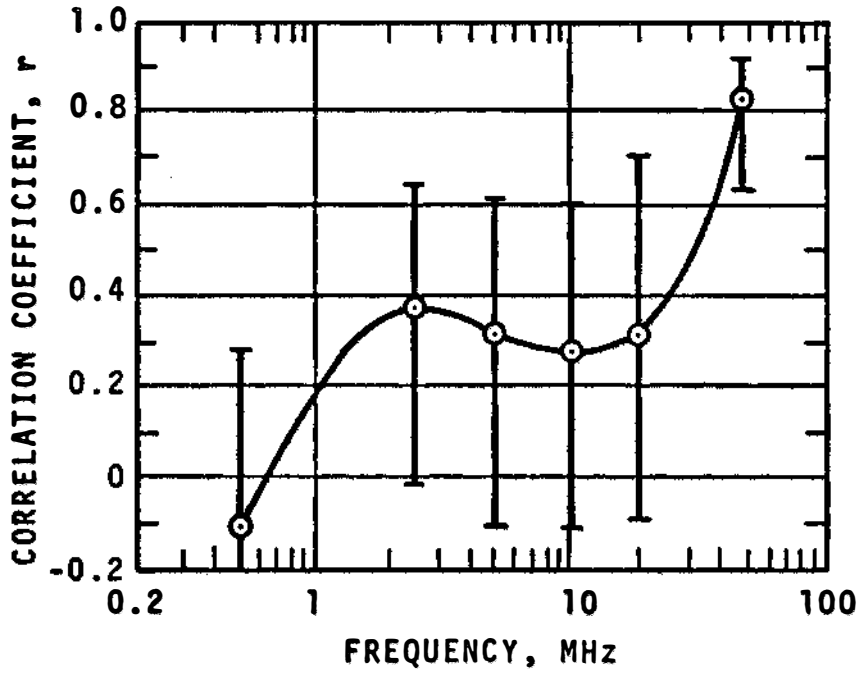


Figure B3. Correlation coefficients along with the 95 percent confidence limits for each of the measurement frequencies,  $F_{a\mu}$  vs. log hourly traffic count.

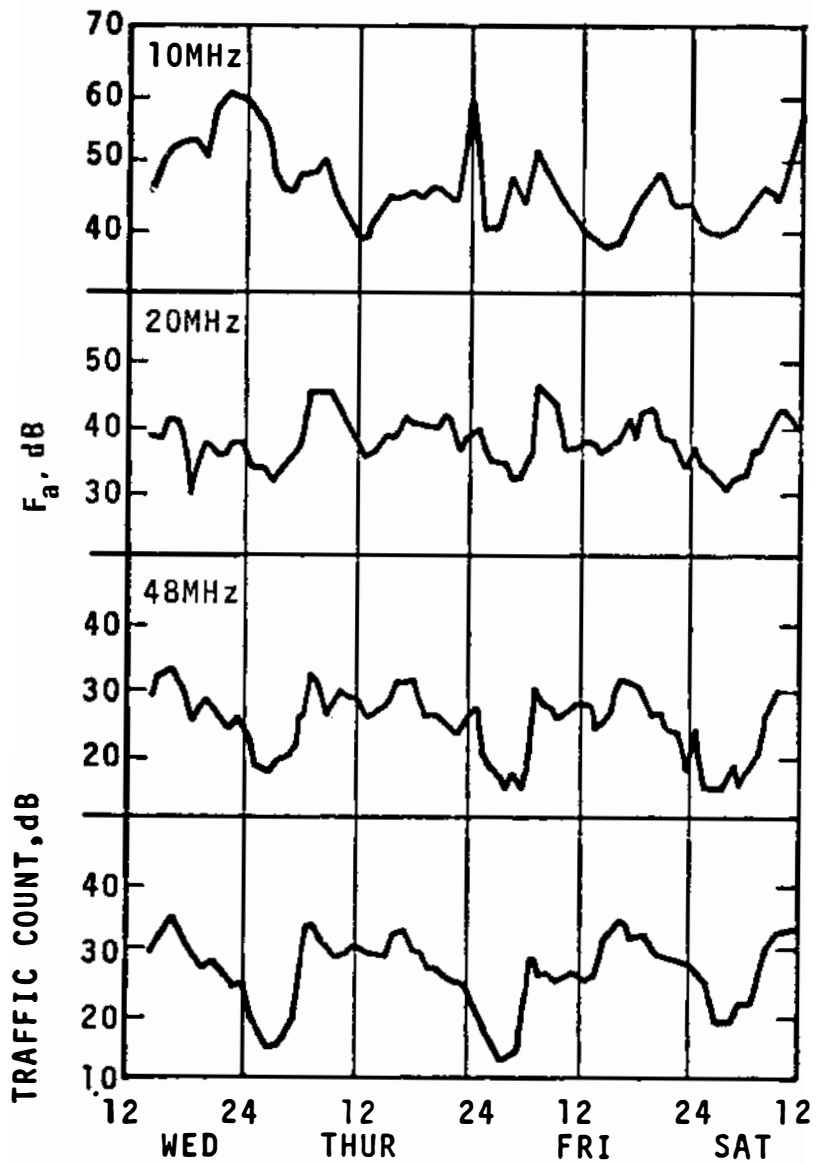


Figure B4. Hourly median values of radio noise power and hourly traffic count. Broadway, Boulder, Colorado, October 25 - 27, 1967, noise values recorded 100 ft west of highway center.

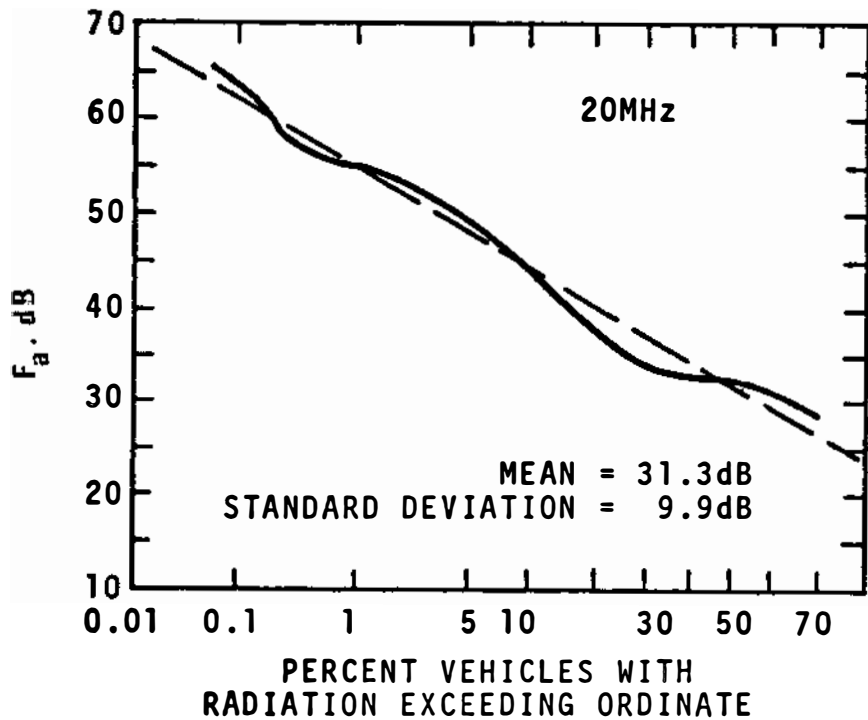


Figure B5. Distribution of radio noise power at 20 MHz radiated from 958 individual vehicles, values measured at 50 ft from vehicle.

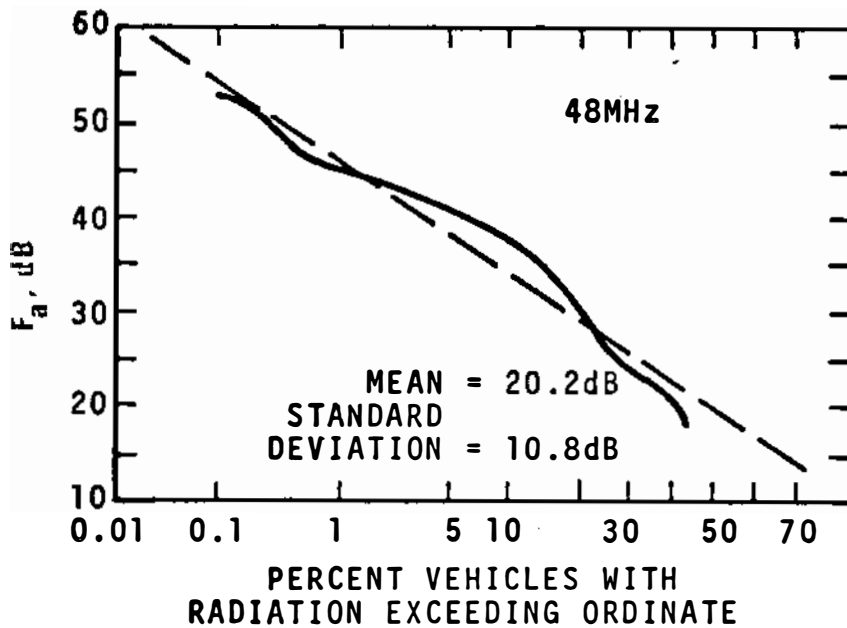


Figure B6. Distribution of radio noise power at 48 MHz radiated from 958 individual vehicles, values measured at 50 ft from vehicle.



**BIBLIOGRAPHIC DATA SHEET**

1. PUBLICATION OR REPORT NO.  OTR 74-38		2. Gov't Accession No.	3. Recipient's Accession No.
4. TITLE AND SUBTITLE Man-Made Radio Noise Part 1: Estimates for Business, Residential, and Rural Areas		5. Publication Date June, 1974	6. Performing Organization Code OT/ITS
		7. AUTHOR(S) Arthur D. Spaulding and Robert T. Disney	9. Project/Task/Work Unit No.
8. PERFORMING ORGANIZATION NAME AND ADDRESS U.S. Department of Commerce Office of Telecommunications Institute for Telecommunication Sciences 325 Broadway, Boulder, Colorado 80302		10. Contract/Grant No.	
		11. Sponsoring Organization Name and Address U.S. Department of Commerce Office of Telecommunications 1325 G Street, N.W. Washington, D.C. 20005	
12. Type of Report and Period Covered		13.	
14. SUPPLEMENTARY NOTES			
15. ABSTRACT (A 200-word or less factual summary of most significant information. If document includes a significant bibliography of literature survey, mention it here.) The Office of Telecommunications, Institute for Telecommunication Sciences (OT/ITS), over the past several years, has accumulated a data base of man-made radio noise measurements in the frequency range from 250 kHz through 250 MHz taken in a number of geographical areas. This data base has been analyzed to provide estimates of the expected characteristics of man-made radio noise in business, residential, and rural areas. The parameters used are the average available power spectral density, the ratio of the rms to the average voltage of the noise envelope, and the ratio of the rms to the average logarithm of the envelope voltage. The variation of these parameters as a function of frequency, location, and time are shown and discussed. Examples of amplitude and time statistics of the received man-made radio noise process also are shown and discussed. The use of the estimates is shown (principally by references in Pt. II, Bibliography) in the solution of <u>problems encountered in frequency management &amp; telecommunication system design.</u>			
16. Key words (Alphabetical order, separated by semicolons)  Impulsive noise; man-made radio noise; noise characteristics; noise levels; non-Gaussian noise; system performance.			
17. AVAILABILITY STATEMENT  <input checked="" type="checkbox"/> UNLIMITED.  <input type="checkbox"/> FOR OFFICIAL DISTRIBUTION.		18. Security Class (This report)  Unclassified	20. Number of pages  133
		19. Security Class (This page)  Unclassified	21. Price: